



LEHIGH  
UNIVERSITY

Library &  
Technology  
Services

The Preserve: Lehigh Library Digital Collections

# Magnetization-transfer NMR analysis of aqueous poly(vinyl alcohol) gels: Effect of hydrolysis and storage temperature on network formation.

## Citation

Stephans, Lori Ellen - Lehigh University. *Magnetization-Transfer NMR Analysis of Aqueous poly(vinyl Alcohol) Gels: Effect of Hydrolysis and Storage Temperature on Network Formation*. 1997, <https://preserve.lehigh.edu/lehigh-scholarship/graduate-publications-theses-dissertations/magnetization>.

Find more at <https://preserve.lehigh.edu/>

*This document is brought to you for free and open access by Lehigh Preserve. It has been accepted for inclusion by an authorized administrator of Lehigh Preserve. For more information, please contact [preserve@lehigh.edu](mailto:preserve@lehigh.edu).*

## **INFORMATION TO USERS**

**This manuscript has been reproduced from the microfilm master. UMI films the text directly from the original or copy submitted. Thus, some thesis and dissertation copies are in typewriter face, while others may be from any type of computer printer.**

**The quality of this reproduction is dependent upon the quality of the copy submitted. Broken or indistinct print, colored or poor quality illustrations and photographs, print bleedthrough, substandard margins, and improper alignment can adversely affect reproduction.**

**In the unlikely event that the author did not send UMI a complete manuscript and there are missing pages, these will be noted. Also, if unauthorized copyright material had to be removed, a note will indicate the deletion.**

**Oversize materials (e.g., maps, drawings, charts) are reproduced by sectioning the original, beginning at the upper left-hand corner and continuing from left to right in equal sections with small overlaps. Each original is also photographed in one exposure and is included in reduced form at the back of the book.**

**Photographs included in the original manuscript have been reproduced xerographically in this copy. Higher quality 6" x 9" black and white photographic prints are available for any photographs or illustrations appearing in this copy for an additional charge. Contact UMI directly to order.**

# **UMI**

**A Bell & Howell Information Company  
300 North Zeeb Road, Ann Arbor MI 48106-1346 USA  
313/761-4700 800/521-0600**



**Magnetization-Transfer NMR Analysis of Aqueous  
Poly(vinyl alcohol) Gels: Effect of Hydrolysis and Storage  
Temperature on Network Formation**

by

Lori Ellen Stephans

A Dissertation

Presented to the Graduate and Research Committee

of Lehigh University

in Candidacy for the Degree of

Doctor of Philosophy

in

Chemistry

1997

**UMI Number: 9730312**

---

**UMI Microform 9730312**  
**Copyright 1997, by UMI Company. All rights reserved.**

**This microform edition is protected against unauthorized  
copying under Title 17, United States Code.**

---

**UMI**  
**300 North Zeeb Road**  
**Ann Arbor, MI 48103**

## Certificate of Approval

Approved and recommended for acceptance as a dissertation in partial fulfillment of the requirements for the degree of Doctor of Philosophy.

07. May 1997  
Acceptance Date

Natalie Foster  
Dissertation Director

Committee Directing the Doctoral Work of Lori Ellen Stephans:

Natalie Foster  
Dr. Natalie Foster

James E. Roberts  
Dr. James E. Roberts

Michael Freund  
Dr. Michael Freund

Mary Jo Kulp  
Dr. Mary Jo Kulp

## Certificate of Presentation

This dissertation is respectfully submitted to the graduate faculty of Lehigh University in partial fulfillment of the requirements for the degree of Doctor of Philosophy.

07 May 1997  
Date Submitted

Lori E Stephens  
Lori Ellen Stephens

## Acknowledgements

I would like to express my sincere gratitude and appreciation to my advisor Dr. Natalie Foster for her guidance and encouragement. Many thanks go to my dissertation committee: Dr. James Roberts, Dr. Michael Freund and Dr. Mary Jo Kulp for their advice and willingness to help. I would like to thank Air Products and Chemicals, Inc. for supplying poly (vinyl alcohol). Many thanks to the instrumentation directors at Lehigh, William Anderson and Dr. D.J. Wang, for their help with understanding pulse programs. I would like to express gratitude to Dr. K. Klier for his encouragement to pursue my Ph.D. I would also like to thank the Chemistry department for financial support.

Last, but not least, I will always be indebted to my family for supporting my efforts and encouraging me to pursue my education. I could not have made it without their love and unconditional support throughout my life.



**This Dissertation is Dedicated to my Dad  
(11/15/21 - 04/19/81)**

## Table of Contents

Certificate of Approval . . . . .	ii
Certificate of Presentation . . . . .	iii
Acknowledgements . . . . .	iv
Dedication . . . . .	v
Table of Contents . . . . .	vi
List of Tables . . . . .	ix
List of Figures . . . . .	xii

<b>Abstract . . . . .</b>	<b>1</b>
---------------------------	----------

### **Introduction**

Statement of Intent . . . . .	3
-------------------------------	---

#### Poly (vinyl alcohol)

Manufacture of Poly (vinyl alcohol) . . . . .	4
Physical Characteristics and Uses of Poly(vinyl alcohol) . . . . .	8
Aqueous Solution Behavior of Poly (vinyl alcohol) . . . . .	9
Aqueous Poly (vinyl alcohol) Gels . . . . .	11

#### NMR Spectroscopy

Relaxation in Polymer Systems . . . . .	11
---	----

##### Theory

Spin-Spin and Spin-Lattice Relaxation . . . . .	17
Polymer-Bound Water . . . . .	19
Magnetization-Transfer . . . . .	20

## Methods

Materials and Methods . . . . .	20
Line-Shape Analysis . . . . .	29
Instrumentation	
NMR Spectroscopy . . . . .	30
Turbidity Measurements . . . . .	34
Rigidity Measurements . . . . .	35

## Results and Discussion

Characterization of Poly (vinyl alcohol) . . . . .	36
<sup>13</sup> C-Nuclear Magnetic Resonance Spectroscopy . . . . .	38
<sup>1</sup> H-Nuclear Magnetic Resonance Spectroscopy . . . . .	47
Spin-Spin and Spin-Lattice Relaxation Measurements . . . . .	51
Polymer Bound Water via T <sub>2</sub> Measurements . . . . .	59
Magnetization-Transfer Nuclear Magnetic Resonance Spectroscopy	
Effect of Concentration on Network Formation . . . . .	61
Effect of Degree of Hydrolysis on Network Formation . . . . .	67
Ageing of Poly (vinyl alcohol) Solutions and Gels . . . . .	69
Turbidity . . . . .	85
Multicomponent Nature of Magnetization-Transfer Profiles . . . . .	89
Gel Point . . . . .	93
Viscosity Stabilization-Destabilization . . . . .	106
Effect of Quench Temperature on Network Formation . . . . .	110
Freeze-Thaw Experiments . . . . .	112

Solvent Extraction . . . . .	114
Preheating Treatment . . . . .	114
Thermoreversibility . . . . .	115
Gel Rigidity . . . . .	123
 <b>Conclusions</b> . . . . .	 125
 <b>References</b> . . . . .	 129
 <b>Vita</b> . . . . .	 135

## List of Tables

Table 1:	Degree of hydrolysis, sodium acetate, ash, volatile content, pH and viscosity of commercial poly (vinyl alcohol) samples . . . . .	37
Table 2:	Projection of triad and tetrad sequences with corresponding frequency of propagation $P_m$ assuming Bernoullian statistics . . . . .	41
Table 3:	Triad tacticity of poly (vinyl alcohol) calculated from $^{13}\text{C}$ NMR methine resonances . . . . .	42
Table 4:	First-order Markov probabilities calculated from the area of the triad methine carbon resonances of poly (vinyl alcohol) . . . . .	44
Table 5:	Tetrad tacticity of poly (vinyl alcohol) calculated from the areas of the $^{13}\text{C}$ NMR methylene resonances . . . . .	46
Table 6:	$^1\text{H}$ NMR chemical shift data for poly (vinyl alcohol) in dimethyl sulfoxide- $\text{d}_6$ . . . . .	49
Table 7:	$^1\text{H}$ NMR chemical shifts of the hydroxyl protons in poly (vinyl alcohol) with corresponding triad tacticities . . . . .	50
Table 8:	Water proton spin-lattice and spin-spin relaxation times as a function of concentration for poly (vinyl alcohol) samples stored at $23^\circ\text{C}$ for 24 hours . . . . .	53
Table 9:	Water proton spin-lattice relaxation times as a function of concentration for aged poly (vinyl alcohol) samples stored at $23^\circ\text{C}$ . . . . .	55

<b>Table 10:</b>	<b>Calculated number of polymer-bound water molecules per repeat unit of poly (vinyl alcohol) for samples stored at 23 °C for 1 day and 14 days . . . . .</b>	<b>59</b>
<b>Table 11:</b>	<b>Poly (ethylene oxide) magnetization-transfer profile area, Lorentzian full-width at half-maximum and viscosity as a function of concentration for samples stored at 23 °C . . . . .</b>	<b>65</b>
<b>Table 12:</b>	<b>Area of the magnetization-transfer profile for 5% poly(vinyl alcohol) samples as a function of storage time at 23 °C and 5 °C . . . . .</b>	<b>72</b>
<b>Table 13:</b>	<b>Area of the magnetization-transfer profile for 10% poly (vinyl alcohol) samples as a function of storage time at 23 °C and 5 °C . . . . .</b>	<b>74</b>
<b>Table 14:</b>	<b>Area of the magnetization-transfer profile for 20% poly (vinyl alcohol) samples as a function of storage time at 23 °C and 5 °C . . . . .</b>	<b>76</b>
<b>Table 15:</b>	<b>Area of the magnetization-transfer profile for 30% poly (vinyl alcohol) samples as a function of storage time at 23 °C and 5 °C . . . . .</b>	<b>79</b>
<b>Table 16:</b>	<b>Measured turbidity as a function of ageing time for 20% poly (vinyl alcohol) samples stored at 23 °C and 5 °C . . . . .</b>	<b>86</b>
<b>Table 17:</b>	<b>Measured turbidity as a function of ageing time for 30% poly (vinyl alcohol) samples stored at 23 °C and 5 °C . . . . .</b>	<b>87</b>
<b>Table 18:</b>	<b>Line shape analysis of 20% poly (vinyl alcohol)-A as a function of storage time at 23 °C . . . . .</b>	<b>91</b>
<b>Table 19:</b>	<b>Line shape analysis of 20% poly (vinyl alcohol)-A as a function of storage time at 5 °C . . . . .</b>	<b>92</b>

Table 20:	Gel point by the gel tilt method and gel point by magnetization-transfer analysis . . . . .	98
Table 21:	Magnetization-transfer profile area of 20% poly (vinyl alcohol)-A, B, C and D as a function of ageing time at 23 °C and 5 °C after the samples were heated at 96 °C after ageing initially for 21 weeks . . .	117
Table 22:	Measured turbidity of 20% poly (vinyl alcohol)-A, B, C and D as a function of ageing time at 5 °C and 5 °C after the samples were heated at 96 °C for 5 hours after ageing initially for 21 weeks . . . . .	118
Table 23:	Magnetization-transfer profile area, Gaussian and Lorentzian areas and percent Gaussian area for 20% poly (vinyl alcohol)heated at various times at 96 °C after bieng aged at 23 °C for 126 days . . . . .	121
Table 24:	Magnetization-transfer profile area, Gaussian and Lorentzian areas and percent Gaussian area for 20% poly (vinyl alcohol)heated at various times at 96 °C after bieng aged at 5 °C for 126 days . . . . .	122

## List of Figures

Figure 1:	Transesterification and hydrolysis reaction schemes for the conversion of poly (vinyl acetate) to poly (vinyl alcohol) . . . . .	5
Figure 2:	Tacticity of a monosubstituted polymer showing syndiotactic, isotactic and atactic arrangements . . . . .	7
Figure 3:	Magnetization-transfer profiles of liquid-like and solid-like polymer samples . . . . .	23
Figure 4:	$^{13}\text{C}$ NMR spectra showing the methylene and methine carbon regions of atactic poly (vinyl alcohol) in dimethyl sulfoxide- $\text{d}_6$ . . . . .	39
Figure 5:	$^{13}\text{C}$ NMR spectra showing the methine carbon atom region of the atactic poly (vinyl alcohol) samples in dimethyl sulfoxide- $\text{d}_6$ . . . .	40
Figure 6:	$^{13}\text{C}$ NMR spectra showing the methylene carbon resonances of atactic poly (vinyl alcohol) in dimethyl sulfoxide- $\text{d}_6$ . . . . .	45
Figure 7:	Proton NMR spectra of the poly (vinyl alcohol) samples in dimethyl sulfoxide- $\text{d}_6$ . . . . .	48
Figure 8:	Water proton spin-lattice and spin-spin relaxation times as a function of polymer concentration for poly (vinyl alcohol) samples stored at $23^\circ\text{C}$ for 1 day . . . . .	54
Figure 9:	Spin-spin and spin-lattice relaxation times as a function of degree of hydrolysis of poly (vinyl alcohol) for samples stored at $23^\circ\text{C}$ for 1 day . . . . .	56



Figure 10:	Spin-lattice relaxation times of water protons as a function of polymer concentration for samples aged at 23 °C .....	57
Figure 11:	Magnetization-transfer profiles of poly (vinyl alcohol)-A quenched and stored at 23 °C for 1 day .....	62
Figure 12:	Area of the magnetization-transfer profiles versus poly (vinyl alcohol) concentration for samples stored at 23 °C for 1 day, profile area measured as a function of concentration for poly (ethylene oxide) stored at 23 °C for 1 day .....	63
Figure 13:	Magnetization-transfer profiles as a function of concentration for poly (acrylic acid) and ethylene glycol stored at 23 °C for 1 day .....	66
Figure 14:	Area of the magnetization-transfer profiles versus degree of hydrolysis for poly (vinyl alcohol) samples stored at 23 °C for 1 day .....	68
Figure 15:	Magnetization-transfer profiles for 30% poly (vinyl alcohol)-A and 30% poly (vinyl alcohol)-D as a function of storage time at 23 °C .....	70
Figure 16:	Area of the magnetization-transfer profiles of 5% poly (vinyl alcohol) samples as a function of storage time at 23 °C and 5 °C .....	73
Figure 17:	Area of the magnetization-transfer profiles of 10% poly (vinyl alcohol) samples as a function of storage time at 23 °C and 5 °C .....	75
Figure 18:	Area of the magnetization-transfer profiles of 20% poly (vinyl alcohol) samples as a function of storage time at 23 °C and 5 °C .....	77
Figure 19:	Area of the magnetization-transfer profiles of 30% poly (vinyl alcohol) samples as a function of storage time at 23 °C and 5 °C .....	80

Figure 20:	Area of the magnetization-transfer profiles as a function of storage time at 23 °C for all poly (vinyl alcohol) samples . . . . .	82
Figure 21:	Area of the magnetization-transfer profiles as a function of storage time at 23 °C for all poly (vinyl alcohol) samples . . . . .	83
Figure 22:	Curve-fitting analysis of magnetization-transfer profile of 30% poly (vinyl alcohol)-A stored at 23 °C for 1 day . . . . .	90
Figure 23:	Percent Gaussian and Lorentzian areas as a function of storage time at 23 °C and 5 °C for 20% poly (vinyl alcohol)-A,B, and C samples . . . . .	97
Figure 24:	Gaussian and Lorentzian full-width at half-maximum as a function of storage time for 20% poly (vinyl alcohol)-A stored at 23 °C and 5 °C . . . . .	100
Figure 25:	Gaussian and Lorentzian full-width at half-maximum as a function of storage time for 20% poly (vinyl alcohol)-B stored at 23 °C and 5 °C . . . . .	102
Figure 26:	Gaussian and Lorentzian full-width at half-maximum as a function of storage time for 20% poly (vinyl alcohol)-C stored at 23 °C and 5 °C . . . . .	104
Figure 27:	Magnetization-transfer profiles for poly (vinyl alcohol)-A stored at 23 °C for 14 days containing viscosity stabilizing and destabilizing agents . . . . .	107
Figure 28:	Magnetization-transfer profiles for poly (vinyl alcohol)-A stored at 23 °C for 14 days containing viscosity stabilizing agents . . . . .	109

Figure 29:	Area of the magnetization-transfer profiles as a function of quench temperature for 20% poly (vinyl alcohol) samples . . . . .	111
Figure 30:	Scheme for the freeze-thaw cycle . . . . .	112
Figure 31:	Magnetization-transfer profiles and the corresponding profile areas of 10% poly (vinyl alcohol) after five freeze-thaw cycles . . . . .	113
Figure 32:	Area of the magnetization-transfer profiles as a function of storage time at 23 °C and 5 °C after reheating at 96 °C for 5 hours . . . . .	116
Figure 33:	Simple schematic of a potential energy surface before and after annealing . . . . .	120
Figure 34:	Gaussian area as a function of gel rigidity for 20% poly (vinyl alcohol) stored at 23 °C for 3 days . . . . .	124

## Abstract

Poly (vinyl alcohol) (PVA) is commercially manufactured from the hydrolysis of poly (vinyl acetate). The degree of hydrolysis can be precisely controlled, yielding copolymers with various vinyl alcohol and vinyl acetate contents. Commercial grades of PVA with degrees of hydrolysis extending from 80 to 99.5% have a broad range of physical properties that ensure numerous and diverse commercial applications. During the production of films, fibers and adhesives, ease of processing relies primarily on solubility, solution viscosity and solution stability. As a result, considerable interest has been focused on understanding the basic principles that govern solution dynamics at a molecular level from the standpoint of both the polymer and the solvent. The ability to predict and interpret the factors that affect solution dynamics is crucial to the development and manufacture of PVA-based products.

Aqueous PVA solutions are unstable. This instability, referred to as ageing, is affected by the degree of hydrolysis, molecular weight, tacticity and concentration of the PVA. Network formation, which develops as the sample ages, is a consequence of chain overlap and entanglement. Once progressed to a critical point, network formation significantly affects the viscosity and viscoelasticity of the solution. In PVA solutions network formation can cause gelation and may ultimately result in phase separation.

Existing analytical methods that provide information about macromolecular structure and order in the bulk require the sample to be in the form of a film or in dilute solutions. Typically, existing techniques are not adaptable to concentrated aqueous

solutions or gels. The goal of this investigation is to probe the effects of the degree of hydrolysis and storage temperature on network formation in aqueous PVA gels over a broad concentration range without physical destruction of the sample using solution-state Nuclear Magnetic Resonance (NMR) Spectroscopy.

This inquiry uses Magnetization-Transfer (MT) NMR to monitor network formation in aqueous PVA solutions and gels. Four commercially available atactic-PVA samples with various degrees of hydrolysis ranging from 87 to 99% were analyzed at concentrations from 2 to 30 wt%. The evolution of physical entanglements promoted by inter- and intrachain hydrogen-bonding between hydroxyl groups was monitored by observing changes in the MT profiles of the samples as they aged at 23 and 5 °C. The relative changes in the amount of immobile and mobile components of the gel were calculated by fitting the MT profiles of aged samples to the sum of a broad Gaussian component and a narrow Lorentzian component. Network formation is discussed in terms of relative changes in the amount of immobile and mobile components of the gel.

## Introduction

### Statement of Intent

This research is aimed at correlating NMR relaxation of solvent protons to the bulk properties and dynamic behavior of aqueous PVA solutions and gels. This work utilizes MT-NMR to nondestructively probe polymer chain dynamics in the gel state. The intent of this inquiry is to correlate the physical properties of the parent polymer to gel phase dynamics. PVA is the polymer targeted for this research because it is structurally simple, well characterized and recognized as a gel forming polymer.

The specific aims of this research are: *i*) to apply existing NMR methods and develop protocols to investigate network formation in aqueous PVA solutions and gels; *ii*) to systematically evaluate the effect of concentration, degree of hydrolysis and storage temperature on network formation; *iii*) to illustrate the advantages and contributions that NMR spectroscopy can make to verifying mechanisms governing gel phase dynamics, and *iv*) to provide a definition of a gel from the perspective of the NMR.

The hypotheses that govern the basis for this work are: *i*) magnetization-transfer can be used to observe the effects of the degree of hydrolysis, concentration, quench and storage conditions on the ageing of polymer solutions and gels; *ii*) magnetization-transfer profiles can yield distinct information about the mobile and immobile components of gels and hence can provide a novel view of the processes at the molecular level that cause transitions in properties between solutions and gels and

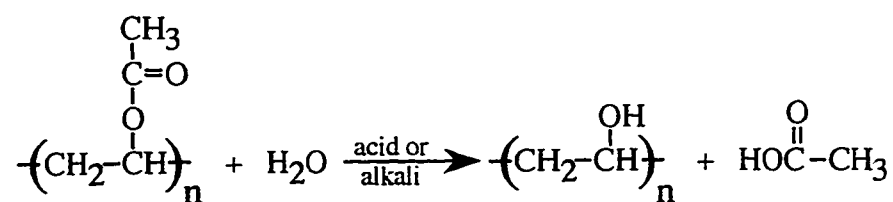
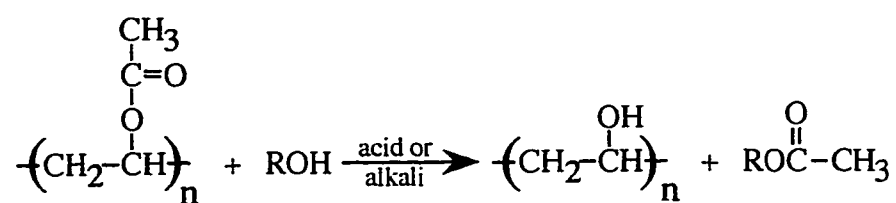
between gels and heterogeneous mixtures, and *iii*) results from magnetization-transfer analysis can be compared to other, more traditional classification methods and can provide a useful definition of a gel based on the view of polymer-solvent systems provided by NMR. The completion of this work has tested these hypotheses, contributed to the characterization of the processes governing network formation in aqueous PVA gels and has provided a definition of a gel from the standpoint of the NMR.

## Poly(vinyl alcohol)

### Manufacture of Poly(vinyl alcohol)

PVA is commercially manufactured by the hydrolysis of poly (vinyl acetate) (PVAc). Polymerization of the vinyl alcohol monomer is not possible due to its instability, which results in its rearrangement to acetaldehyde. The physical properties of PVA are closely correlated to the physical properties of the PVAc. PVAc is commercially manufactured by free radical emulsion or solution polymerization, during which propagation occurs nearly exclusively by head-to-tail addition.<sup>1-2</sup>

Commercially, PVAc is converted to PVA by acid or base catalyzed transesterification or hydrolysis (Figure 1). The percent conversion is termed the degree of hydrolysis or saponification (for transesterification reactions) and is reported as mol % vinyl alcohol. Commercially available grades of PVA are classified as super hydrolyzed (>99.5%), fully hydrolyzed (99.5-98%), intermediately hydrolyzed (98-89%) and partially hydrolyzed (80-89%). The degree of polymerization (dp) of PVA

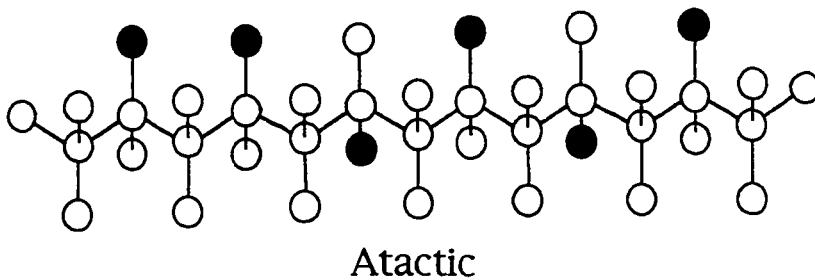
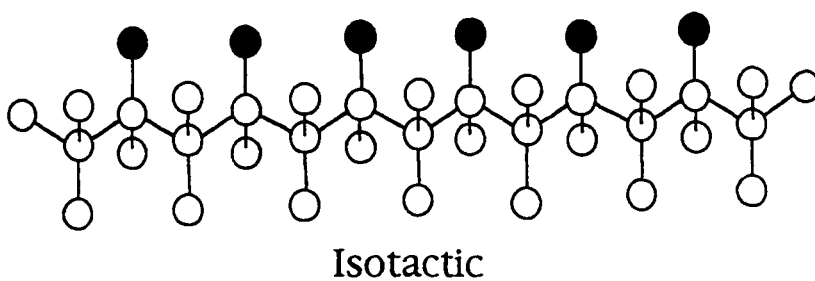
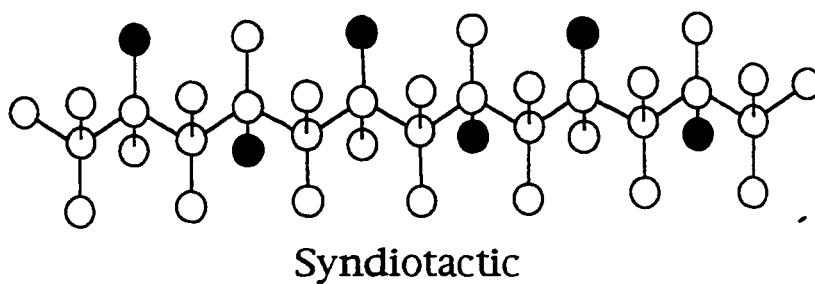


**Figure 1.** Transesterification (a) and hydrolysis (b) reaction schemes for the conversion of poly (vinyl acetate) to poly (vinyl alcohol).



is controlled during the polymerization of PVAc. PVA is also classified in terms of  $\overline{DP}$  based on the viscosity in centipoise (cP) of a 4% aqueous solution, where low viscosity (5 cP), medium viscosity (20-30 cP) and high viscosity (40-50 cP) classifications correspond to degrees of polymerization of 500, 1700 and 2000, respectively.

The tacticity, which is the arrangement of functional groups along the backbone of the polymer chain, is a consequence of the reaction conditions during the polymerization of PVAc. Commercially available PVA typically contains 25 to 30% of both syndiotactic and isotactic arrangements with a 40 to 50% atactic arrangement. The tacticities of PVA are illustrated in Figure 2. Tacticity has a pronounced effect on crystallinity, water solubility and tensile strength of PVA films and fibers.<sup>3</sup> The solubility of PVA decreases with increasing syndiotacticity.<sup>4-6</sup> Syndiotactic PVA, manufactured under controlled conditions, has unique physical properties and is targeted for special applications requiring high crystallinity and low solubility.<sup>4-6</sup>



**Figure 2.** Tacticity of a monosubstituted polymer showing syndiotactic, isotactic and atactic arrangements, where the black dots represent hydroxyl or acetate functional groups in poly (vinyl alcohol).

## **Physical Characteristics of Poly(vinyl alcohol) in Relation to Its Uses**

PVA has a wide range of physical properties that make it useful in a myriad of applications.<sup>7</sup> The degree of hydrolysis, degree of polymerization, crystallinity and tacticity are the characteristics of PVA that most significantly effect its physical properties. Diverse physical properties allow for a wide range of desired physical and chemical characteristics that include: water solubility, tensile strength, abrasion resistance, adhesion properties, grease and oil resistance, and film forming capabilities. As a result, these diverse characteristics afford uses such as non-woven materials, strippable coatings, water soluble films, fibers, textile and paper sizing, adhesives, emulsifiers and binders for pigments.<sup>1-3,7</sup>

Partially hydrolyzed grades of PVA have the best adhesive properties to hydrophobic surfaces and hence are used most widely for sizing polyesters.<sup>2</sup> In general, fabric and textile sizing applications require PVA having a low degree of crystallinity, and as a result the fabrics can be desized easily. Conversely, fully hydrolyzed grades with a high degree of crystallinity are used for sizing paper because they exhibit high tensile strength, flexibility and resistance to water.

PVA used in applications that include film and fiber production must have a high degree of hydrolysis and high crystallinity but low viscosity so that it can be extruded. Alternatively, films can be made from high viscosity PVA by spreading PVA in the gel state on a heated drum.<sup>7</sup> As the water evaporates from the gel, the resulting film attains sufficient mechanical strength so that it can be removed from the drum. With subsequent heat stretching, the films attain a high degree of crystallinity that renders

them useful for applications requiring high water resistance and mechanical strength.<sup>8-9</sup>

Ease of initial solubility as well as long term stability of aqueous solutions are required for all applications. As a result, considerable effort has been expended to understand the effect that the physical properties of PVA have on its solution behavior. Researchers have found ways to modify the physical and chemical structure of PVA such that the desired physical characteristics are enhanced and the applications of PVA are broadened.

### **Behavior of Aqueous Solutions of Poly(vinyl alcohol)**

Many studies that involve determining the correlation between the physical properties of PVA and the behavior of aqueous solution have been justified by the practical importance of aqueous solutions in the manufacture of PVA products. Aqueous PVA solutions are unstable due to the formation of aggregates upon storage. Aggregation has been studied by light scattering and turbidity measurements.<sup>10-11</sup> Aggregates are formed in aqueous solutions that are 5-7% by weight PVA. At concentrations of 15% by weight PVA, solution viscosity increases and gels are formed upon storage at room temperature. It has been suggested that gel formation is the result of partial crystallization of PVA molecules due to chain orientation as a result of hydrogen bonding. X-ray diffraction has confirmed that crystallization occurs in aqueous PVA gels upon long-term storage.<sup>12</sup>

Both the association of chains in solution and the subsequent formation of aggregates are highly dependent on the conditions of synthesis and hydrolysis, concentration and the conditions of dissolution.<sup>1-2</sup> Small-angle neutron-scattering, a technique highly sensitive to structure formation in aqueous solutions, has shown that methods of synthesis of PVAc and conditions of hydrolysis that decrease the crystallinity of the parent polymer significantly affect the formation of supermolecular structures in solution.<sup>13-14</sup> When dissolved, samples with higher initial crystallinity have a high degree of order in solution that results in an increased tendency toward aggregation. Any residual crystallinity not destroyed in the dissolution process is believed to “seed” the formation of crystallites or aggregates depending on dissolution conditions. Upon storage, the number and size of the aggregates increase with time. The rate of growth of ordered structures is slower for samples of ultrahigh molecular weight and high vinyl acetate contents.<sup>13-14</sup>

The viscosity and turbidity of aqueous solutions of PVA increase upon long-term storage which, depending on the storage conditions, may result in gelation.<sup>15-19</sup> Gelation is affected by the PVA concentration, degree of hydrolysis, molecular weight and storage temperature.<sup>20</sup> Storage temperature has a pronounced effect on gelation, whereby the formation of physical entanglements and aggregates is appreciably enhanced as the storage temperature is decreased.<sup>17</sup> Viscosity measurements have shown that at 2-4 wt % solutions of PVA are dispersed and fully hydrated. At higher concentrations of 10-12 wt%, chains are entangled, forming a net-like structure which renders the solution non-Newtonian.<sup>15</sup> PVA solutions with concentrations above 10 wt % used industrially behave as non-Newtonian liquids and are referred to as liquified gels.

It has been suggested that hydrophilic and hydrophobic areas of the polymer chain are oriented in solution, whereby the hydrophobic portions of the molecule are turned inward toward each other and the hydrophilic groups are directed outward, solvated by water molecules in solution.<sup>21</sup> At and below a critical temperature, the hydroxyl groups are hydrated and the system is homogeneous. As the temperature increases, partial hydration promotes changes in the hydrophilic-lipophilic balance that result in phase separation. This critical temperature increases with the degree of hydrolysis of the PVA, and samples with a higher degree of hydrolysis have a greater affinity for hydration as a result of the increased number of hydrophilic hydroxyl groups. The critical temperature also increases with the concentration of the PVA.

### Poly(vinyl alcohol) Aqueous Gels

In general, the main effort in the study of gels has been directed toward explaining gel properties and the gelation process in terms of gel structure and changes in structure as a function of the physical properties of the polymer. As early as 1926, Jordan Lloyd, who in a paper entitled "The Problem of Gel Structure" noted that gels are easier to recognize than they are to study and define.<sup>22</sup> In 1949, P.H. Hermans defined gels as a coherent dispersed system containing at least two components that extend themselves continuously throughout the whole system.<sup>23</sup> Flory<sup>24</sup> and Ferry,<sup>25</sup> both concerned with the structural characteristics of polymers, defined a gel as a system that exhibits no steady-state flow as result of the formation of a network, aggregates or well-ordered lamellar structures.

A discrete unambiguous definition of a gel is difficult because the physical properties that are used to define gels are technique dependent. For example, from a mechanical standpoint, a substance is a gel when it has the mechanical properties of a solid, i.e., it can maintain its form under the stress of its own weight and under mechanical stress displays the phenomenon of strain. From the stand point of other existing analytical techniques used to study gels such as dynamic light scattering, x-ray diffraction, differential scanning calorimetry, this definition of a gel is meaningless. For this reason, a definition of a gel must be stated with reference to the technique used to study it. It is therefore our intent to provide a definition of a gel from the standpoint of NMR and to contribute to the overall definition of a gel.

Simplistically, polymer gels are complex, three-dimensional networks comprised of liquid and solid components. The liquid/polymer and polymer/polymer interactions that occur in the gel system influence macromolecular organization, which in turn affect the bulk physical properties of the gel. The liquid component, while providing the polymer chain with mobility and the gel with fluidity, can be exploited as a tool for probing gel phase dynamics.

The manufacture and product quality of PVA-based products depend on their ability to be processed as solutions and gels.<sup>1-3,7</sup> As a result, considerable interest has been focused on understanding the basic principles governing the formation, integrity and degradation of gels at a molecular level from the standpoint of both the polymer and the liquid component. Specifically, for aqueous PVA gels, the network structure and the bulk physical properties of the gel change with age and storage conditions.<sup>15-19</sup> These changes promote both desirable and undesirable product performance. The ability to

predict and interpret either consequence is crucial to the development and manufacture of PVA-based products.

Diverse efforts have focused on characterizing the network structure of PVA gels and its effect on the physical properties of the gel. Prokopova and coworkers<sup>15-19</sup> were first to report network formation in ageing PVA gels. They found that the network structure in the gel consisted of amorphous and crystalline regions, and the amount of crystallinity depended predominately on the age, dissolution conditions and storage temperature. The process of ageing, reflected by a rise in viscosity and elasticity, promotes the formation of a supermolecular structure that is affected by the thermal prehistory of the solutions, the temperature at which the ageing takes place, and the physical characteristics of the polymer such as concentration and molecular weight of the parent polymer.<sup>17,26</sup>

## NMR Spectroscopy Applied to the Study of Polymers

NMR, used in its most classical sense, is a valuable tool which provides structural information through measurements of chemical shifts, line intensities and coupling constants. From these measurements, detailed structural information such as connectivity, tacticity and branching can be determined in the most complex polymer systems in solid and solution state. Through time-dependent spectra or time domain decay of signal, NMR can provide dynamic information about the motional characteristics of both the polymer and solvent. For example, the amount of polymer



bound water, polymer surface coverage on colloids, crosslink densities, concentration of chain entanglement and crystallinity can be determined by NMR.<sup>27-30</sup>

## Relaxation of Water Protons in Polymer Systems

The relaxation characteristics of polymer-bound water differ from that of bulk water. The presence of the polymer results in large variations in the relaxation time of water as a result of hindered motion. Studies which involve correlating relaxation properties to macromolecular structure and organization in aqueous polymer systems are important in many different areas of science: in biology and medicine, where a large quantity of water is associated with cellular membranes; in the study of the stability of proteins and peptides where hydration is crucial for molecular association and interaction. NMR also plays a major role in the study of absorbed water in systems such as silica, wood, cellulose and membranes.<sup>28-35</sup>

NMR relaxation times,  $T_1$  (spin-lattice) and  $T_2$  (spin-spin), are extremely sensitive to changes in molecular mobility and macromolecular environment.<sup>36-37</sup> As a result, the  $T_1$  and  $T_2$  relaxation times of the water protons furnish information about the dynamics of polymer chains involved in the network of the gel.

## Polymer Bound Water

Cha and Ikada<sup>38</sup> examined the relationship between the amount of polymer-bound water and the properties of PVA gels by differential scanning calorimetry (DSC). They found a smaller bound-water fraction when a gel was prepared by low temperature crystallization than when a gel was prepared by high temperature annealing. These results suggested that the structure and the physical properties of PVA gels depend on the quantity of polymer-bound water. Prokopova *et al.*<sup>26</sup> used DSC and polarizing microscopy to evaluate network formation and crystallinity in aqueous PVA samples. The results of the DSC analysis showed that the degree of network formation and crystallinity was dependent on the amount of polymer-bound water.

The interaction of water with polymers having hydrophilic groups has been studied by various experimental techniques where “associated/bound” water has been distinguished from “free/bulk” water. The amount of polymer-bound water in natural and synthetic polymers has been probed by NMR relaxation measurements in systems including polymer adsorbed on silica,<sup>28-29</sup> wood,<sup>31-33</sup> cellulose<sup>34</sup> and lipid bilayers.<sup>35</sup> For example, Froix and Nelson<sup>39</sup> have shown that the structure and physical properties of cellulose change with variations in degree of hydration and hence the amount of polymer-bound water. A water binding analysis of aqueous poly (ethylene glycol) obtained from various methods including light scattering, neutron scattering, calorimetry and NMR has shown that there are 2-4 molecules of bound water per repeat unit of poly (ethylene glycol). Katayama *et al.*<sup>40-41</sup> estimated the number of bound water molecules to be 1-2 per repeat unit in polyacrylamide gels.

Hatakeyema *et al.*<sup>40</sup> quantified the amount of bound and free water in PVA crosslinked with <sup>60</sup>C γ-ray irradiation by DSC. From the enthalpy of melting, it was determined that three states of water exist in PVA gels: free, associated and polymer bound water. They determined that there are 1-1.5 molecules of non-freezing/bound-water per hydroxyl group and 5-6 molecules of freezing/associated-water per hydroxyl group, where the amount of free water depended markedly on the crosslink density of the PVA. Hatakeyema *et al.*<sup>40</sup> corroborated these observations with NMR relaxation measurements and found that the NMR relaxation times of water were related to the crosslink density and leveled off at a crosslink density of  $2.0 \times 10^{-4}$  crosslinks/cm<sup>3</sup>.

The observed proton relaxation time of water is governed by the time the water molecules spend exchanging between the “rigid” polymer and “free” water environments and, therefore, is inherently dependent on the interaction with and relaxation behavior of the polymer.<sup>42</sup> NMR methods were chosen for this study because relaxation times of solvent protons yield information about the motional characteristics of the polymer.<sup>27-31</sup> The ability to quantify the amount of polymer-bound water allows us to make correlations between the degree of hydration of the polymer and the physical behavior of the PVA gel.

## Magnetization-Transfer NMR Spectroscopy

The network structure and the amount of polymer-bound water in natural and synthetic polymers have been probed by magnetization-transfer (MT) NMR in systems

that include lipid bilayers,<sup>35</sup> starch,<sup>43</sup> fruit <sup>44</sup> and poly(ethylene glycol).<sup>45</sup> Eads and Wu found MT to be a valuable tool for monitoring the changes in crystallinity in waxy maize starch.<sup>43</sup> Eads and Wu determined that, as the starch aged, the total area and Gaussian component of the MT profiles were directly related to the crystallinity of the starch. Similarly, we plan to use NMR to characterize the network structure formed as a result of gelation and ageing in aqueous poly (vinyl alcohol) solutions and gels.

## Theory

### Spin-Spin and Spin-Lattice Relaxation

The dynamics of the solvent reflect the motional characteristics of the polymer with which it interacts.<sup>46-47</sup> As a result, the observed relaxation time of the water protons in an aqueous polymer system is governed by the time the water molecules spend exchanging between the “rigid” polymer and “free” water environments and, therefore, is inherently dependent on the interaction with and relaxation behavior of the polymer.<sup>48-50</sup>

Spin-lattice relaxation involves loss of energy by the excited nucleus to the surrounding lattice. As the system returns to equilibrium, the number of excited nuclei in the high energy population decreases exponentially with time, and the value  $T_1$  represents the time required for the magnetization to return to equilibrium.

The spin-lattice relaxation time is measured by an inversion-recovery sequence that consists of a 180 ° preparation pulse followed by a delay and a 90 ° read pulse.<sup>51</sup> The 180 ° pulse inverts the bulk magnetization vector along the z axis so that the vector is initially negative. With time, the magnetization vector in the z direction passes through zero and then grows toward equilibrium. The read pulse rotates the magnetization vector into the y axis for detection. The  $T_1$  value is calculated from

$$M_{y(t)} = M_{y(0)} \exp (-t/T_1) \quad (1)$$

where  $M_{y(t)}$  is the measured magnetization after the relaxation delay  $t$ ,  $M_{y(0)}$  is the initial magnetization and  $T_1$  is the spin-lattice relaxation time.

Spin-spin relaxation involves a redistribution of energy within the spin system. This interchange of energy between spins results in some spins precessing slower and some faster causing the magnetization vector to fan out in the xy plane resulting in a loss of phase coherence. The value for  $T_2$  is measured by a Carr-Purcell pulse sequence in which a series of 180 ° pulses is applied to refocus the magnetization at variable times after a 90 ° pulse.<sup>52</sup> Loss of coherence manifests itself as a decay of the transverse magnetization expressed as

$$M_{y(t)} = M_{y(0)} \exp (-t/T_2) \quad (2)$$

where  $M_{y(t)}$  is the measured magnetization after the relaxation delay  $t$ ,  $M_{y(0)}$  is the initial magnetization and  $T_2$  is the spin-spin relaxation time.

## Quantification of Polymer-Bound Water

Experimental determination of bound and free water by NMR is feasible assuming a two phase model. Component A (free water) consists of all water molecules that are not influenced by the polymer and exhibit relaxation characteristics of pure bulk water. Component B (bound water) consists of all water molecules that have reduced mobility as a result of interaction with the polymer. Carles and Scallan determined the amount of polymer-bound water and the percent of accessible hydroxyl groups on cellulose by NMR spectroscopy.<sup>53</sup> They evoked a two-state model where  $T_{2B}$  is the spin-spin relaxation time of the water protons “bound” to the polymer and  $T_{2F}$  is that of the water in the free, bulk state. The ensemble average spin-spin relaxation time that is experimentally measured ( $T_2$ ) is defined as

$$1/T_2 = P_B (1/T_{2B}) + P_F (1/T_{2F}) \quad (3)$$

where  $P_B$  and  $P_F$  are the probabilities that a proton is in the bound or free state, respectively. Assuming the quantity  $1/T_{2F}$  to be negligible compared to either  $1/T_2$  or  $1/T_{2B}$ , the second term on the right-hand side can be neglected. The probability of the water proton residing in the bound state  $P_B$  is then a function of the concentration of each state of water

$$P_B = [H_2O]_B / [H_2O]_T \quad (4)$$

where  $[H_2O]_T$  is the total concentration of water in the sample and  $[H_2O]_B$  is the concentration of the water bound to the polymer. The quantity  $T_{2B}$ , which can not be measured easily experimentally, can then be approximated from a plot of  $T_2$  versus  $[H_2O]_T$  where the intercept of the  $T_2$  axis is taken to be  $T_{2B}$ . The quantity  $[H_2O]_B$ ,

which is the maximum number of water molecules in the bound state, is calculated by:

$$[\text{H}_2\text{O}]_B = (T_{2B}) \cdot [\text{H}_2\text{O}]_T / T_2 \quad (5)$$

This method for calculating the number of polymer bound water is presented, but because of the experimental difficulty in determining the exact spin-spin relaxation time of bound water, only upper limits can be defined for the amount of bound water.

## Magnetization-Transfer

Proton relaxation in a heterogeneous sample containing both liquid and solid components involves magnetic relaxation coupling between the components. Although this magnetic coupling may complicate our understanding of heterogeneous systems, it may be exploited to examine a spin system that is difficult to observe accurately, namely the solid, via the readily observed component, the liquid. The MT experiment utilized in this study was first described by Grad and Bryant<sup>54-55</sup> and has been successfully used to study naturally occurring, macroscopically heterogeneous polymer systems.<sup>43-44, 56-58</sup> Grad and Bryant simplified the set of six coupled Bloch equations to describe a model system containing a pair of spin baths, A (liquid) and B (solid), interacting via intermolecular dipole-dipole interactions in the rotating frame in the presence of a radio frequency field.<sup>58</sup> The observed magnetization ( $\overline{M}_A^S(t)$ ) can be written in terms of a reduced form:

$$\overline{M}_A^S(t) = [M_A^O - M_A^S(t)] / 2M_A^O \quad (6)$$

which is a measure of the deviation of the longitudinal magnetization of the A spin bath from equilibrium at time (t) in the absence of a RF field, where ( $M_A^S$ ) is the magnetization of the A signal in the presence of the off-resonance saturation of the B spins and ( $M_A^O$ ) is the magnetization of the A signal in the absence of saturation.

The steady-state solution of the Bloch equations for a single population of nuclear spins is simplified in equation (7) and contains the relaxation parameters of the solid as well as those of the liquid. When the MT rate between the liquid and solid spin baths is much greater than unity, the measured liquid signal intensity ( $\overline{M}_A^S(t)$ ) is affected by the magnetic relaxation parameters of the solid spin system and, therefore, by the molecular dynamics of the solid component. The quantity  $f$  refers to the ratio of

$$\overline{M}_A^S(t) = 1/2 \{ (\omega_1 / T_{1B} T_{2B}) / (1 + 4\pi^2 T_{2B}^2 \Delta^2) (1 + T_{1B} / f T_{1A}) + \omega_1 2 T_{1B} T_{2B} \} \quad (7)$$

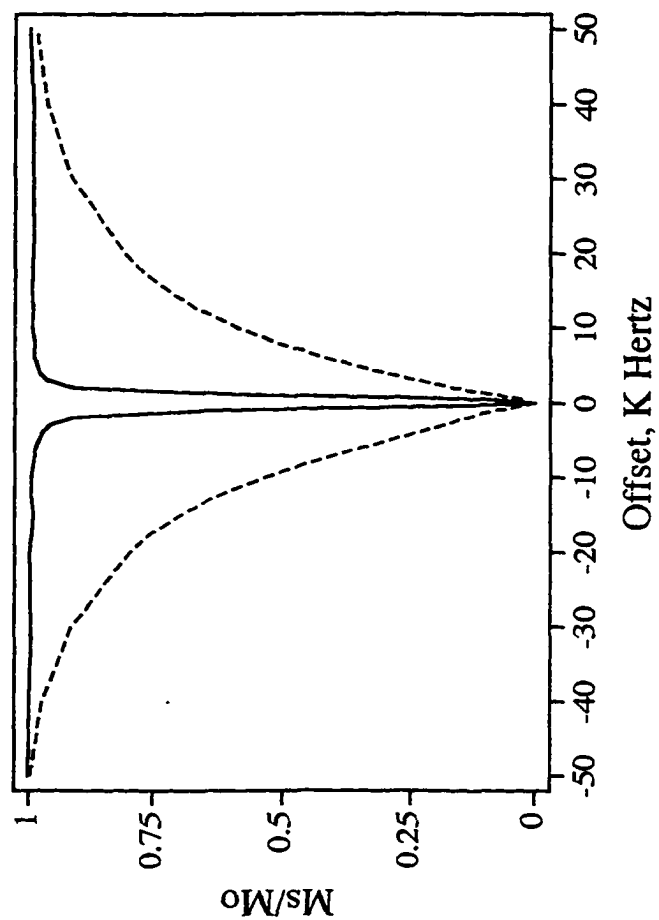
the number of B spins (solid) to the number of A spins (liquid),  $\Delta$  represents the frequency-offset of the radio-frequency preparation pulse from the A resonance frequency, and the quantities  $T_{1A,B}$  and  $T_{2A,B}$  are the spin-lattice and spin-spin relaxation times of the protons in the liquid-like (A) and solid-like (B) components.

In the aqueous PVA system studied here, the slow-relaxing protons of the liquid-like, mobile component transfer magnetization to the fast relaxing protons of the solid-like, rigid component. This interaction between the rigid and mobile components of the gel is measured by saturating the proton NMR signal of the rigid component off-



resonance from water while avoiding any direct saturation of the relatively mobile, bulk water spins. The effect that the off-resonance saturation has on the signal intensity of the water protons is measured by a pulse on-resonance with water. In the MT experiment, the intensity of the water proton signal is measured as a function of the off-resonance frequency and is interpreted in the form of a MT profile whose shape, intensity and line-width is characteristic of the dynamics of the polymer. The line-width of the MT profile increases with decreasing  $T_{2B}$ , i.e. increasing rigidity.<sup>43</sup> The intensity of the MT profile depends on the solid to liquid proton ratio  $f$ ; thus the area of the MT profile increases as the number of protons in the solid component increases.

MT profiles of samples with and without a rigid component are shown in Figure 3. The MT profile of a sample without a rigid component appears narrow and can be fit to a single Lorentzian function. The MT profile of a sample containing a rigid component is broad and is best fit to the sum of a narrow Lorentzian and broad Gaussian function. The areas of the Lorentzian and Gaussian components provide information about the degree of chain immobilization in the gel. For example, a Gaussian component with a large profile area would indicate chain immobilization and conversely, a sample with no Gaussian component would indicate no chain immobilization. The full-width at half-maximum of the individual components provides information about the relative immobilities of each component.



**Figure 3** . Magnetization-transfer profiles of a liquid-like ( — ) and solid-like samples ( - - - - - ).

## Methods

### Materials

Poly (vinyl alcohol) samples (A,B, C, D and E) with an average degree of polymerization of 1250-1300 and the following degrees of hydrolysis: A: 99.5, B: 98.5, C: 97.4, D: 87.6 and E: 96.1(mole % hydrolysis) were manufactured under similar conditions and were supplied by Air Products and Chemicals, Inc., Allentown, PA. All the PVA samples analyzed in this study have the same tacticity as determined by  $^{13}\text{C}$ - NMR spectroscopy. Analyses were performed on samples A through D to establish trends based on the degree of hydrolysis. Sample E was analyzed to verify the sharp decrease in network formation observed in the 98 - 87% hydrolysis range. Poly(ethylene oxide) (PEO), a non-network forming polymer, was used to verify that MT analysis is sensitive to network formation independent of changes in viscosity. PEO with a viscosity average molecular weight of 100,000 was obtained from Aldrich, Milwaukee, WI. Poly (acrylic acid) with a viscosity average molecular weight of 200,000 and ethylene glycol were purchased from Aldrich. Deionized/distilled water with a conductivity of 4 micromohs/cm and with a pH of 5.4 was used to prepare all samples. ACS grade ethylene glycol, sodium hydroxide, hydrochloric acid, sulfuric acid, sodium sulfate, ammonium thiocyanate, potassium thiocyanate, methanol, isopropanol and 1-butanol were used as received from Aldrich, Milwaukee, WI.

## General

The samples used for MT analysis were prepared by placing weighed quantities of PVA and room temperature distilled water in 10 mm NMR tubes. The tubes were capped with parafilm to prevent water loss during heating. The samples were heated in a water bath at 96 °C for 5 hours until the PVA samples appeared visually homogeneous. The prepared samples were quenched immediately from 96 °C to the storage temperature and stored in a water bath at 23 °C or 5 °C for varying periods of time. PEO was dissolved in water at room temperature by vortexing. All samples were capped to prevent water loss. The concentration of PVA or PEO is reported as percent polymer by weight. Viscosity stabilizing and destabilizing agents were added as 10% by weight of the aqueous portion of the sample. All samples were equilibrated at 23 °C for 15 minutes prior to MT analysis.

## Sodium Acetate Content

The sodium acetate content was determined according to published procedure.<sup>1</sup> A 5 g sample, for PVA greater or equal to 97% degree of hydrolysis, was weighed and dissolved in 150 ml of deionized water with heating. Upon cooling the solution was titrated with 0.1 N HCl using methylene blue/methyl yellow indicator. A blank titration was carried out using 150 ml of water. A 12 g sample, for PVA samples with a degree of hydrolysis less than 97% degree of hydrolysis, was weighed and placed in a Soxhlet extractor and extracted with 150 ml of methanol for 100 cycles. The methanol was removed from the sample by vacuum and 20 ml of deionized water was added. After dissolution, the sample was titrated with 0.1 N HCl using methylene

blue/methyl yellow indicator. A blank titration was carried out using 20 ml of water.

The sodium acetate content was calculated by:

$$N_o = [0.0082 \times (a - b) F / s] \times 100$$

where  $N_o$  is the sodium acetate content,  $s$  is the mass of sample,  $F$  is the normality of HCl,  $a$  is the sample volume of HCl, and  $b$  is the blank volume of HCl.

### Volatile Content

Volatile content was determined as the loss of mass (%) when the PVA was dried at  $105 \pm 2^\circ\text{C}$  until a constant mass was obtained.

### Ash Content

The ash content was determined according to published procedure.<sup>1</sup> PVA was extracted with methanol in a Soxhlet extractor for 100 cycles and dried under vacuum to remove the methanol until a constant mass was obtained. Approximately 5 g of the dried sample was accurately weighed in a porcelain crucible of known mass. The sample was heated at  $450^\circ\text{C}$  for one hour, then at  $750^\circ\text{C}$  for 5 hours in a muffle furnace. After cooling to constant mass, the sample was weighed and the ash content was calculated as:

$$K_o = a (100 - R - N_o) / b + 0.38N_o$$

where  $K_o$  is the ash content of sample as received,  $N_o$  is the sodium acetate content,  $a$

is the mass change, R is the volatile content and b is the mass of extracted sample.

## Degree of Hydrolysis

The degree of hydrolysis was determined according to published procedure.<sup>1</sup> A 3 g sample, for PVA equal to or greater than 97% degree of hydrolysis, or 0.5 g of sample, for PVA less than 97% degree of hydrolysis, was weighed and dissolved in 100 ml of deionized water with heating. Upon cooling, 25 ml of 0.1N NaOH ( $\geq 97\%$  DH) or 0.2 N NaOH ( $< 97\%$  DH) was added and the sample was allowed to sit at room temperature for 2 hours. A 25 ml portion of 0.1N sulfuric acid ( $\geq 97\%$  DH) or 0.2 N sulfuric acid ( $< 97\%$  DH) was added and the excess was titrated with 0.1 N NaOH to a pink endpoint with phenolphthalein. A blank titration was performed. The degree of hydrolysis was calculated by:

$$A = 0.60 \times (a - b) F \times 100 / s \times p$$

$$B = 44.05A / 60.06 - 0.42A$$

$$C = 100 - B$$

where A is the mass of acetate, p is the pure component, B is the residual acetate (mol %), F is the normality of sodium hydroxide, C is the degree of hydrolysis (mol %), a is the sample volume of NaOH, s is the mass of sample and b is the blank volume of NaOH. The pure component is the mass percent of the sample that remains after subtracting the percent volatiles, percent sodium acetate and percent ash content.

## pH

The pH of 5% solutions of PVA prepared with deionized water by heating at 96 °C for 1 hour was measured at 23 °C using a Corning 150 digital pH meter.

## 1,2-Glycol Content

The 1,2-glycol content was determined for PVA according to published procedure.<sup>2</sup> A weighed sample of PVA, 0.25g, was dissolved in 40 ml of hot distilled water. Sodium periodate was added in a two fold excess to cleave the 1,2-glycol units. After approximately 30 minutes, 1 g of sodium bicarbonate was added to render the solution alkaline. An exact quantity of excess 0.10 M arsenious acid, 10.00 ml, and 0.1 g of potassium iodide were added to the solution. The sample was titrated with (V) ml of (N) normal standard iodine. A blank titration was performed and the volume of titer is  $V_0$ . The percent 1,2-glycol content was calculated as

$$(V - V_0) N M / W$$

where M is 44.1 for the molecular weight of one  $\text{CH}_2\text{CHOH}$  segment. The literature reports the accuracy of this method to be  $\pm 2\%$ .

## Gel Point Measurements

PVA was dissolved in glass test tubes (i.d. 1 cm) under the conditions outlined in the methods section. Visual investigation of the sol-gel transition was carried out according to published procedure at 23 and 5 °C by tilting the test tube at a 90 ° angle for 30 s.<sup>59</sup> If the meniscus deformed under its own weight, the sample was judged to be a solution. Conversely, if the meniscus did not deform, the sample was judged a gel.

## Line-Shape Analysis

The line-shapes of the MT profiles were analyzed using simple line-shape functions in accordance with the procedure first described by Eads.<sup>43</sup> Typically, NMR spectral line-shapes can be approximated by either Lorentzian (8) or Gaussian (9) functions whose mathematical forms are:

$$I_L = \frac{C_L}{1 + (2(\nu - \nu_0) / (\Delta \nu_L))^2} \quad (8)$$

$$I_G = C_G \exp \left( -\frac{\ln 2 (2(\nu - \nu_0))^2}{(\Delta \nu_G)^2} \right) \quad (9)$$

where  $I$  is the intensity,  $C$  is the coefficient,  $(\nu - \nu_0)$  is the frequency-offset in Hz,  $\Delta \nu$  is the line width at half-height in Hz, and the subscripts L and G denote Lorentzian and Gaussian. The MT profile is a plot of the normalized intensity of the water peak,  $(M_A^S)$  (with presaturation) /  $(M_A^O)$  (without presaturation), versus the frequency-offset  $\Delta$ . This plot must be inverted for curve-fitting analysis; thus the function  $1 - (M_A^S) / (M_A^O)$  was used. The line-shape was fit by a routine using a least squares procedure (Sigma Plot, Jandel Scientific, Corte Madera, CA) to the sum of Lorentzian and Gaussian functions:

$$1 - M_A^S(\Delta) / M_A^O = \frac{C_L}{1 + (2000 \Delta / \Delta \nu_L)^2} + C_G \exp \left( -\frac{\ln 2 (2000(\Delta))^2}{(\Delta \nu_G)^2} \right) \quad (10)$$



where  $C_L$ ,  $C_G$ ,  $\Delta\nu_L$ , and  $\Delta\nu_G$  are obtained from curve fitting. The areas of the MT profile and its components were calculated as the sum of the values at intervals of 500 Hz over the frequency range of -70 to 70 kHz. The profile area and the Gaussian (11) and Lorentzian (12) areas were calculated by :

$$\text{Area}_G = \sum_{\Delta_i=-70}^{70} \frac{C_L}{1 + (2000 \Delta / \Delta\nu_L)^2} \quad (11)$$

$$\text{Area}_L = \sum_{\Delta_i=-70}^{70} C_G \exp\left(-\frac{\ln 2 (2000(\Delta))^2}{(\Delta\nu_G)^2}\right) \quad (12)$$

and were expressed in arbitrary units. The Gaussian percentage of the MT profile is defined as the area of the Gaussian component divided by the total area of the profile; the Lorentzian percentage of the MT profile is defined analogously.

## Instrumentation

### Magnetization-Transfer NMR Spectroscopy

MT profiles of aqueous PVA samples were obtained from the offset-frequency dependence of the water proton signal intensity. The high-resolution spectra used to construct MT profiles were obtained on a Brüker AMX 360 wide-bore spectrometer operating at 360.13 MHz for the detection of protons. The spectrometer was equipped

with a 25-mm single-frequency ( $^1\text{H}$ ) single-coil probe. The pulse sequence was D1(relaxation delay)-P18(preparation pulse)-P1( $90^\circ$  pulse)-acquisition. In all MT measurements, the preparation pulse was applied for 3 s at a radio-frequency field strength of 500 Hz (proton precession frequency). The frequency offset ( $\Delta$ ) of the preparation pulse from the water resonance was varied from -70 kHz to +70 kHz and randomized. Thirty-two data points were acquired from -70 kHz to +70 kHz. Other acquisition parameters were: relaxation delay (D1) 20 s,  $90^\circ$  pulse (P1) 56  $\mu\text{s}$ , spectral width 8196 Hz. All measurements consisted of a single scan and were carried out at  $23 \pm 2^\circ\text{C}$ . Samples were equilibrated at  $23^\circ\text{C}$  for 15 minutes prior to data acquisition, then returned to the temperature bath. The typical time for measurement of a MT profile was 9 minutes.

### Optimization of MT-NMR Parameters

Several experiments were conducted to ensure full saturation and reproducibility of the data. The MT experimental parameters were optimized to: *i*) ensure full saturation, *ii*) minimize radio-frequency heating and *iii*) reduce scatter by minimizing radiation damping.

### Optimization of the Duration of the Preparation Pulse

The duration of the preparation pulse was set to 500 ms, 1 s, 3 s and 5 s. The maximum saturation occurred within 3 s.

### Amplitude of the Preparation Pulse

The preparation pulse amplitude was varied by changing the attenuation (HL2) of

the preparation pulse. A value of 18 dB was used, which gave a preparation pulse amplitude of 532 Hz.

### Minimization of RF Heating and Radiation Damping

Sample scatter was minimized by minimizing the parameters that contribute to radio-frequency heating. A maximum duration of the preparation pulse of 3 s and a 12 s relaxation delay were used. Initially, RF heating occurred at the beginning of the experiment and was manifested as scatter in the initial eight downfield data points of the MT profile. To reduce radio-frequency heating, the variable frequency-offset list was randomized and the scatter decreased considerably. To minimize radiation damping, the sample size was adjusted so that when it was in the 10 mm NMR tube the sample remained within the 2 cm height of the RF coil. A 10 mm NMR tube in the 10 mm insert caused considerable scatter in the data, possibly due to the filling factor of the insert and radiation damping. A 10 mm NMR tube in 25 mm insert provided the least scatter.

### Sample Equilibration Time

The samples were allowed to equilibrate in the NMR at 23 °C. Those samples that were above or below 23 °C were deemed equilibrated when the water resonance remained stationary to within  $\pm 0.1$  Hz. MT profiles were checked at 15 min, 30 min and 1 hour to determine the minimum equilibration time; 15 minutes was sufficient.

## Carbon-13 Nuclear Magnetic Resonance Spectroscopy

Carbon-13 NMR spectra were obtained at 125.77-MHz using a Brüker AM 500 high-resolution spectrometer. The samples were examined as 10% (w/w) solutions in dimethyl- $d_6$  sulfoxide (DMSO- $d_6$ ) in 10 mm NMR tubes. Spectra were acquired at 323 K, using the standard Brüker variable-temperature unit. So that data collection parameters could be chosen to ensure quantitative results, the spin-lattice relaxation times ( $T_1$ ) from the literature were relied upon.<sup>60</sup> The  $T_1$  values were determined for the methine and methylene carbons for 10 % (w/v) solutions of PVA in DMSO- $d_6$  at 323 K. The  $T_1$  values were 0.29-0.32 s and 0.17-0.18 s for the methine carbons and the methyl carbon, respectively. Based on these  $T_1$  values, the relaxation delay was set to 1.8 s. Spectra were acquired with a 45 ° pulse, a spectral width of 10 kHz, and 32 K data points to give an acquisition time of 1.41 s. The relaxation delay of 1.8 s was the time between the end of one acquisition and the start of the next during which the decoupler was gated off to provide complete relaxation and suppression of Overhauser effects. A 0.5 Hz line broadening was used.

## Proton Nuclear Magnetic Resonance Spectroscopy

Proton NMR spectra were obtained at 360.13-MHz using a Brüker AMX 360 high-resolution spectrometer equipped with an Oxford (8.45 Tesla) wide-bore magnet at 296 K. Proton spectra of 5% (w/w) solutions of polymer in DMSO- $d_6$  in 5 mm NMR tubes were acquired with a 90° pulse, a relaxation delay of 5 s and 32 k data points. Spin-lattice relaxation times of the water protons were measured using the

180°-τ-90° inversion-recovery technique.<sup>51</sup> Spin-spin relaxation times of the water protons were measured using the standard 90°-τ-180° spin echo sequence by Carr-Purcell-Meiboom-Gill (CPMG).<sup>52</sup> For T<sub>1</sub> and T<sub>2</sub> measurements the temperature was controlled to within ± 1 °C. A 2.0 Hz line broadening was used for all proton spectra.

## Turbidity Measurements

The turbidity of aqueous solutions of PVA at various concentrations was measured at 520 nm in a 1 cm cell with a Spec-20 spectrophotometer. Percent light transmittance was recorded at various intervals in time as the samples aged at 23 °C and 5 °C. Samples stored at 5 °C were equilibrated at 23 °C for 15 minutes prior to measurement. The transmitted light intensity (I<sub>t</sub>) and the incident intensity (I<sub>o</sub>) are related by the sample turbidity (T) and the path length (L),

$$I_t/I_o = e^{-TL} \quad (13)$$

The conversion from absorbance (A) to turbidity was performed using equation (14),

$$T = A \ln(10)/L \quad (14)$$

where L is the sample path length.<sup>61-63</sup>

## Rigidity and Viscosity Measurements

Dynamic viscoelastic measurements were acquired with a stress-controlled rheometer (Rheometrics RDA II, Piscataway, NJ) using a 50 mm diameter parallel plate geometry. The storage and loss moduli,  $G'(\omega)$  and  $G''(\omega)$ , of the samples were measured at a strain of 0.7 % over an angular frequency range from 0.15 Hz to 15 Hz at 23 °C. The sample rigidity is expressed in terms of the limiting value of the frequency-dependent storage modulus (17)

$$E = \lim_{\omega \Rightarrow 0} G'(\omega) \quad (15)$$

where  $\omega$  is the angular frequency and  $E$  is the relaxed shear modulus. The gel rigidity is expressed as the limiting value of  $G'(\omega)$  at the lowest attainable experimental value of  $\omega$ , 0.15 Hz.<sup>64-66</sup>

The viscosity of the 5 and 10% poly(ethylene oxide) samples were acquired at 23 °C by a steady state-single point measurement using a cup and bob geometry with the following conditions: cup inner diameter 27 mm, bob outer diameter 25 mm, bob length 32 mm, gap 0.5 mm, shear rate 10 s<sup>-1</sup> and measurement time 5 s. The viscosities of the 20, 30 and 40% poly(ethylene oxide) samples were acquired under the same conditions using a 50 mm parallel plate geometry and the previously specified experimental conditions.

## Results

### Characterization of Poly(vinyl alcohol)

#### General

Physical characteristics such as degree of hydrolysis, pH, sodium acetate, ash and volatile contents were evaluated by standard methods to verify the purity of the PVA samples.<sup>1</sup> The results are listed in Table 1. The concentration of sodium acetate, a side product of hydrolysis, increases as expected with increasing degree of hydrolysis. The pH of 5% solutions of PVA increases with increasing degree of hydrolysis and sodium acetate concentration. This observation is consistent and expected; increasing sodium acetate content should increase alkalinity. The volatile content is similar for all samples. The degree of hydrolysis measured experimentally agrees with the values reported by the manufacturer. The 1,2-glycol contents are reported as the average of four measurements. The 1,2-glycol contents are PVA-A: 0.88%, PVA-B: 0.88%, PVA-C: 0.85% and PVA-D: 0.96%. These physical characteristics were determined to verify the values reported by the manufacturer and to assure continuity between samples so that the samples could be evaluated based solely on their differences in degree of hydrolysis.

Sample	Degree of Hydrolysis	Sodium Acetate	Ash	Volatile Content	pH	Viscosity <sup>a</sup>
PVA-A	99.5%	0.91%	0.14%	4.3%	6.4	27.6
PVA-B	98.5%	0.43%	0.10%	3.9%	6.1	31.1
PVA-C	97.3%	0.28%	0.07%	3.2%	5.7	27.8
PVA-D	87.6%	0.16%	0.02%	3.5%	4.8	24.5
PVA-E	96.1%	0.18%	0.03%	3.6%	5.5	27.6

<sup>a</sup>Viscosity: 4% aqueous solution at 23 °C in cps as reported by the manufacturer.

**Table 1.** Degree of hydrolysis, sodium acetate, ash, volatile content, pH and viscosity of poly (vinyl alcohol).

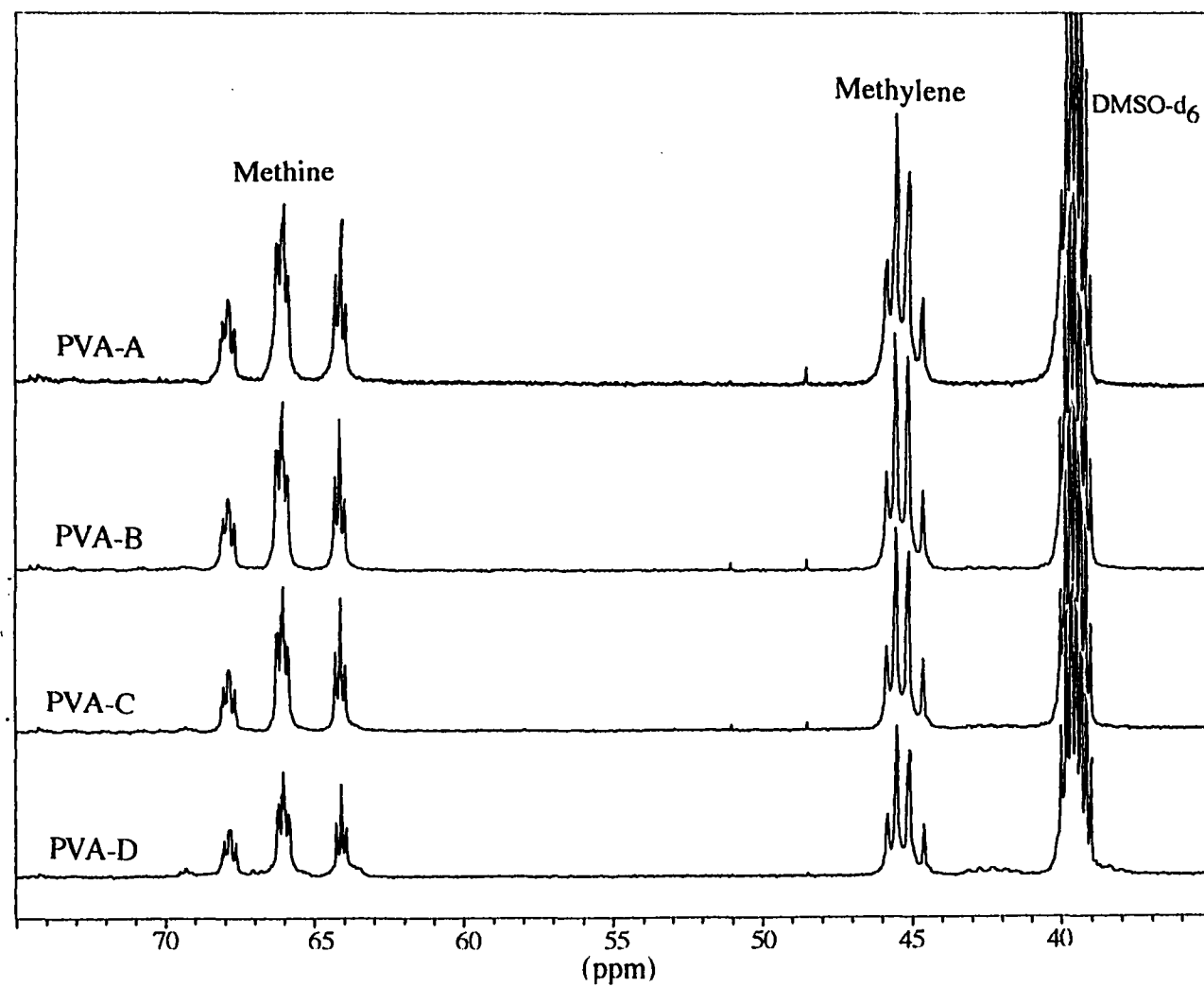


## Tacticity by $^{13}\text{C}$ Nuclear Magnetic Resonance Spectroscopy

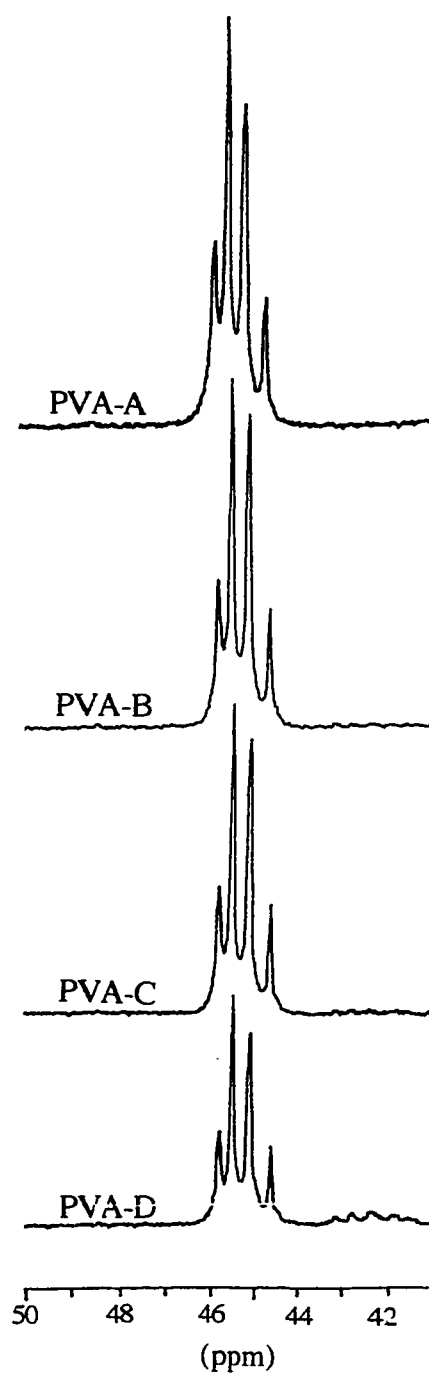
Even at a low concentration of vinyl acetate, the distribution of acetate groups along the polymer backbone has a pronounced effect on the physical properties of PVA and its solutions. Changes in intramolecular distribution of the vinyl acetate units and the tacticity of the polymer backbone cause pronounced differences in crystallinity, melting point, solubility, surface tension and structure formation in solution.<sup>1-4</sup> For this reason it is necessary to verify the tacticity and statistical randomness of the functional groups along the backbone of the polymer. Verification of tacticity and randomness by Bernoulian and Markov statistics will provide assurance that the observed differences in the network structure of solutions and gels are a direct consequence of differences in inter- and intramolecular hydrogen-bonding as a result of differences in the degree of hydrolysis. The PVA samples analyzed in this study came from one manufacturer and were polymerized and hydrolyzed under similar conditions.

Figure 4 shows the 125.77-MHz  $^{13}\text{C}$  NMR spectra of PVA-A, B, C and D in DMSO- $\text{d}_6$  solution at 323 K. The four resonances from 44 ppm to 46 ppm and the three groups of resonances from 64 ppm to 68 ppm are assigned to the methylene and methine carbons, respectively. The heptet at 39.5 ppm is due to the solvent DMSO- $\text{d}_6$ .






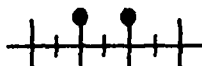



The three resonance lines of the methine carbon region are shown in Figure 5 and are assigned to isotactic triads (mm) at 64 ppm, heterotactic at (mr) 66 ppm and syndiotactic (rr) at 68 ppm (refer to Table 2 for structural arrangements).<sup>67</sup> The triad tacticities determined from the area of the methine carbon resonances, mm, mr and rr, for PVA-A, PVA-B, PVA-C and PVA-D are shown in Table 3 and indicate that all PVA samples are atactic. The Bernoulli statistical values were calculated and are also



**Figure 4.**  $^{13}\text{C}$  NMR spectra showing the methylene and methine carbon atom regions of atactic poly(vinyl alcohol) samples in dimethyl sulfoxide- $\text{d}_6$ .



**Figure 5.** Methine carbon atom region of atactic poly (vinyl alcohol) samples in DMSO-d<sub>6</sub>.

$\alpha$ Substituent			$\beta$ Substituent					
Designation	Projection	Bernoullian Probability	Designation	Projection	Bernoullian Probability			
Triad	Isotactic, mm		$Pm^2$	Tetrad	mmm		$Pm^3$	
	Heterotactic, mr		$2Pm(1 - Pm)$		mmr		$2Pm^3(1 - Pm)$	
	Syndiotactic, rr		$(1 - Pm)^2$		rmr		$Pm(1 - P)^2$	
					mrm		$Pm^2(1 - Pm)$	
					rrm		$2Pm(1 - Pm)^2$	
					rrr		$(1 - Pm)^3$	

m and r denote meso and racemic, respectively

**Table 2.** Projection of triad and tetrad sequence projections with corresponding frequency of propagation  $P_m$  assuming Bernoullian propagation.

Triad	PVA-A		PVA-B		PVA-C		PVA-D	
	Obs <sup>a</sup>	Bernoulli Trial <sup>b</sup> $P_m=0.448$	Obs	Bernoulli Trial $P_m=0.473$	Obs	Bernoulli Trial $P_m=0.458$	Obs	Bernoulli Trial $P_m=0.477$
mm <sup>c</sup>	0.203	0.201	0.231	0.224	0.204	0.210	0.240	0.227
mr	0.490	0.494	0.485	0.498	0.509	0.496	0.475	0.499
rr	0.298	0.305	0.284	0.278	0.287	0.294	0.285	0.273

<sup>a</sup> Obtained from the area of the methine carbon resonances in Me<sub>2</sub>SO-d<sub>6</sub> solution at 323 K. <sup>b</sup> The probability of generating a meso sequence when a new monomer unit is formed at the end of a growing chain. <sup>c</sup> Chemical shifts: mm (64 ppm), mr (66 ppm) and rr (68 ppm).

**Table 3.** Triad tacticity of poly (vinyl alcohol) calculated from <sup>13</sup>C NMR methine resonances.

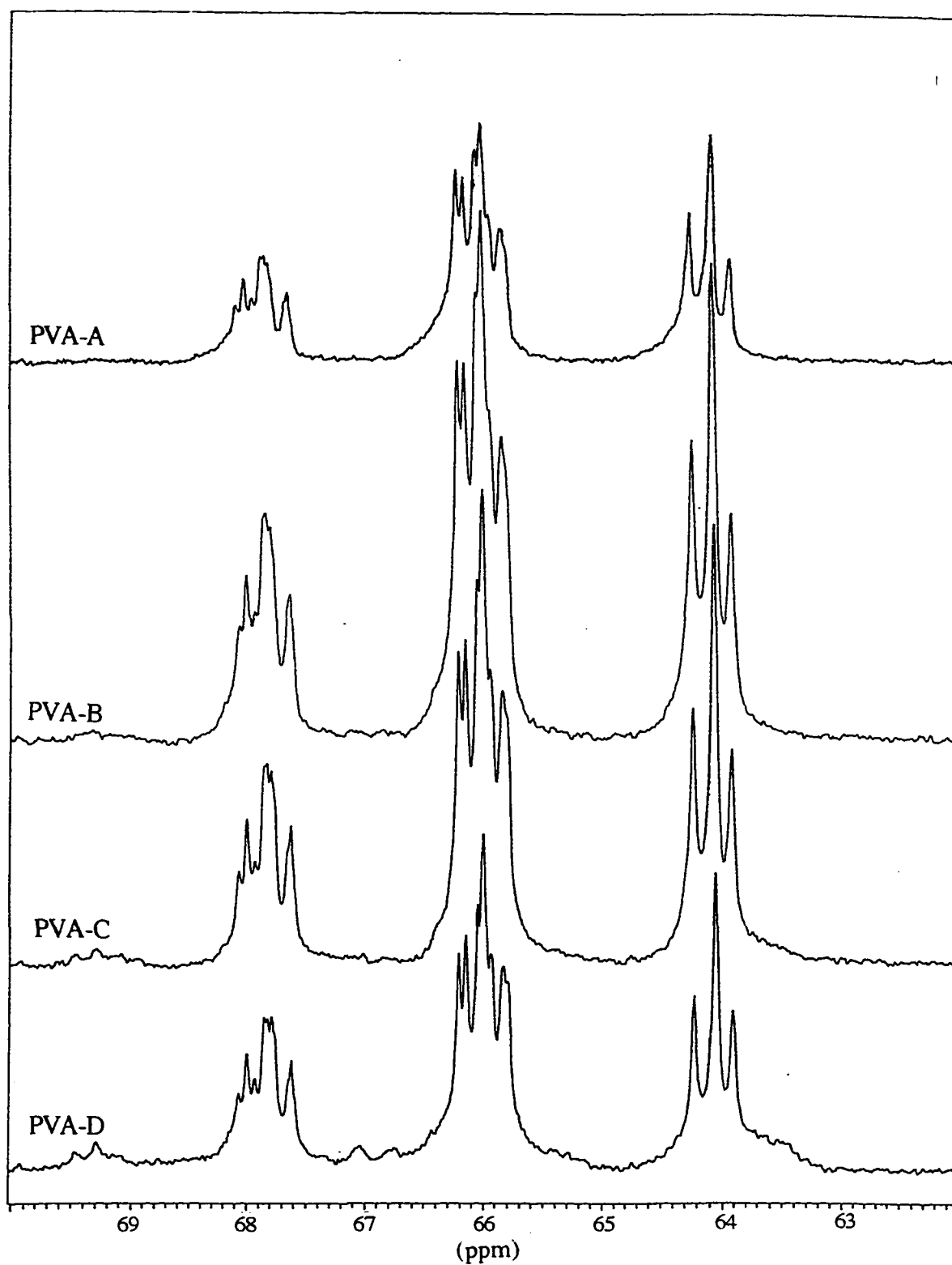
shown in Table 3 for comparison. Close correlation between the experimentally determined propagation probability and the Bernoullian probability suggests that the triad tacticities can be described by Bernoulli statistics corresponding to a strictly random atactic configuration.<sup>67</sup> All samples are atactic and have random configurations, which provides assurance that differences in polymer-polymer interaction can be deemed the result of the differences in the degree of hydrolysis of the PVA and not the result of configurational differences.

Wu and Sheer<sup>68</sup> and Ovenall<sup>69-70</sup> determined that the sequencing in PVA does not always follow Bernoullian statistics, depending on the mode of polymerization. As a result, in some cases they found that the sequencing could be described by a first-order Markov probability model. Wu and Sheer obtained  $P_{m/r} = 0.158$  and  $P_{r/m} = 0.655$  while Ovenall found  $P_{m/r} = 0.145$  and  $P_{r/m} = 0.613$ . The slight difference between the two sets of data are probably due to low signal-to-noise ratios and resolution obtained by Wu and Sheer.<sup>68</sup> The sums of  $P_{m/r}$  and  $P_{r/m}$  obtained from these authors are significantly different from unity. Wu and Sheer concluded that the PVA used in their study, prepared by the hydrolysis of a cationically polymerized vinyl trimethylsilyl ether, does not follow Bernoullian statistics. Ovenall<sup>69</sup> found that the triad tacticities could be described by the first-order Markov model. The data presented in Table 4 shows that the PVA analyzed in this study follows the first-order Markov model where the quantity  $P_{m/r} + P_{r/m}$  is close to unity which indicates a strictly random atactic configuration.<sup>71</sup>

The methylene carbon atom resonances for PVA, shown in Figure 6, appear as four features from overlapping tetrads. The four resonances are assigned to tetrads rrr at 44.8 ppm, rmr and mmr at 45.4 ppm, mrm and mmm at 45.6 ppm and mmm at 45.8

	PVA-A	PVA-B	PVA-C	PVA-D
$P_{m/r}$	0.547	0.512	0.555	0.497
$P_{r/m}$	0.451	0.460	0.470	0.454
$P_{m/r} + P_{r/m}$	0.998	0.972	1.025	0.951

**Table 4.** First-order Markov probabilities calculated from the area of the triad methine carbon resonances in poly (vinyl alcohol).



**Figure 6.** Methylene carbon resonances of atactic poly (vinyl alcohol) in  $\text{DMSO-d}_6$ .



Tetrad	PVA-A		PVA-B		PVA-C		PVA-D	
	Obs <sup>a</sup>	Bernoulli Trial $P_m=0.409^b$	Obs	Bernoulli Trial $P_m=0.477$	Obs	Bernoulli Trial $P_m=0.482$	Obs	Bernoulli Trial $P_m=0.478$
rrr	0.176	0.206	0.159	0.143	0.155	0.139	0.154	0.142
rmr <sup>c</sup> mmr	0.392	0.429	0.377	0.391	0.376	0.388	0.389	0.390
mr <sup>c</sup> mmr	0.309	0.297	0.337	0.357	0.336	0.361	0.327	0.363
mmm	0.123	0.068	0.127	0.108	0.133	0.112	0.130	0.109

<sup>a</sup> Obtained from the area of the methylene carbon resonances in  $\text{Me}_2\text{SO}-d_6$  solution at 323 K. <sup>b</sup> The probability of generating a meso sequence when a new monomer unit is formed at the end of a growing chain. <sup>c</sup> The tetrads (rmr,mmr) and (mr<sup>c</sup>,mmr) are unresolved. Chemical shifts: rrr (44.8 ppm), rmr,mmr (45.4 ppm), mr<sup>c</sup>,mmr (45.6 ppm) and mmm (45.8 ppm)

**Table 5.** Tetrad tacticity calculated from the areas of the  $^{13}\text{C}$  NMR methylene resonances of poly(vinyl alcohol).

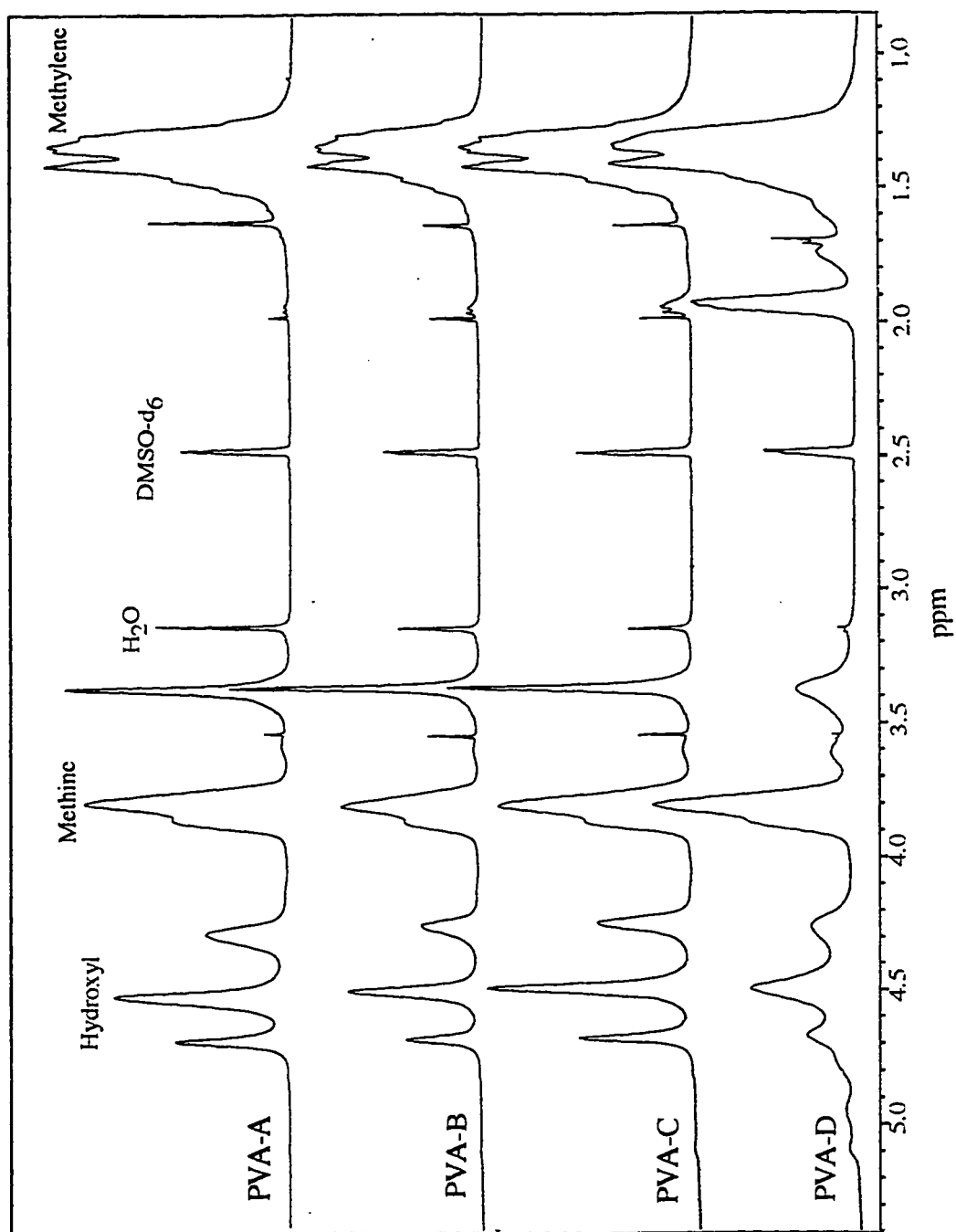
ppm (refer to Table 2 for structural arrangements). The observed tetrad tacticities and the Bernoulli trial statistics determined from the methylene carbon resonances for PVA-A, PVA-B, PVA-C and PVA-D are tabulated in Table 5. The variation between the experimentally calculated propagation probabilities and the theoretical Bernoullian propagation probabilities is due to peak overlap as a result of poor resolution. Higher order tacticities are also difficult due to peak overlap as a result of poor resolution.

### Proton Nuclear Magnetic Resonance Spectroscopy

The 360.13-MHz proton NMR spectra of PVA-A, B, C and D in DMSO- $d_6$  solution at 296 K are shown in Figure 7. The resonances assigned to the methylene protons of PVA appear at 1.37 ppm. Down field from the methylene resonances, there appear resonances assigned to the solvent DMSO- $d_6$  (2.48 ppm), residual water in DMSO- $d_6$  (3.15 ppm), the methine protons (3.82 ppm) and hydroxyl protons (4.26, 4.50 and 4.75 ppm). All assignments are shown in Table 6 and correlate with the literature.<sup>72</sup>

A number of workers have shown that three distinct hydroxyl resonances corresponding to triad sequences can be observed when DMSO- $d_6$  is used as the solvent.<sup>73</sup> The three hydroxyl resonances can be assigned to the isotactic (mm), heterotactic (mr) and syndiotactic (rr) triad configurations in order of increasing field strength.

The triad probabilities calculated from the area of the hydroxyl resonances were determined and reported as percent area (Table 7). The triad probabilities show that all



**Figure 7.** Proton NMR spectra of poly(vinyl alcohol) in dimethyl sulfoxide-d<sub>6</sub>.

Chemical Shift, (ppm)	Structural Assignment
1.37	methylene PVA
1.70	methylene PVAc
1.95	methyl PVAc
3.82	methine PVA
2.00	methyl sodium acetate
2.48	DMSO-d <sub>6</sub>
3.15	residual water in DMSO-d <sub>6</sub>
3.38	methine PVA (PVA, <u>PVA</u> , PVAc)
3.55	methine PVA (PVAc, <u>PVA</u> , PVAc)
4.26	(rr) <sup>a</sup> Hydroxyl PVA
4.50	(mr) Hydroxyl PVA
4.75	(mm) Hydroxyl PVA

<sup>a</sup>The three hydroxyl resonances are assigned to the isotactic (mm), heterotactic (mr) and syndiotactic triad configurations.

**Table 6.** Proton NMR chemical shifts for poly (vinyl alcohol) samples in DMSO-d<sub>6</sub>.

Triad <sup>a</sup>	Chemical <sup>b</sup> Shift (ppm)	Percent Area of the Triad Sequences			
		PVA-A	PVA-B	PVA-C	PVA-D
mm	4.75	20.5	21.8	22.1	21.1
mr	4.50	47.9	48.8	50.4	52.2
rr	4.26	31.5	29.4	27.5	26.7

<sup>a</sup> The abbreviations: mm, mr and rr denote isotactic, heterotactic and syndiotactic triads, respectively. <sup>b</sup> In dimethyl sulfoxide-d<sub>6</sub> at 23 °C.

**Table 7.** Chemical shifts and the corresponding percent area of the triad tacticities for the hydroxyl protons of poly (vinyl alcohol).

four samples are atactic with a slightly higher syndiotacticity than isotacticity. The tacticity calculated from the hydroxyl protons correlates well with the methine carbon triad probabilities calculated from  $^{13}\text{C}$ -NMR data (Table 3).

The resonance at 1.95 ppm appearing in all four spectra is due to the methyl protons of poly(vinyl acetate). The area of this resonance increases with decreasing degree of hydrolysis as expected and is particularly pronounced in the PVA-D where the concentration of vinyl acetate is the greatest. The resonance at 1.7 ppm in PVA-D is due to the methylene protons of poly(vinyl acetate). The sharp resonance at 2.0 ppm in the spectra of PVA-A, PVA-B and PVA-C is due to the methyl protons on sodium acetate. This resonance is not present in PVA-D due to the relatively low concentration of sodium acetate in samples with low degrees of hydrolysis. The area of the sodium acetate peak is highest in sample A due to the sodium acetate produced as a byproduct of the hydrolysis of PVAc to PVA. The resonance at 3.38 ppm is due to the methine proton of PVA sequenced between PVA and PVAc sequences. The resonance at 3.55 ppm is due to the methine protons of PVA between two PVAc sequences. The resonance at 1.65 ppm in PVA-A, PVA-B and PVA-C is undefined but probably due to methanol, the residual polymerizing solvent.

## Characterization of Poly(vinyl alcohol) Solutions and Gels

### Measurements of Spin-Lattice and Spin-Spin Relaxation Times of Water Protons

The spin-lattice and spin-spin relaxation times of water protons were measured as a function of concentration for PVA-A, B, C and D stored at 23 °C for 24 hours (Table 8). A plot of relaxation time as a function of concentration shows that  $T_1$  and  $T_2$  both decrease with increasing concentration of PVA (Figure 8). From Figure 8 it is apparent that differentiation between the four PVA samples with different degrees of hydrolysis by  $T_1$  and  $T_2$  is not possible.

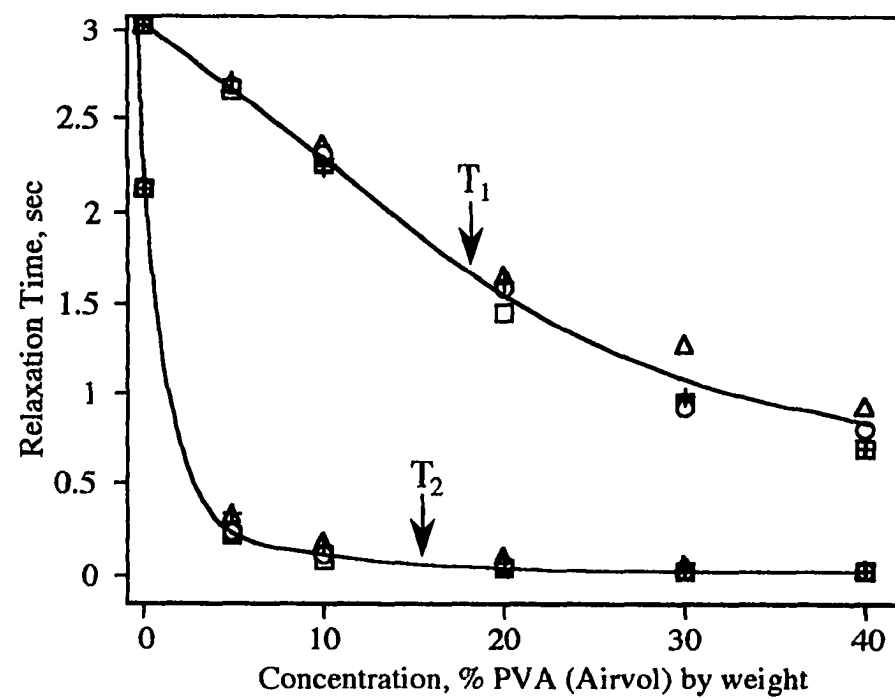
The water proton  $T_1$  and  $T_2$  values are plotted as a function of the degree of hydrolysis (Figure 9). The  $T_1$  relaxation time is constant with degree of hydrolysis at every concentration. A minimum in the  $T_2$  relaxation time occurs for PVA-C, the sample with a degree of hydrolysis of 97.3%, at every concentration. Two maxima occur at the highest and lowest degrees of hydrolysis at every concentration.

As aqueous solutions of PVA age, viscosity increases because the mobility of the water molecules in the system decreases. In some systems, the mobility of the water molecules can be measured by  $T_1$  relaxation times which are sensitive to the molecular environment and molecular mobility. The  $T_1$  relaxation times of water protons for PVA-A were measured as a function of concentration as the samples aged at 23 °C over a period of 8 weeks (Table 9). It is apparent that a decrease in molecular mobility as a result of ageing is not detectable by  $T_1$  measurements in the PVA system (Figure 10).

Concentration	Spin-Lattice Relaxation Time $T_1$ , Sec				Spin-Spin Relaxation Time $T_2$ , Sec			
	PVA-A	PVA-B	PVA-C	PVA-D	PVA-A	PVA-B	PVA-C	PVA-D
5	2.71	2.68	2.65	2.69	0.34	0.23	0.22	0.32
10	2.26	2.31	2.27	2.36	0.16	0.11	0.09	0.17
20	1.62	1.58	1.45	1.65	0.07	0.05	0.04	0.09
30	0.99	0.93	0.96	1.27	0.04	0.03	0.03	0.06
40	0.70	0.81	0.70	0.93	0.02	0.02	0.02	0.03

**Table 8 .** Water proton spin-lattice and spin-spin relaxation times as a function of concentration for poly(vinyl alcohol) samples stored at 23 °C for 24 hours. Error:  $T_1 \pm 0.1$  s,  $T_2 \pm 15$  ms.

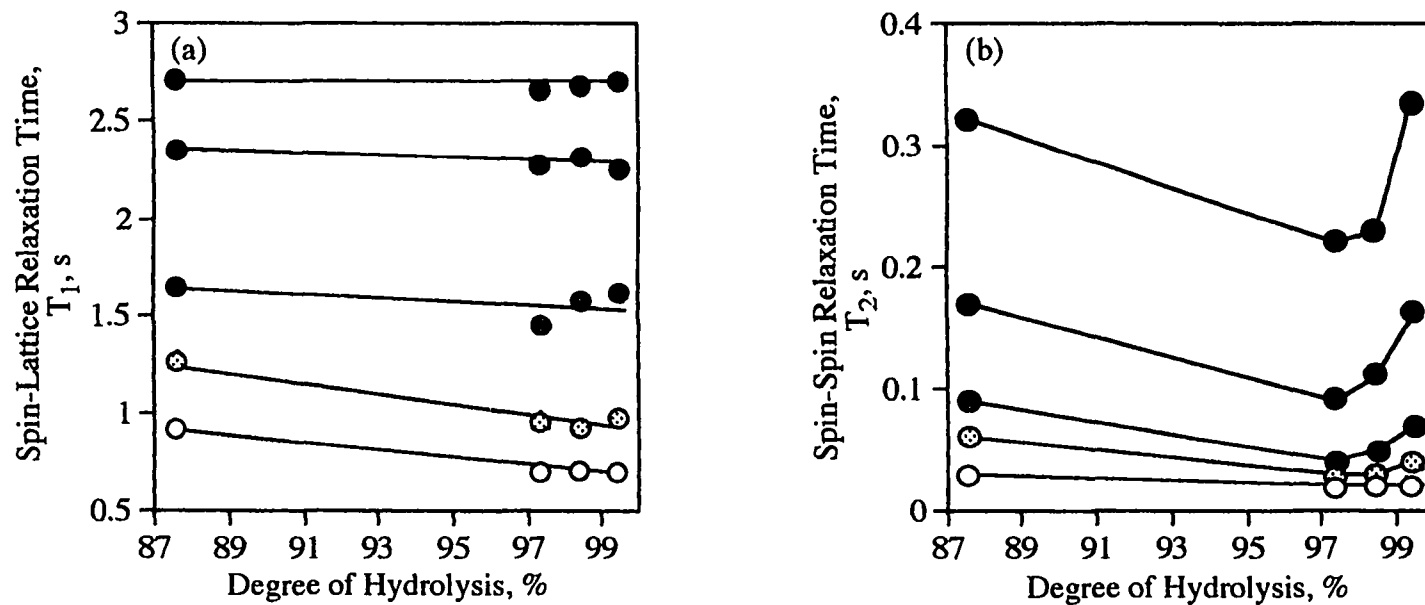




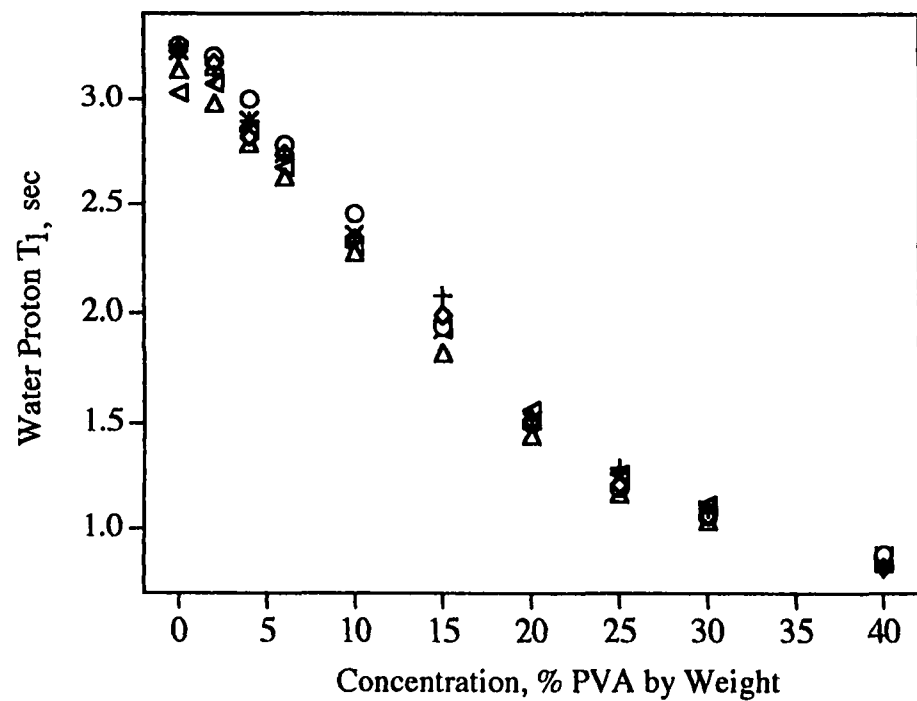
**Figure 8.** Water proton spin-lattice and spin-spin relaxation times as a function of concentration for PVA-A ( + ), PVA-B ( O ), PVA-C ( □ ) and PVA-D ( Δ ) stored at 23 °C for 24 hours.

Concentration, PVA by weight	Spin-lattice Relaxation Time, sec					
	1 Day	4 Day	10 Day	21 Day	36 Day	60 Day
0	3.03	3.08	3.03	3.01	3.02	3.03
2	3.02	3.02	3.03	2.98	3.02	3.01
4	2.89	2.82	3.00	2.79	2.90	2.85
6	2.73	2.74	2.79	2.63	2.74	2.68
10	2.34	2.34	2.45	2.28	2.36	2.30
15	2.08	1.99	1.94	1.82	1.93	1.93
20	1.52	1.51	1.50	1.45	1.52	1.56
25	1.29	1.21	1.19	1.16	1.25	1.26
30	1.10	1.06	1.06	1.04	1.09	1.11
40	0.81	0.82	0.88	0.84	0.87	0.86

**Table 9 .** Water proton spin-lattice relaxation times as a function of concentration for PVA-A stored at 23 °C. Error in the measurement is  $\pm 0.1$  s for one standard deviation.



**Figure 9.** Spin-spin (a) and spin-lattice (b) relaxation times as a function of the degree of hydrolysis of PVA at 5% (●), 10% (●), 20% (●), 30% (⊗) and 40% (○) samples stored at 23 °C for 1 day. The size of the circles represent the error in the measurements,  $\pm 0.1$  s for  $T_1$  and  $\pm 15$  ms for  $T_2$  measurements.



**Figure 10** . Spin-lattice relaxation times of water protons as a function of polymer concentration for PVA-A stored at 23 °C for 1 day (+), 4 days (◊), 10 days (O), 21 days (Δ), 36 days (X) and 60 days (◄).

## Quantification of Polymer-Bound Water Using Measurements of $T_2$ Relaxation

The number of water molecules per repeat unit of PVA was calculated according to the procedure outlined in the theory section. The number of bound water molecules per repeat unit is reported as an upper limit of bound water because the determination of the spin-spin relaxation time of the polymer bound water is not exact. For three different samples the reproducibility in the number of bound water molecules is  $\pm 0.5$  (1 standard deviation) for a series of four measurements.

The number of water molecules per repeat unit decreases with increasing concentration for PVA-A, PVA-B and PVA-C samples stored for 1 day at 23 °C (Table 10). The number of polymer bound water molecules per repeat unit of PVA-D is 2 and remains constant with increasing concentration in the samples stored for 1 day and 14 days. The average number of water molecules per repeat unit in PVA-A is 3, PVA-B is 4, PVA-C is 4 and PVA-D is 2 over the entire concentration range for samples stored at 23 °C for both 1 day and 14 days of storage.

The number of polymer bound water molecules per repeat unit of PVA is the lowest in PVA-D because it has the largest number of vinyl acetate groups that do not hydrogen bond with water. The large number of vinyl acetate groups ( $>12\%$ ) in PVA-D also disrupts inter- and intramolecular polymer-polymer hydrogen bonding, and hence decreases network formation. The number of polymer bound water molecules per repeat unit is low in PVA-A because polymer-polymer inter- and intramolecular hydrogen bonding is favored, therefore leaving fewer hydroxyl groups available for hydrogen bonding with water. Both circumstances result in the same net situation, in

Concentration, % PVA	1 Day of Storage at 23 °C				14 Day of Storage at 23 °C			
	PVA-A	PVA-B	PVA-C	PVA-D	PVA-A	PVA-B	PVA-C	PVA-D
5	4	5	5	2	3	5	5	2
10	3	4	4	2	3	4	4	2
15	3	4	4	2	3	4	4	2
20	3	4	3	2	3	4	4	2
30	3	4	4	2	3	4	4	2

**Table 10** . Calculated number of bound water per repeat unit of poly (vinyl alcohol) for samples stored at 23 °C for 1 day and 14 days.

PVA-A and PVA-D fewer water molecules bind.

The largest number of polymer bound water molecules per repeat unit of PVA is in the 5% samples where polymer-solvent interactions are favored due to minimal polymer entanglement. The number of polymer bound water molecules per repeat unit of PVA decreases with increasing concentration because at high polymer concentrations polymer-polymer interactions are favored which promote entanglement. The number of polymer bound water molecules per repeat unit does not change significantly between 1 day of storage and 14 days of storage for all samples.

Hatakeyema *et al.* quantified by DSC the amount of bound and free water in PVA covalently cross-linked with  $^{60}\text{C}$   $\gamma$ -ray irradiation.<sup>41</sup> From the enthalpy of melting, it was determined that three states of water exist in PVA gels: 1-1.5 molecules of non-freezing water bound water per hydroxyl group, 5-6 molecules of freezing associated water per hydroxyl group, and free bulk water. Hatakeyema *et al.* reported that the amount of bound water was independent of crosslink density, the amount of associated water leveled off at a crosslink density of  $2.0 \times 10^{-4}$  crosslinks/ $\text{cm}^3$ , and the amount of free water depended markedly on the crosslink density of the PVA. The range of polymer bound water molecules determined by NMR in this study, 2 to 5 water molecules per PVA repeat unit, is within the range of values calculated by DSC for a similar PVA system. This NMR method for the determination of bound water cannot discriminate between polymer bound and polymer associated water but estimates the sum of the water molecules in both populations.<sup>74-76</sup>

## Characterization of PVA Solutions and Gels by MT-NMR

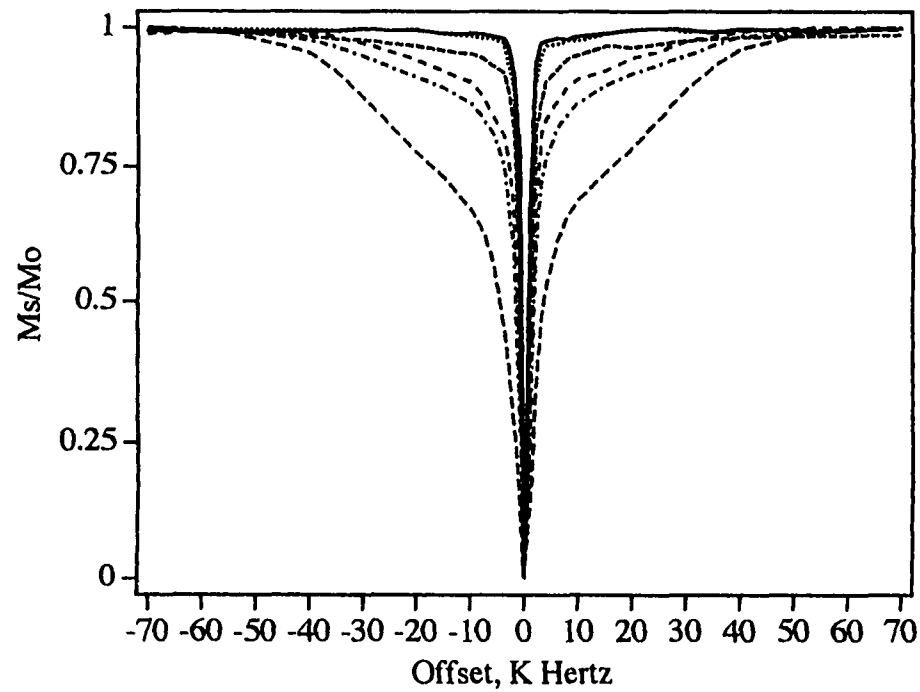
### Effect of Concentration and Degree of Hydrolysis on Network Formation

MT analysis was used to observe the influence of concentration on the degree of network formation in aqueous solutions of PVA. The MT profiles for sample PVA-A (99.5%) quenched and stored at 23 °C for 24 hours are shown in Figure 11. As concentration increases the area of the MT profiles increases dramatically. The MT profiles of 5% and 10% PVA samples are narrow, representative of samples with a single motional component characterized by relatively long spin-lattice ( $T_1$ ) and spin-spin ( $T_2$ ) relaxation times on the order of 2 s and 100-300 ms, respectively. At concentrations greater than 10%, the MT profiles are broad, indicating the existence of regions of restricted molecular motion characterized by relatively short values of  $T_1$  and  $T_2$  on the order of 1-1.5 s and 20-50 ms, respectively. It is likely that several  $T_2$  values characterize subdomains of varying mobility within the generally immobile portion of the sample.

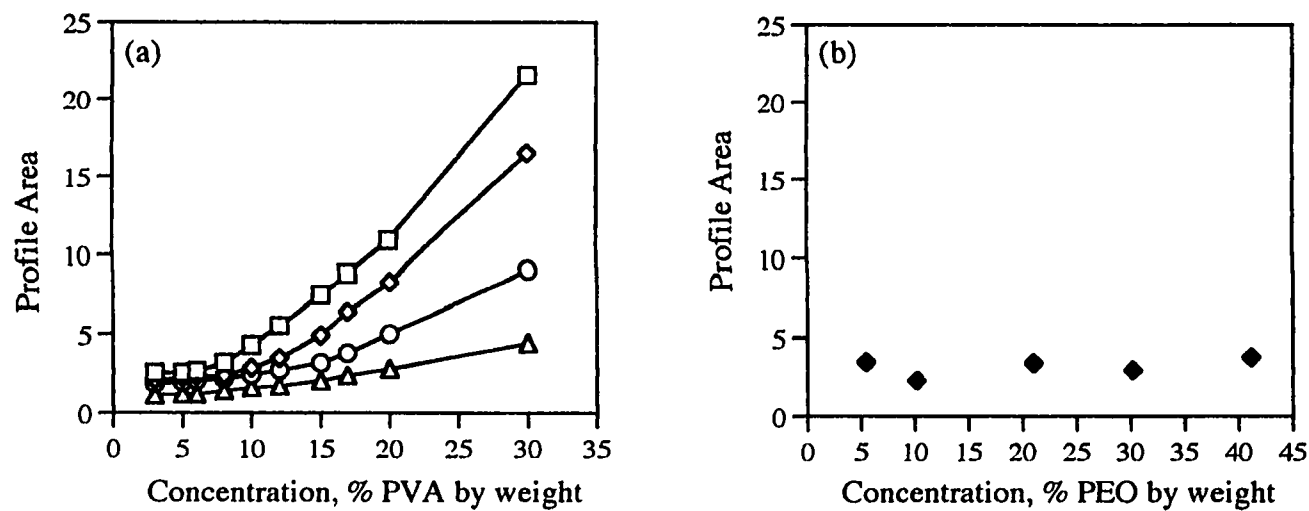
To a first approximation, the total area of the MT profile may be used as an index of chain immobilization.<sup>43</sup> The area of the profile increases nonlinearly with increasing polymer concentration for all PVA samples stored for 1 day at 23 °C (Figure 12a). The nonlinear increase in profile area indicates more extensive network formation at higher PVA concentrations. A greater deviation from linearity as the degree of hydrolysis increases is also evident in the data. This behavior suggests the emerging dominance of polymer-polymer hydrogen-bonding over polymer-solvent associations as the degree of hydrolysis increases and hence as the number of residual acetate groups on the polymer backbone decreases.



The magnification transfer profiles of PVAc-5 quenched and stored at 23 °C for 24 hours: 5% (-----), 10% (-----), 13% (-----), 17% (-----), 20% (-----) and 30% (-----).



**Figure 11** . The magnetization-transfer profiles of PVA-A quenched and stored at 23 °C for 24 hours: 5% (—), 10% (.....), 12% (-----), 17% (-----), 20% ( - · - · - ) and 30% (-----).

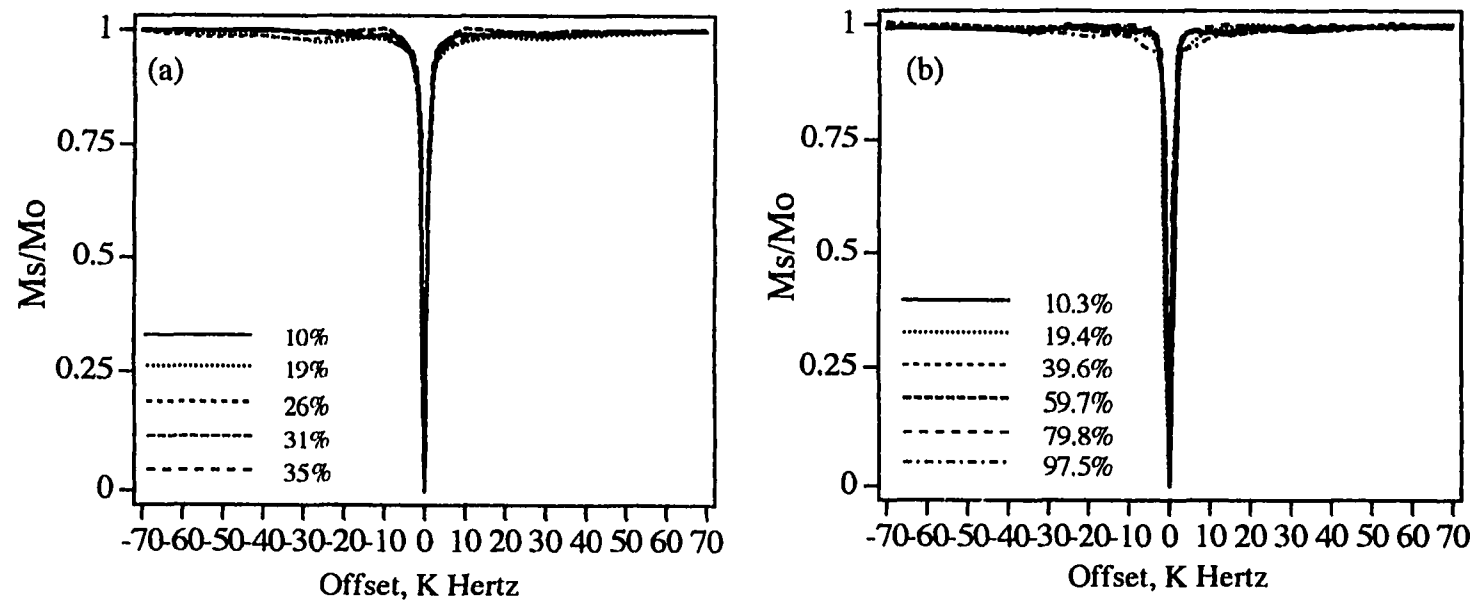


**Figure 12** . (a) Profile area measured as a function of PVA concentration for samples A (—□—), B (—◇—), C (—○—) and D (—△—) stored at 23 °C for 24 hours. (b) Profile area measured as a function of PEO concentration stored at 23 °C for 24 hours.

In polymer systems, changes in molecular mobility with increasing polymer concentration also result in increases in solution viscosity and gel viscoelasticity. To confirm that MT analysis is sensitive to network formation and not simply to solution viscosity, solutions of poly(ethylene oxide) (PEO), poly (acrylic acid) (PAA) and ethylene glycol were analyzed by MT analysis over a broad concentration range. PEO, a water soluble polymer that does not contain hydrophilic, pendent groups that allow for hydrogen bonding, were analyzed by MT analysis in the 5-40% concentration range. MT profiles of the PEO samples were fit to a single narrow Lorentzian function (full-width at half-maximum <2 KHz) and did not increase with increasing polymer concentration (Figure 12b). The MT profiles of the PEO solutions did not broaden as the viscosity increased (Table 11). MT analysis was also performed on solutions of PAA in the 11-35% concentration range and ethylene glycol in the 10-95% concentration range. The MT profile areas did not increase with increasing concentration indicating a lack of appreciable network formation in these samples (Figure 13). The MT profiles of PAA do not indicate network formation even at the highest concentration. PAA does not readily inter- and intramolecular hydrogen bond and therefore has no potential for network formation confirmed by narrow MT profiles. Ethylene glycol, which contains hydroxy groups that readily hydrogen bond, does not form a network due to the low molecular weight and nonpolymeric nature of the ethylene glycol molecule. The results for the PEO, PAA and ethylene glycol prove that MT analysis is sensitive to network formation and not simply an artifact of an increase in viscosity within the system. As a result, the change in profile area of the PVA solutions and gels may be ascribed with surety to chain immobilization.

PEO Concentration	MT Profile Area	Lorentzian FWHM	Viscosity, cps
5.4	3.5	1146.0	29.4
10.2	3.3	1168.0	157.1
21.0	3.4	1392.0	3224.2
30.2	3.7	1603.0	24240.0
41.2	3.5	1611.0	11780.0

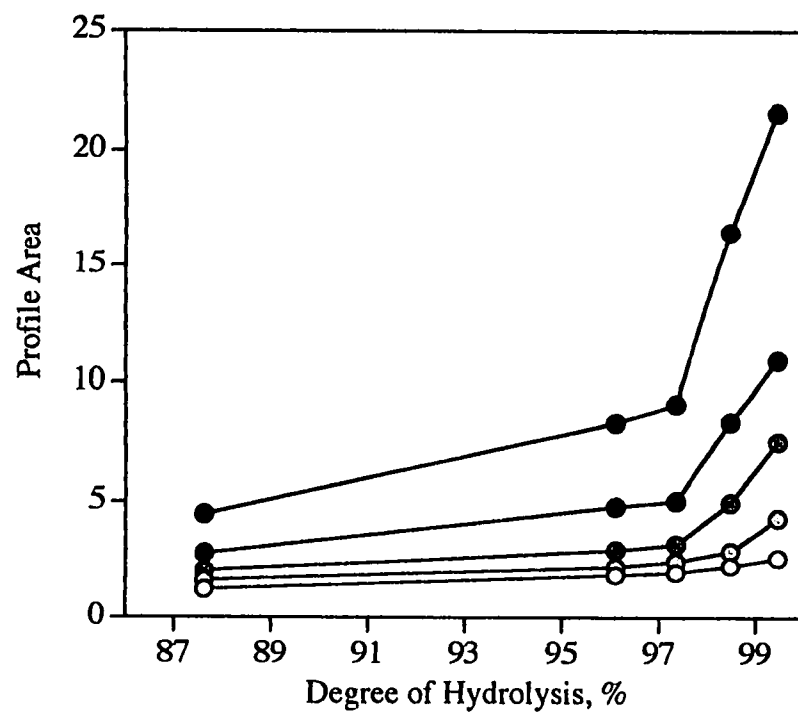
**Table 11.** Poly (ethylene oxide) magnetization-transfer profile area, Lorentzian full-width at half-maximum (FWHM: Hertz) and viscosity as a function of concentration for samples stored at 23 °C.



**Figure 13** . (a) Magnetization-transfer profiles of poly (acrylic acid) in the 10 - 35% concentration range and (b) ethylene glycol in the 10 - 97% concentration range. Samples were stored for 1 day at 23 °C.

The MT profiles of 5, 10, 15, 20 and 30% samples of PVA-A, B, C, and D were acquired after the samples were quenched and stored at 23 °C for 24 hours. The area of each profile was calculated and plotted as a function of degree of hydrolysis (Figure 14). The degree of network formation is negligible in 5% PVA samples stored for 1 day at all degrees of hydrolysis as indicated by narrow MT profiles. The onset of chain overlap and entanglement has been reported to occur in aqueous solutions of PVA with a degree of polymerization (dp) of 1700 and a concentration of polymer from 2-4% by weight as determined by dynamic light scattering.<sup>10-11</sup> It is highly likely that the degree of network formation in a 5% solution of PVA (dp 1250-1300) after only 1 day of storage, at any degree of hydrolysis, is below the critical concentration at which entanglement takes place. Of course, it is also possible that the degree of network formation in the 5% sample stored at 23 °C for one day is simply below the detection limits of MT analysis.

The differentiation between the four samples with different degrees of hydrolysis increases with increasing polymer concentration. In samples containing 20% and 30% PVA a significant change in profile area occurs for samples with degrees of hydrolysis between 97 and 99.5%, whereas the change between the 87 and 97% degree of hydrolysis samples is small. In the PVA-D sample, network formation is minimal at all concentrations indicated by relatively low MT profile areas. The PVA-D sample contains 12.4% vinyl acetate which apparently corresponds to enough bulky, hydrophobic acetate groups to disrupt polymer-polymer inter- and intrachain hydrogen-bonds and favor polymer-solvent interactions. A small increase in profile area occurs in the samples over the degree of hydrolysis range from 87 to 97%, while large changes in profile area occur between samples in the 97 to 99.5% hydrolysis range. Small changes in the degree of hydrolysis above 97% significantly affect the extent of



**Figure 14** . Profile area measured as a function of degree of hydrolysis for 5% ( —○—), 10% ( —○●—), 15% ( —●●—), 20% ( —●—) and 30% ( —●—) samples of PVA stored at 23 °C for 1 day

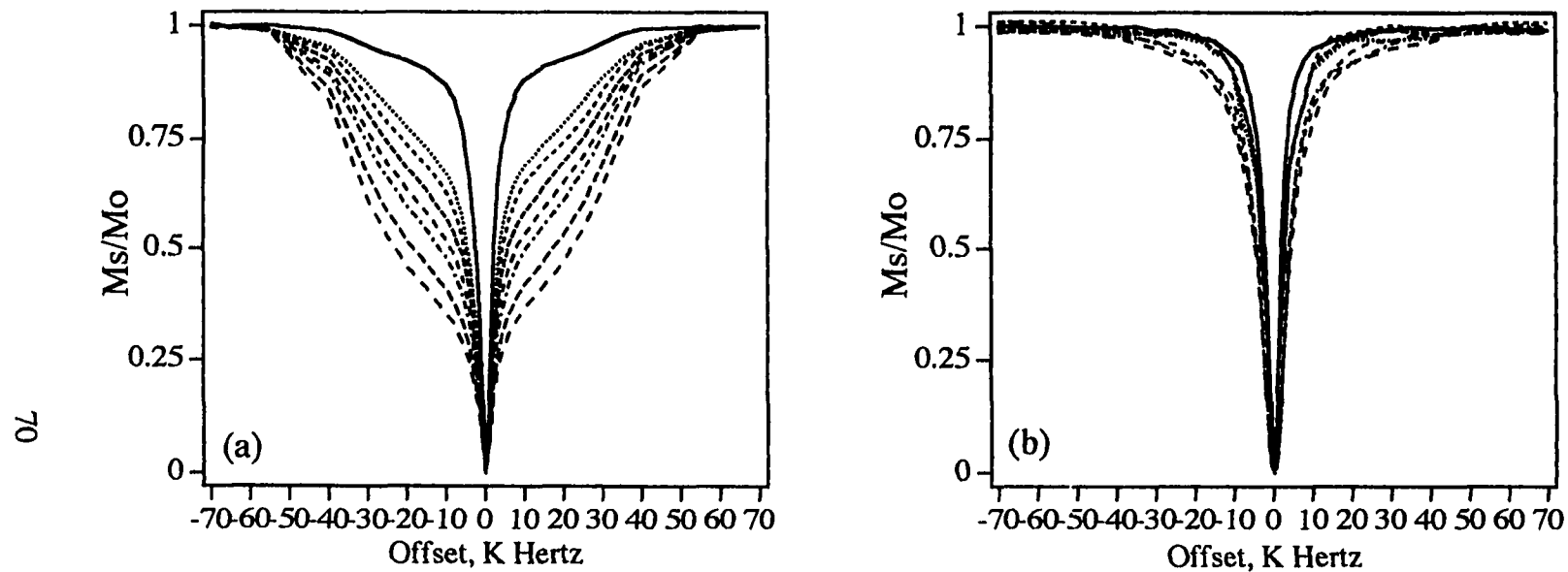


network formation. In the PVA-A, PVA-B and PVA-C samples containing 0.5%, 1.5% and 2.7% vinyl acetate, respectively, polymer-polymer hydrogen bonding dominates. As a result, a critical concentration of acetate necessary to disrupt polymer-polymer hydrogen bonding is approximately 3%.

These results are consistent with the number of polymer associated water molecules determined by spin-spin relaxation. PVA-A and PVA-D are the extreme cases. The large number of hydroxyl groups in PVA-A inter- and intramolecular hydrogen bond promoting a network that decreases the number of polymer associated water molecules. In PVA-D, the lower number of hydrophilic hydroxyl groups reduces the number of polymer associated water molecules while the significant amount of vinyl acetate (12.4%) disrupts hydrogen bonding, reducing network formation and crystallization. The highest number of polymer bound water molecules occurred in PVA-C (2.7% vinyl acetate) where the number of hydrophilic groups is high while the amount of vinyl acetate is sufficient promoting a loosely entangled network that allows for the entrapment of water.

## Ageing of Poly (vinyl alcohol) Solutions and Gels

For aqueous PVA gels, the development of a physically entangled network proceeds over many weeks in a process that can be monitored by observing changes in the MT profiles as the gels age. Based on the results presented herein, network formation is characterized by an increase in the area of the MT profile with time. Figure 15 shows profiles for 30% PVA-A (15a) and 30% PVA-D (15b) as the samples age at 23 °C over 18 weeks. The MT profile of PVA-A broadens and its area increases



**Figure 15.** MT profiles of: (a) 30% PVA-A and (b) 30% PVA-D stored at 23 °C for: 15min (————), 1 Day (······), 3 Day (-----), 8 Day (-----), 14 Day (-----), 21 Day (-----), 49 Day (-----) and 126 Day (-----).

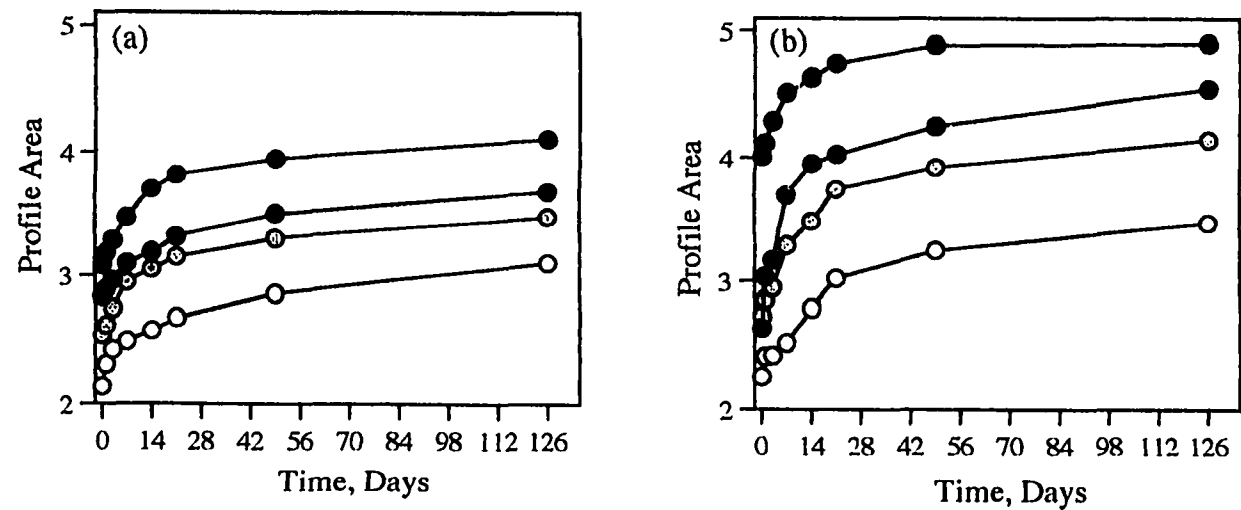
significantly with storage time. After only one day of storage the breadth of the profile indicates considerable chain immobilization, which continues to increase over time. In contrast, the MT profile of PVA-D does not broaden or increase greatly in area over the entire storage period, indicating negligible network formation as the sample ages. PVA-A with 0.5% residual acetate groups experiences more extensive polymer-polymer inter- and intrachain hydrogen bonding and hence network formation. PVA-D, with 12.4% residual acetate, is more likely to participate in polymer-solvent hydrogen bonding and is therefore not expected to form an extensive network.

The MT profiles of 5% PVA samples with varying degrees of hydrolysis were monitored as a function of storage time at 23 °C and 5 °C. The MT profile areas were calculated (Table 12) and plotted as a function of storage time (Figure 16). The evolution of network formation in 10% PVA samples with varying degrees of hydrolysis was monitored as a function of storage time at 23 °C and 5 °C. The MT profile areas were calculated (Table 13) and plotted as a function of storage time (Figure 17). The 10% PVA samples have only slightly larger profile areas than the 5% samples stored under the same storage conditions. From the data it is evident that the samples that were quenched and stored at 5 °C have large profile areas and hence more network formation than similar samples quenched and stored at 23 °C. In all 5 and 10% PVA samples, the degree of network formation increases with increasing degree of hydrolysis and decreasing storage temperature.

The evolution of network formation in 20% PVA samples with varying degrees of hydrolysis was monitored as a function of storage time at 23 °C and 5 °C (Table 14 and Figure 18). The initial profile areas of samples quenched and stored at 5 °C are larger for all samples of a given degree of hydrolysis than those quenched and stored at 23 °C.

Time, Days	23 °C				5 °C			
	PVA-A	PVA-B	PVA-C	PVA-D	PVA-A	PVA-B	PVA-C	PVA-D
0	3.1	2.8	2.0	1.3	4.0	2.6	2.7	2.3
1	3.2	2.9	2.1	1.5	4.1	3.0	2.9	2.4
3	3.3	3.0	2.2	2.0	4.3	3.2	2.9	2.4
7	3.5	3.1	2.4	2.2	4.5	3.7	3.3	2.5
14	3.7	3.2	2.5	2.3	4.6	3.9	3.5	2.8
21	3.8	3.3	2.6	2.4	4.7	4.0	3.7	3.0
49	3.9	3.5	2.8	2.7	4.9	4.3	3.9	3.2
126	4.1	3.7	2.9	2.7	4.9	4.5	4.1	3.5

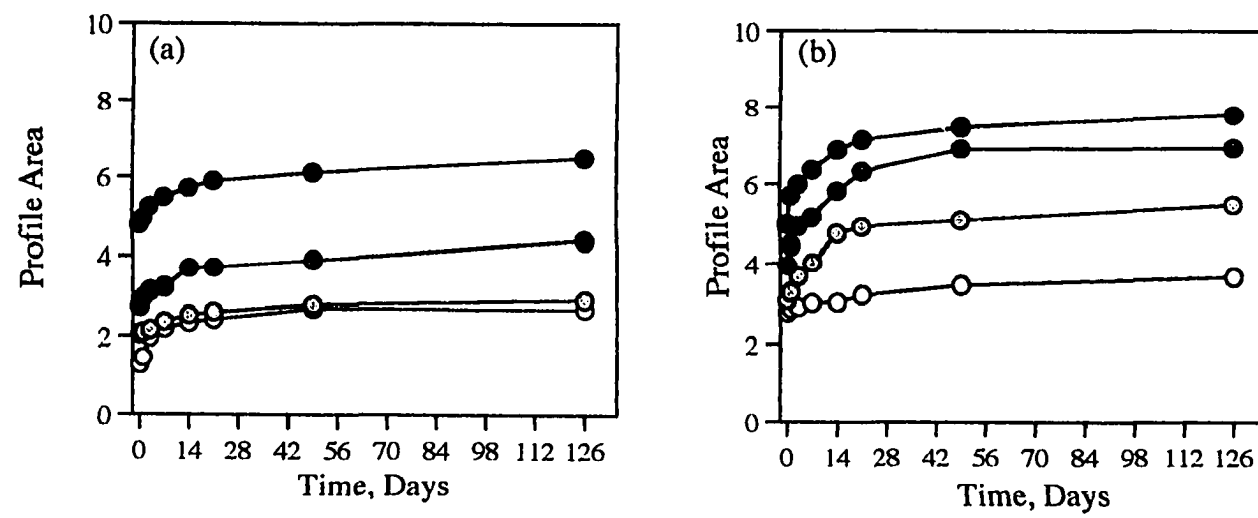
**Table 12 .** Area of the magnetization-transfer profiles for 5% samples of PVA-A, B, C and D stored at 23 °C and 5 °C as a function of storage time. Error in the measurements is  $\pm 0.2$



**Figure 16.** Area of the magnetization-transfer profile as a function of storage time at (a) 23 °C and (b) 5 °C for 5% PVA-A ( —●— ), PVA-B ( —●— ), PVA-C ( —○— ) and PVA-D ( —○— ).

Time, Days	23 °C				5°C			
	PVA-A	PVA-B	PVA-C	PVA-D	PVA-A	PVA-B	PVA-C	PVA-D
0	4.8	2.7	2.5	2.1	5.0	3.9	3.1	2.8
1	4.9	3.0	2.6	2.3	5.7	4.4	3.3	2.9
3	5.2	3.1	2.7	2.4	6.0	4.9	3.7	2.9
7	5.5	3.2	2.9	2.5	6.4	5.1	4.0	3.0
14	5.7	3.7	3.0	2.6	6.9	5.8	4.7	3.0
21	5.9	3.7	3.1	2.7	7.1	6.3	4.9	3.2
49	6.1	3.9	3.3	2.9	7.5	6.9	5.1	3.5
126	6.5	4.4	3.5	3.1	7.8	6.9	5.5	3.7

**Table 13** . Area of the magnetization-transfer profiles for 10% PVA-A, B, C and D stored at 23 °C and 5 °C as a function of storage time. Error in the measurements is  $\pm 0.2$ .

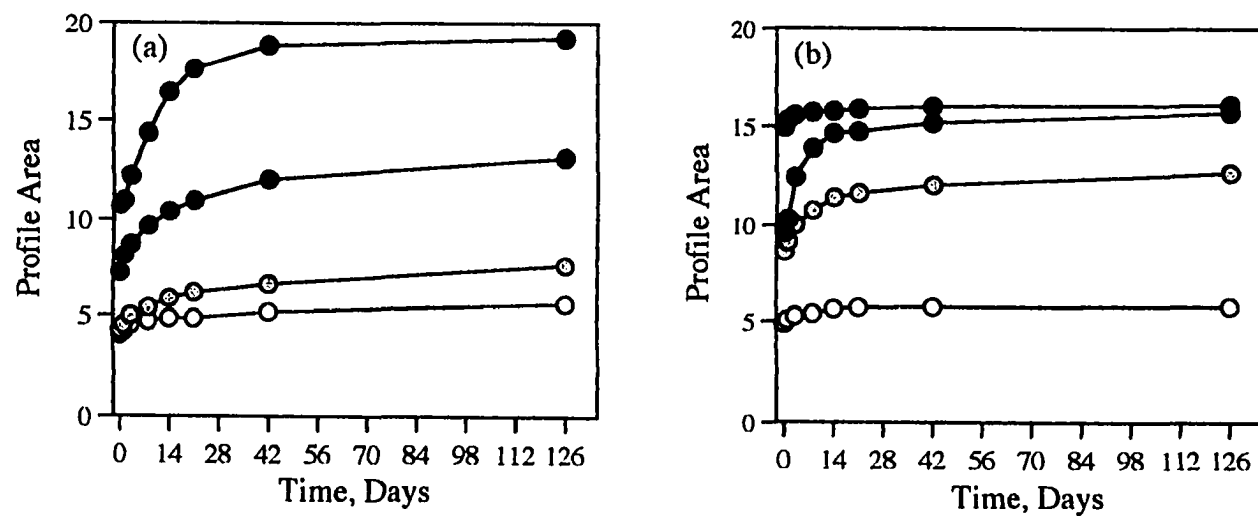


**Figure 17 .** Magnetization-transfer profile area as a function of storage time at (a) 23 °C and (b) 5°C for 10% PVA-A (—●—), PVA-B (—●—), PVA-C (—○—) and PVA-D (—○—).

Time, Days	23 °C				5 °C			
	PVA-A	PVA-B	PVA-C	PVA-D	PVA-A	PVA-B	PVA-C	PVA-D
0	10.7	7.2	4.2	4.0	15.0	9.6	8.6	4.9
1	11.0	8.1	4.5	4.2	15.3	10.3	9.1	5.1
3	12.2	8.7	5.0	4.5	15.6	12.4	10.0	5.3
8	14.4	9.7	5.4	4.7	15.7	13.9	10.8	5.4
14	16.4	10.4	5.9	4.8	15.7	14.6	11.4	5.6
21	17.6	10.9	6.2	4.8	15.9	14.7	11.7	5.7
42	18.9	12.0	6.6	5.1	16.0	15.2	12.1	5.7
126	19.2	13.1	7.6	5.6	16.1	15.7	12.0	5.8

**Table 14 .** Area of the magnetization-transfer profiles for 20% samples of PVA-A, B, C and D stored at 23 °C and 5 °C as a function of storage time. Error in the measurement is  $\pm 0.2$ .





**Figure 18.** Magnetization-transfer profile area as a function of storage time at (a) 23 °C and (b) 5 °C for 20% PVA-A (—●—), PVA-B (—●—), PVA-C (—⊙—) and PVA-D (—○—).

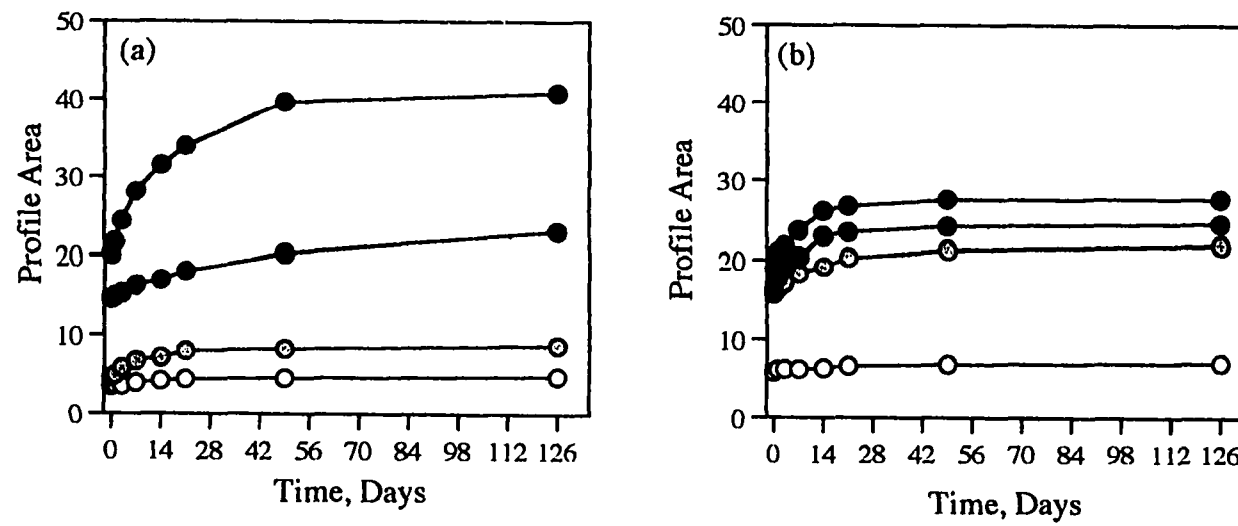
This appears to be a direct consequence of the fast quench from the dissolution temperature of 96 °C to the storage temperature of 5 °C. In all samples quenched and stored at 5 °C, the quench appears to promote network formation which results in extensive chain immobilization indicated by broad initial MT profiles.

The evolution of network formation in 30% PVA samples with varying degrees of hydrolysis was monitored as a function of storage time at 23 °C and 5 °C (Table 15 and Figure 19). At 23 °C, PVA-A has a larger initial profile area than PVA-A stored at 5 °C. The 5 °C quench appears to significantly hinder initial network formation. The PVA-B, C and D stored at 5 °C have larger initial profile areas than at 23 °C. In the 30% PVA-B and PVA-C samples, the 5 °C quench promotes network formation as it has in all other samples. The profile areas of PVA-C stored at 5 °C are significantly larger over the entire storage period than the profile areas of PVA-C stored at 23 °C. The initial profile areas of PVA-D stored at 5 °C are only marginally larger than the profile areas of PVA-D stored at 23 °C. The 5 °C quench and storage temperature does not have a significant effect on network formation in any of the PVA-D samples.

Over the entire 18 week storage period, all 5 and 10% samples show an increase in profile area indicating measurable network formation. In all cases the 5 and 10% samples stored at 5 °C show more network formation than the corresponding samples stored at 23 °C. Even at low concentrations where chain entanglement is minimal, the relatively low degree of network formation is detectable by MT analysis. At these low concentrations, the 5 °C quench and storage temperature enhances measurable network formation.

Time, Days	23 °C				5 °C			
	PVA-A	PVA-B	PVA-C	PVA-D	PVA-A	PVA-B	PVA-C	PVA-D
0	20.2	14.6	4.7	3.5	18.9	16.1	15.8	5.9
1	21.6	14.9	5.0	3.6	20.9	17.7	16.4	6.2
3	24.3	15.3	5.9	3.6	21.6	19.0	17.1	6.3
7	28.0	16.3	6.8	4.0	23.6	20.4	18.3	6.3
14	31.5	17.0	7.2	4.3	26.1	22.9	19.2	6.4
21	34.0	18.1	8.0	4.5	26.7	23.4	20.3	6.7
49	39.6	20.3	8.3	4.6	27.5	24.1	21.3	6.9
126	40.9	23.0	8.8	4.9	27.6	24.5	21.9	7.1

**Table 15** . Area of the magnetization-transfer profiles for 30% samples of PVA-A, B, C and D stored at 23 °C and 5 °C as a function of storage time. Error in the measurements is  $\pm 0.2$ .



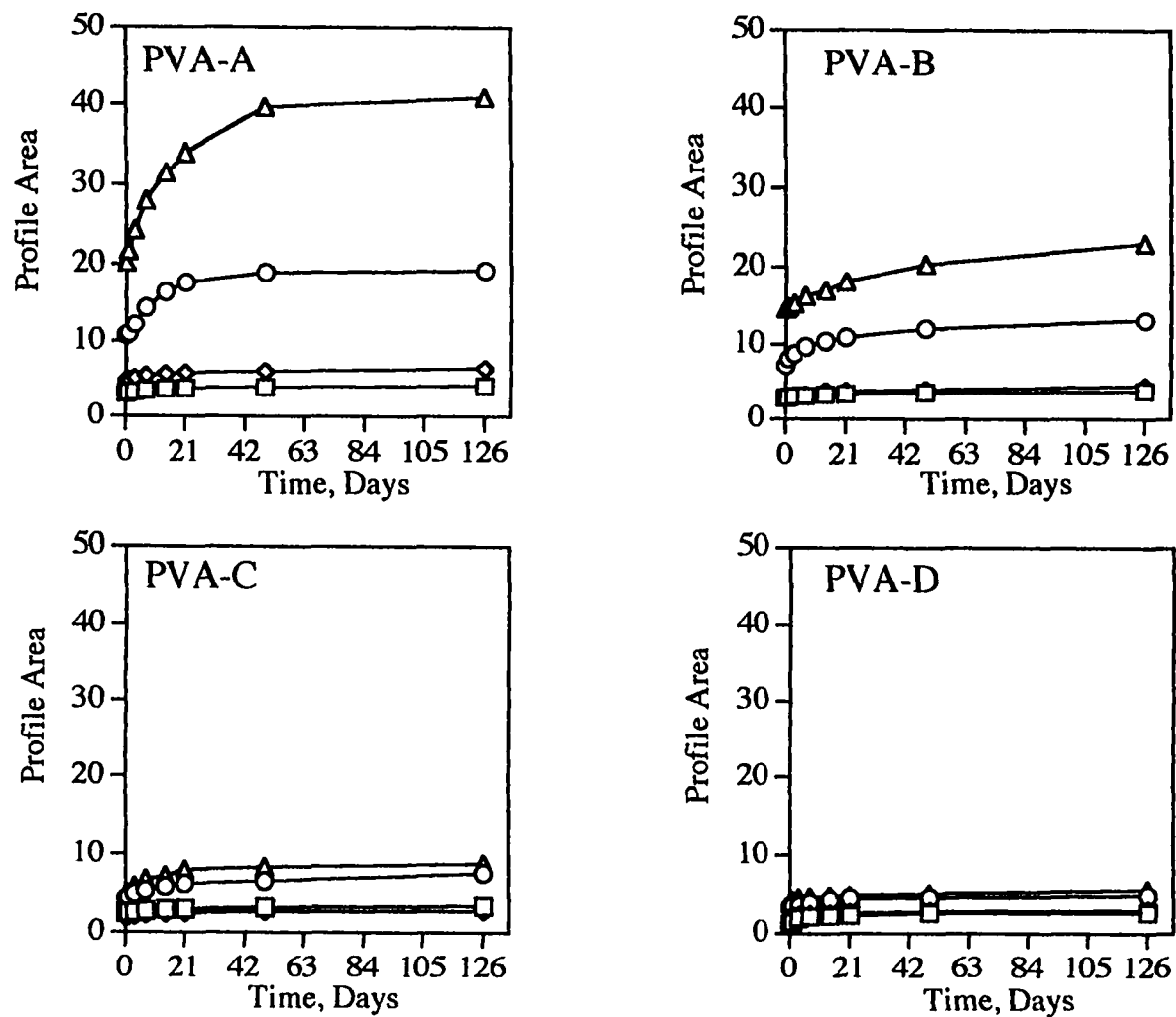
**Figure 19.** MT profile area as a function of storage time at (a) 23 °C and (b) 5°C for 30% PVA-A (—●—), PVA-B (—●—), PVA-C (—○—) and PVA-D (—○—).

The progression of network formation over 18 weeks in 20% PVA-A stored at 5 °C is significantly hindered by the low quench and storage temperature relative to the corresponding sample stored at 23 °C (Figure 18). In contrast, 20% PVA-B and PVA-C samples develop a more extensive network over time at 5 °C than at 23 °C. The 5 °C quench seems to hinder the progression of network formation in PVA-A but promotes network formation in PVA-B and especially promotes network formation in PVA-C.

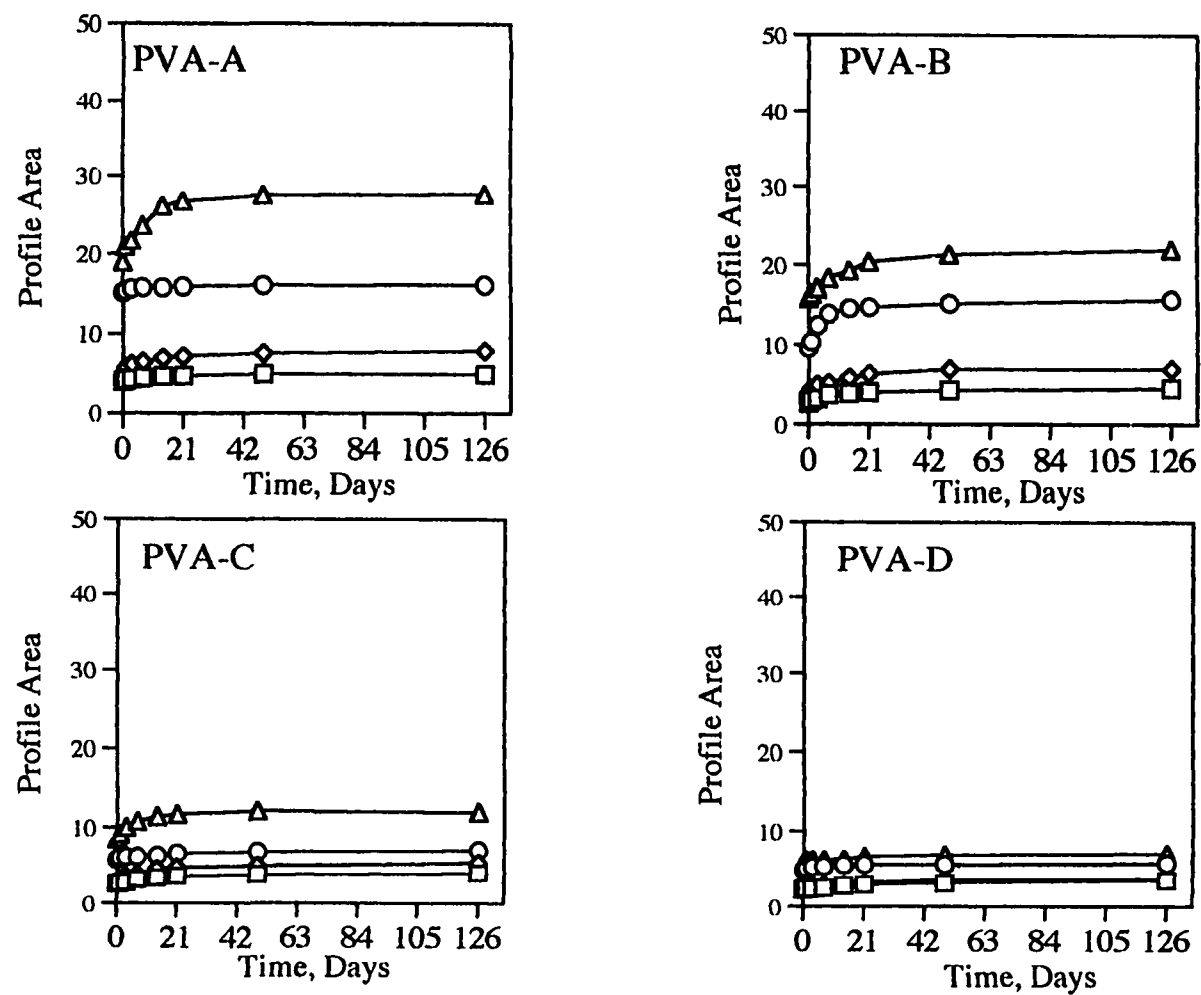
All initial profile area for the 30% PVA samples are considerably larger than the corresponding 20% PVA samples, and after 18 weeks of ageing all 30% samples except PVA-D have considerably larger profile areas. In general, the 30% PVA samples stored at 23 °C and 5 °C follow the same trend as the 20% PVA samples regarding increasing profile area with storage time.

The profile areas of all samples are plotted as a function of storage time at 23 °C (Figure 20) and at 5 °C (Figure 21) for each PVA sample over the 5 to 30% concentration range. These figures are useful for putting the degree of network formation over the range of degree of hydrolysis and concentration into perspective. The degree of network formation in PVA-C and PVA-D is considerably less than the degree of network formation in the PVA-A and PVA-B samples.

In general, network formation increases with the age of the sample as indicated by an increase in profile area with time. Network formation is most pronounced in the samples with the highest degree of hydrolysis at all concentrations at both storage temperatures. Network formation in PVA-D is small, but measurable, relative to the samples with the higher degree of hydrolysis. Quench and storage temperature has an



**Figure 20** . Area of the magnetization-transfer profile as a function of storage time at 23 °C for 30% ( —□— ), 20% ( —◇— ), 10% ( —○— ) and 5% ( —△— ) for PVA-A, B, C and D.



**Figure 21** . Area of the magnetization-transfer profile as a function of storage time at 5 °C for 30% ( —△— ), 20% ( —○— ), 10% ( —◇— ) and 5% ( —□— ) for PVA-A, B, C and D.

effect on network formation even at low concentrations and even to a small degree in PVA-D. The effect of the quench and storage temperature is not entirely systematic for samples at the higher concentrations (20-30%) and does not follow a consistent trend with degree of hydrolysis. The low quench and storage temperature has a network enhancing effect on PVA-B and, to a large degree, on PVA-C in the 20 and 30% samples. The low quench and storage temperature seems to hinder the progression of network formation in 20 and 30% PVA-A samples, whereas for the low temperature quench promotes network formation the low concentration samples (5 and 10%). An explanation for these observations may lie in the fact that as polymer concentration increases, the dynamics of the system become more complex.

In the 20% samples, the differences in the degree of network formation resulting from the differences in storage temperature is directly related to the degree of polymer-polymer self interaction. At 5 °C, the smaller change in profile area of 20% PVA-A over time reflects the diminished molecular mobility resulting from a tightly entangled network promoted by polymer-polymer self interaction.<sup>77-78</sup> At 5 °C, the polymer chains in PVA-B and PVA-C are still mobile enough to continue to form extensive network over time. The PVA-B and PVA-C samples have a lower affinity for polymer-polymer interaction than PVA-A and loosely entangled network forms in the PVA-B and PVA-C samples that further tightens with time. The sample with the highest affinity for polymer-polymer self interaction, in this case PVA-A, may illustrate the limiting value of network development for all 20% PVA samples at a given temperature.

The overall trend in network formation with increasing age of the sample and degree of hydrolysis is similar for 20% and 30% samples. A closer comparison of the data for



the 20% samples (Figure 18) and the 30% samples (Figure 19) reveals subtle differences between the data sets. Consideration of the glass transition allows us to interpret the 20% data. The 30% samples, however, behave differently indicating that other processes must be occurring in the system that effect the overall rigidity of the sample.

Indeed, the turbidity of the samples may provide a clue to the other processes occurring in the samples as concentration increases. The 30% samples stored at 23 °C become visually turbid over the 18 week storage period, while the analogous 20% samples remain visually transparent over the 18 week storage period. The 30% samples stored at 5 °C also become slightly turbid over the 18 week storage period, while the analogous 20% samples remain visually transparent over the 18 week storage period. The difference in turbidity between the 20% and 30% samples is due to differences in the size of aggregates, where smaller aggregates are formed at the lower concentration. Phase separation is occurring in the 30% samples, and the attendant formation of large regions of crystalline or amorphous polymer accompanied by the extrusion of water may be the dominant dynamic process going on in the system.

The turbidity of the 20% (Table 16) and 30% (Table 17) samples stored at 23 °C and 5 °C was measured as a function of time at 520 nm. The measured turbidity of the 30% samples stored at 23 °C increases with degree of hydrolysis. The measured turbidity is greater in the set of 30% samples stored at 5 °C than in the set of 30% samples stored at 23 °C. As the samples age, the turbidity significantly increases in the samples stored at 23 °C, eventually becoming marginally greater than the turbidity of the samples stored at 5 °C. This may indicate that the initial turbidity in the 5 °C sample is due to aggregates or crystallites and the significant increase in turbidity in the samples

Ageing Time, Days	23 °C				5 °C			
	PVA-A	PVA-B	PVA-C	PVA-D	PVA-A	PVA-B	PVA-C	PVA-D
15 min	0.020	0.018	0.016	0.010	0.051	0.046	0.041	0.030
1 hr	0.041	0.020	0.015	0.010	0.051	0.049	0.041	0.030
17 hr	0.060	0.041	0.030	0.020	0.083	0.072	0.052	0.039
2 d	0.062	0.041	0.030	0.020	0.083	0.078	0.064	0.051
5 d	0.062	0.041	0.030	0.020	0.083	0.078	0.068	0.051
9 d	0.062	0.041	0.030	0.020	0.083	0.079	0.069	0.051
18 d	0.062	0.041	0.030	0.020	0.083	0.079	0.069	0.051
47 d	0.062	0.041	0.030	0.020	0.083	0.079	0.069	0.051
126 d	0.062	0.041	0.030	0.020	0.083	0.080	0.069	0.051

**Table 16 .** The measured turbidity as a function of ageing time at 520 nm for 20% PVA samples stored at 23 °C and 5 °C.

Ageing Time, Days	23 °C				5°C			
	PVA-A	PVA-B	PVA-C	PVA-D	PVA-A	PVA-B	PVA-C	PVA-D
15 min	0.186	0.116	0.083	0.020	0.211	0.127	0.051	0.024
1 hr	0.198	0.174	0.105	0.025	0.223	0.133	0.056	0.029
17 hr	0.236	0.223	0.111	0.030	0.236	0.139	0.062	0.030
2 d	0.274	0.261	0.128	0.030	0.301	0.162	0.068	0.030
5 d	0.328	0.301	0.151	0.034	0.357	0.168	0.068	0.030
9 d	0.386	0.328	0.174	0.034	0.360	0.169	0.068	0.030
18 d	0.523	0.357	0.174	0.034	0.368	0.169	0.068	0.030
47 d	0.733	0.358	0.186	0.034	0.370	0.169	0.068	0.030
126 d	0.994	0.478	0.186	0.034	0.370	0.169	0.068	0.030

**Table 17** . The measured turbidity as a function of ageing time at 520 nm for 30% PVA samples stored at 23 °C and 5 °C.

stored at 23 °C is due to phase separation. The occurrence of phase separation in the 30% samples may be the major contributing factor to the overall rigidity detected by MT analysis, which complicates the process of network formation.

Turbidity measurements show that the increase in turbidity in the 20% PVA is negligible over the entire 18 weeks of storage at either temperature (Figure 16). The 20% PVA-A samples stored at 5 °C are slightly more turbid, however, than the corresponding samples stored at 23 °C. Since the turbidity is extremely slight in PVA-A stored at 5 °C (not detectable by the naked eye), the samples stored at 5 °C may have crystallites with a size on the same order of the wavelength of light used to measure the turbidity (520 nm). The presence of ordered structure or crystallites in the 20% PVA-A sample stored at 5 °C may be the reason for the reduced degree of network formation in this sample relative to the sample quenched and stored at 23 °C.

In the 20% samples gelation occurs without considerable phase separation. The presence of measurable but not visually detectable turbidity indicates the existence of ordered structure without the occurrence of macroscopic phase separation.<sup>26,79-80</sup> In contrast, visually perceptible phase separation occurs in the 30% samples and dominates the dynamic processes occurring in the gel. The processes that control the rigidity of the gels change as a function of concentration, with phase separation as the ultimate process causing the transition from homogeneous gel to heterogeneous mixture dominating the system at high polymer concentration.

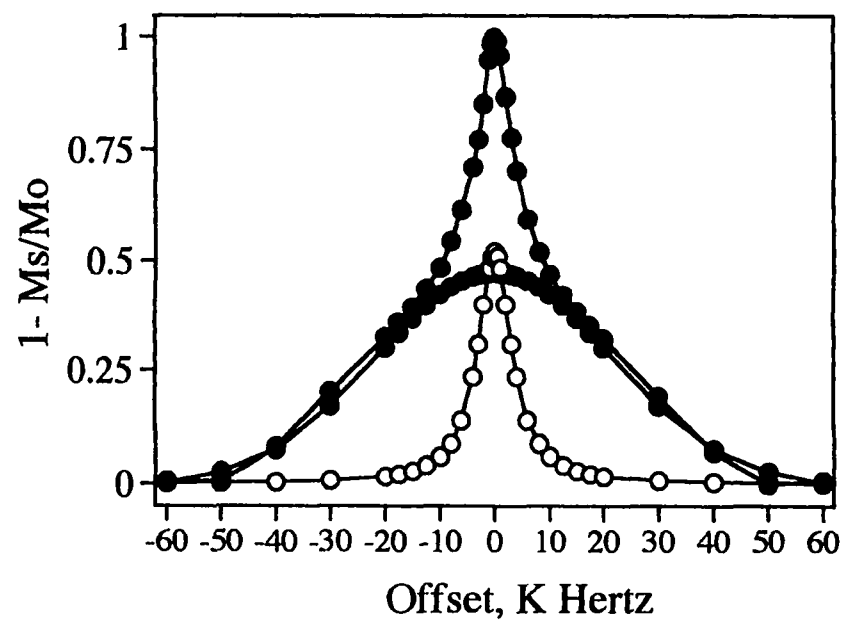
These observations of turbidity suggest that the ageing process in the 20% and 30% samples is complex. In effect, phase separation in the 30% samples determines the rigidity of the samples and dominates. As concentration increases, the dominant

process that contributes to the rigidity of the gel changes. At 20%, gelation occurs as a result of network formation without considerable phase separation. At 30%, phase separation is the dominate mechanism that contributes to the overall rigidity of the sample.

## Multi-component Nature of Magnetization-Transfer Profiles

Insight into the effect of degree of hydrolysis and temperature on network formation may be gained by evaluating the multicomponent nature of the MT profiles.<sup>43-44</sup> In general, the spectral line-shape of a sample with a single motional component with a characteristic transverse relaxation time can be described by a Lorentzian function.<sup>23-25</sup> The MT profiles of aged PVA samples, however, cannot be described by a single Lorentzian function; they contain an additional component with a short transverse relaxation time due to immobilized polymer. These complex MT profiles were fit to a function which is the sum of a narrow Lorentzian component and a broad Gaussian component (Figure 22). The mobile component is the portion of the system containing both polymer and water that gives rise to the Lorentzian line shape, while the immobile component is the portion of the system containing both polymer and water with collective restricted motion that gives rise to a Gaussian line shape.

The MT profiles of 20% samples of PVA-A, B and C stored at 23 °C (Table 18) and 5 °C (Table 19) were fit to the sum of a broad Gaussian component and a narrow Lorentzian component as the samples aged over 18 weeks. Curve fitting analysis reveals information regarding the balance between the polymer-rich and solution-rich portions of the sample as it ages. Upon dissolution the freely moving chains become



**Figure 22** . Curve fitting analysis of the magnetization-transfer profile for 30% sample of PVA-A stored for 24 hours at 23 °C. Actual profile area (—●—), Lorentzian (—○—), and Gaussian curve (—●—).

Storage Time, Days	PVA-A				PVA-B				PVA-C			
	Profile Area	Gaussian Area	Lorentzian Area	% Gaussian	Profile Area	Gaussian Area	Lorentzian Area	% Gaussian	Profile Area	Gaussian Area	Lorentzian Area	% Gaussian
0	10.7	5.5	5.2	51.4	7.2	1.3	5.9	18.1	4.2		4.2	
1	11.0	6.8	4.2	61.8	8.1	3.7	4.4	45.7	4.5		4.5	
3	12.2	8.6	3.6	70.5	8.7	4.8	3.9	55.2	5.0	1.1	3.9	22.0
7	14.9	10.9	4.0	73.2	9.7	7.1	2.6	73.2	5.4	1.3	4.1	24.1
14	16.4	12.8	3.6	78.0	10.4	7.7	2.7	74.0	5.9	1.4	4.5	23.7
21	17.6	14.1	3.5	80.1	10.9	7.9	3.0	72.5	6.2	1.6	4.6	25.8
42	18.9	15.7	3.2	83.1	12.0	8.6	3.4	71.7	6.6	1.8	4.8	27.3
126	20.0	16.3	3.7	81.5	13.1	9.5	3.6	72.5	7.6	1.9	5.5	25.0

**Table 18 .** Line shape analysis of 20% PVA-A, PVA-B and PVA-C stored at 23 °C over 18 weeks.

Storage Time, Days	PVA-A				PVA-B				PVA-C			
	Profile Area	Gaussian Area	Lorentzian Area	% Gaussian	Profile Area	Gaussian Area	Lorentzian Area	% Gaussian	Profile Area	Gaussian Area	Lorentzian Area	% Gaussian
0	15.0	10.5	4.5	70.0	9.6	4.8	4.6	47.9	8.6	3.9	4.7	45.3
1	15.3	11.2	4.1	73.2	10.3	5.0	5.1	49.5	9.1	4.5	4.2	50.0
3	15.6	11.5	4.1	73.7	12.4	7.9	4.6	63.7	10.0	5.1	4.4	50.8
7	15.7	11.7	4.0	74.5	13.9	10.7	3.9	77.0	10.8	5.5	5.1	51.0
14	15.7	11.8	3.9	75.2	14.6	10.8	3.8	74.0	11.4	5.9	5.5	51.7
21	15.9	12.0	3.9	75.5	14.7	11.0	3.7	74.8	11.7	6.2	5.7	52.8
42	16.0	12.1	3.9	75.6	15.2	11.4	3.8	75.0	12.1	6.5	6.0	53.8
126	16.1	12.2	3.9	75.8	15.7	11.6	4.1	73.9	12.0	6.6	5.9	55.0

**Table 19** . Line shape analysis of 20% PVA-A, PVA-B and PVA-C stored at 5 °C over 18 weeks.



increasingly entangled and ultimately form an immobile network as the system ages. This decrease in the mobility of polymer chains is indicated by the growth of the Gaussian area. Evaluation of the areas of the Lorentzian and Gaussian components as a function of storage time furnishes information concerning changes in each component in the gel as it ages.

The total profile and Gaussian areas of 20% samples of PVA-A, PVA-B and PVA-C increase with the age of the sample. The total profile and Gaussian areas are largest for the sample with the highest degree of hydrolysis. The initial MT profile of the 20% PVA-A sample stored at 23 °C is 51% Gaussian. This sample is a gel according to the definition of a gel according to Komatsu; the meniscus of the sample, when tilted at a 90° angle, does not deform.<sup>59</sup>

The MT profile of a 20% PVA-B sample stored at 23°C is initially only 18% Gaussian (Table 18). When tilted, the meniscus of this 20% PVA-B sample deforms; therefore, the sample is a solution. When stored for 18 weeks at 23 °C, the MT profile of the 20% PVA-B sample is 72% Gaussian and the material is a gel; the meniscus does not deform when the sample is tilted. A sample with a MT profile that is 50% Gaussian or greater is more solid-like than liquid-like and, as a result, may be considered a gel from the standpoint of the NMR.

The MT profile of a 20% sample of PVA-C quenched at 23 °C and stored for 1 day at 23 °C does not contain a Gaussian component. The Gaussian component is not detected in the system for 3 days of storage. This means that prior to 3 days of storage the degree of entanglement of the chains has not developed enough to be detected by MT analysis. The MT profile of the 20% PVA-C sample stored for 3 days at 23 °C is

22% Gaussian and remains low for the remainder of the storage period, whereby the sample after 18 weeks of storage is still only 25% Gaussian. The meniscus of this sample, when the sample is tilted, deforms; the sample is a solution over the entire storage period of 18 weeks. Based on the idea that the sample has become a gel when the sample is 50% Gaussian, NMR appears to be accurate at detecting whether the sample is a gel or a solution.

The total profile area and Gaussian area of the samples stored at 5 °C increase with the age and are the largest for the samples with the highest degree of hydrolysis (Table 19). The initial MT profile of a 20% PVA-A sample stored at 5 °C is 70% Gaussian. This sample, which is a gel, is more rigid than the corresponding sample that was stored at 23 °C, whose initial MT profile is 51% Gaussian. After 18 weeks of storage at 5 °C, the MT profile of the 20% PVA-A sample is 76% Gaussian. The corresponding 20% PVA-A sample, after 18 weeks of storage at 23 °C, is 82% Gaussian and is slightly more rigid. It appears that the 5 °C quench promotes initial chain organization that restricts further progression of the network. In the PVA-A sample quenched and stored at 23 °C, the organization of chains and the development of the network is slow.

The MT profile of the 20% PVA-B sample quenched at 5 °C is 50% Gaussian and rises to 74% Gaussian after 18 weeks of storage at 5 °C. The MT profile of the corresponding sample quenched at 23 °C is only 18% Gaussian and rises to 72% Gaussian after 18 weeks of storage at 23 °C. The maximum in the percent Gaussian area occurs within 7 days of storage at both temperatures. The low quench temperature appears to promote initial network formation in PVA-B, but the overall network formation in the system after 7 days of storage are very similar. The initial quench and

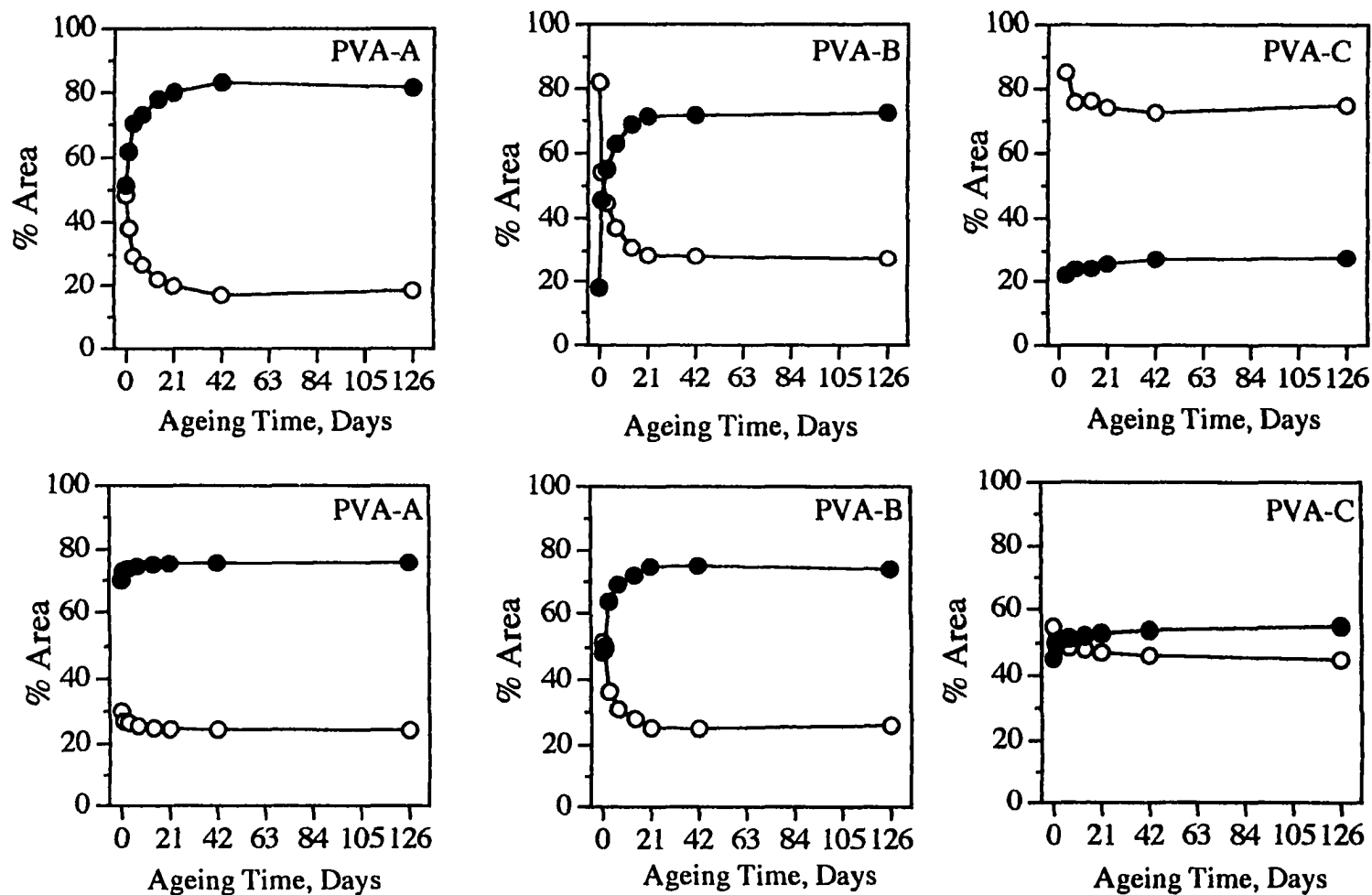
storage temperature of 5 °C does not have as pronounced an effect on network formation in PVA-B as it does in PVA-A over long storage periods.

The MT profile of the 20% PVA-C sample quenched at 5 °C is 45% Gaussian and rises to 51% Gaussian after 18 weeks of storage at 5 °C. The majority of the network in the PVA-C sample stored at 5 °C is due to initial chain organization as a result of the low temperature quench. The MT profile of the corresponding PVA-C sample stored at 23 °C does not contain an initial Gaussian component; a Gaussian component of 22% does not develop until 3 days of storage. At 23 °C the chains are extremely mobile, reducing network formation. The MT profile of the corresponding PVA-C sample stored at 23 °C for 18 weeks is only 25% Gaussian. The low temperature quench has a large effect on the overall degree of network formation in PVA-C relative to the PVA-C sample quenched and stored at 23 °C. The low temperature effect has the opposite effect on network formation than it had on PVA-A. Network formation is promoted by the low temperature quench and the further progression of network formation is not hindered.

This analysis of the percent Gaussian area exactly parallels the analysis of the total profile area. In addition, however, the full evaluation of the multicomponent nature of the MT profiles allows the determination the gel point of the sample from the perspective of the NMR, whereby samples with a percent Gaussian area 50% or greater may be defined as a gel. With this in mind, 20% PVA-A samples stored at 23 °C and 5 °C are gels initially and over the entire storage period of 18 weeks. PVA-B is always a gel at 5 °C. PVA-B becomes a gel after 3 days of storage at 23 °C. PVA-C is not a gel over the entire storage period at 23 °C but becomes a gel after 1 day of storage at 5 °C.

A comparison of the gel point determined by NMR and the gel point determined by the 90 ° tilt method reveal that NMR may be more sensitive to the true gel point of the system. The percent Gaussian and percent Lorentzian areas are plotted as a function of ageing time for PVA-A, B and C samples stored at 23 °C and 5 °C (Figure 23). The point at which the percent Gaussian reaches 50% is defined as the gel point from the perspective of the NMR. The point taken from the graph by extrapolation to the exact time at which the percent Lorentzian and Gaussian lines cross. The gelation times determined from the data in Figure 23 were determined and are tabulated and compared to the gelation time determined by the 90 ° tilt method (Table 20). The gelation time determined by NMR is consistently longer for all samples than the gelation time determined by the 90 ° tilt method. The difference in values may arise from an obvious difficulty with the tilt method: samples of PVA and other polymers may crust over, forming a surface layer that is much less resilient than the bulk. Hence the surface may not deform when the sample is tilted, but the bulk of the sample may still be relatively fluid. In the NMR method, the signal is derived from the bulk sample; hence, it gives an assessment of the state of the entire sample and is much less influenced by the quality of the surface.

97



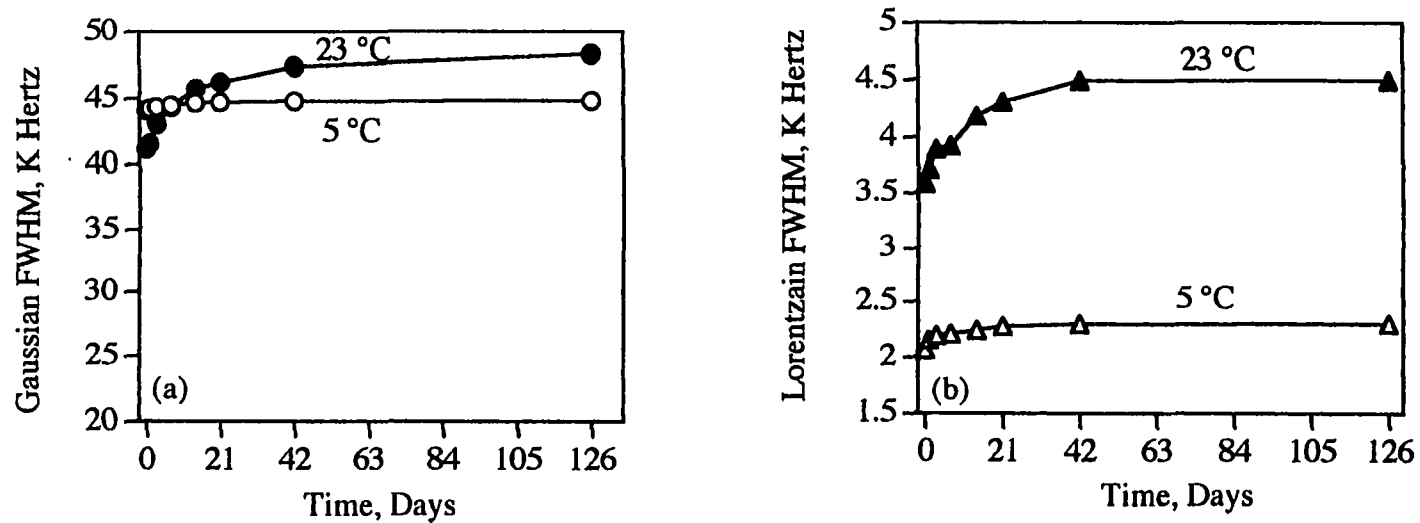
**Figure 23** . Percent Gaussian area ( —●— ) and percent Lorentzian area ( —○— ) as a function of ageing time at 23 °C (top three graphs) and 5 °C (bottom three graphs) for 20 % PVA-A, B and C.

Storage Temperature: 23 °C					Storage Temperature: 5 °C				
Gelation Time					Gelation Time				
	PVA-A	PVA-B	PVA-C	PVA-D		PVA-A	PVA-B	PVA-C	PVA-D
<b>30% Samples</b>					<b>30% Samples</b>				
NMR	15 m	15 m	32 h	21 d	NMR	15 m	15 m	32 h	7 d
Tilt Method	15 m	15 m	12 h	4 d	Tilt Method	15 m	15 m	4 h	1 d
<b>20% Samples</b>					<b>20% Samples</b>				
NMR	15 m	24 h	s	s	NMR	15 m	1 d	18 h	s
Tilt Method	15 m	12 h	18 d	s	Tilt Method	15 m	6 h	12 h	3 d
<b>10% Samples</b>					<b>10% Samples</b>				
NMR	s	s	s	s	NMR	s	s	s	s
Tilt Method	s	s	s	s	Tilt Method	6 h	s	s	s
<b>5% Samples</b>					<b>5% Samples</b>				
NMR	s	s	s	s	NMR	s	s	s	s
Tilt Method	s	s	s	s	Tilt Method	s	s	s	s

**Table 20.** Gelation time determined by the time at which the area of the magnetization-transfer profile is 50% Gaussian and by gel point measurements for PVA samples stored at 23 °C and 5 °C. The letter "s" designates that the sample is a solution. These measurements were recorded over a 126 day storage period.

Evaluation of the full-width at half-maximum (FWHM) of the Gaussian and Lorentzian components provides information about the mobility of the chains in the immobile and mobile components of the sample. Wu and Eads found that the FWHM of the Gaussian component corresponded closely to the rigidity of a starch gel.<sup>43-44</sup> The Lorentzian FWHM and Gaussian FWHM for 20% PVA-A are plotted as a function of storage time at 23 °C and 5 °C (Figure 24). The initial FWHM of the Gaussian (immobile) component is greater for the 20% PVA-A sample stored at 5 °C than the corresponding sample stored at 23 °C. As the sample ages, the FWHM of the Gaussian component of the sample stored at 23 °C becomes larger and reaches a higher limiting value than the corresponding sample stored at 5 °C. The 5 °C quench appears to initially promote network formation but hinders the further progression of the network. The chains in the Gaussian component of the sample stored at 5 °C are initially more immobilized than the chains in the Gaussian component of the sample stored at 23 °C. The 5 °C quench induces macromolecular structure such as dense aggregates or crystallites that hinder the further progression of the network. It appears from this data that crystallization, although initially contributing to the bulk rigidity of the network, ultimately hinders network formation.

The Lorentzian FWHM of 20% PVA-A stored at 23 °C and 5 °C is plotted as a function of ageing time (Figure 24b). The Lorentzian FWHM of the sample stored at 23 °C is larger than the Lorentzian FWHM of the sample stored at 5 °C, indicating that the chains in the Lorentzian component of the sample stored at 23 °C are less mobile than the chains in the Lorentzian component of the sample stored at 5 °C. Although it may initially seem counterintuitive that chains at 23 °C are less mobile than those at 5 °C, consideration of the effect of greater mobility in the Gaussian component on the

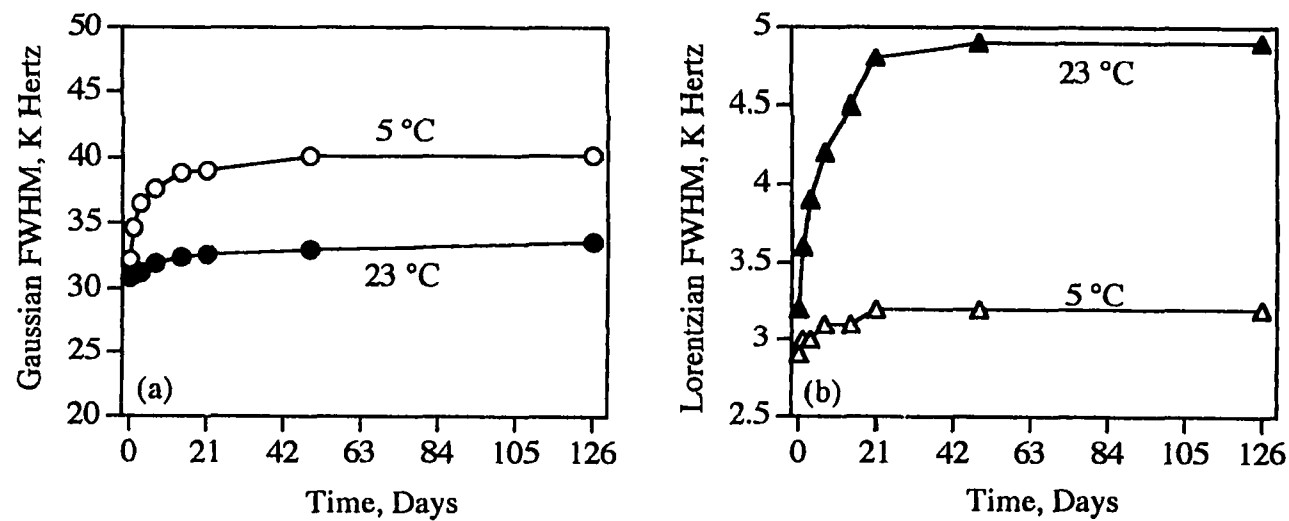


**Figure 24** . (a) Gaussian FWHM versus storage time at 23 °C ( —●— ) and 5 °C ( —○— ) and (b) Lorentzian FWHM versus storage time at 23 °C ( —▲— ) and 5 °C ( —△— ) for 20% PVA-A. Error in the measurements is  $\pm 200$  Hz.



volume available for the mobile chains may elucidate this observation. At 5 °C, the chains in the immobile component are tightly entangled and occupy a smaller free volume than the chains in the immobile component of the sample stored at 23 °C. This provides a greater available free volume to the mobile component and in effect dilutes the chains in the mobile component enabling them to move more freely at the lower storage temperature.

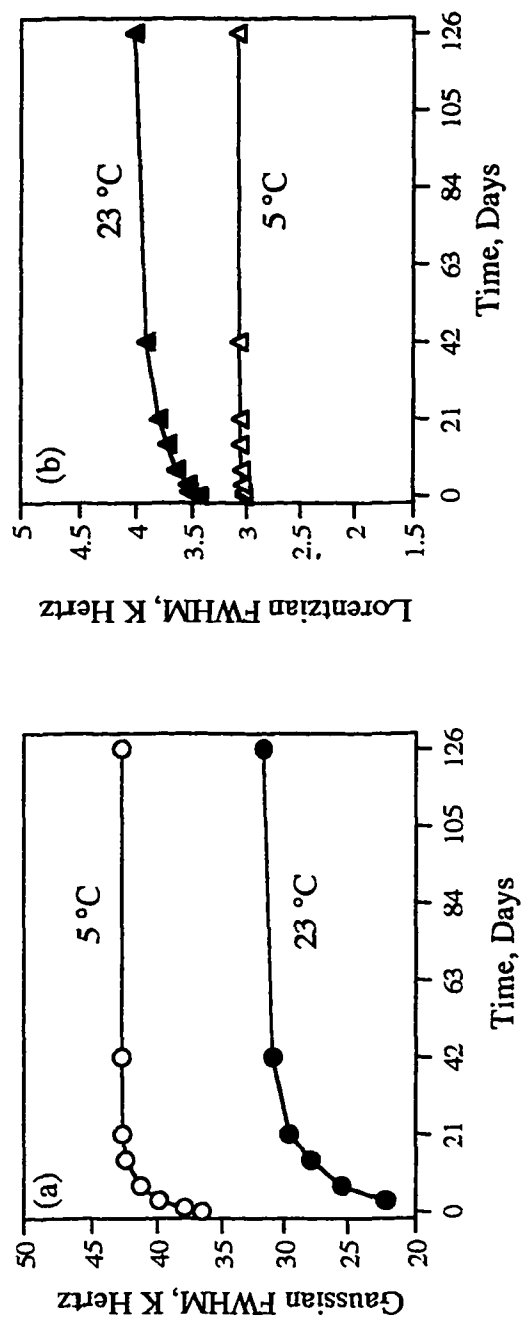
The Lorentzian FWHM and Gaussian FWHM for 20% PVA-B are plotted as a function of storage time at 23 °C and 5 °C (Figure 25). The FWHM of the Gaussian and Lorentzian components of 20% PVA-B follow the same general trend as the PVA-A sample. Close evaluation of the data reveals that the Gaussian FWHM is always greater for the sample stored at 5 °C (Figure 25a). The progression of network formation appears to be enhanced by the 5 °C quench and storage temperature unlike PVA-A. The 5 °C temperature promotes network formation possibly by inducing loosely entangled structures that nucleate further network formation or that become increasingly entangled as the sample ages. The Lorentzian FWHM is larger for the sample stored at 23 °C indicating less mobility than the Lorentzian component of the sample stored at 5 °C (Figure 25b). The chains in the immobile component of the sample stored at 23 °C become increasingly entangled as the sample ages. The chains in the immobile component of the sample stored at 5 °C do not become increasingly entangled as the sample ages. This may indicate that the progression of network formation in the PVA-B sample stored at 5 °C occurs by further tightening of the chains in the loosely entangled network. Network formation in the 20% PVA-B sample stored at 23 °C occurs by an overall entanglement of chains in both components.



**Figure 25** . (a) Gaussian FWHM versus storage time at 23 °C ( —●— ) and 5 °C ( —○— ) and (b) Lorentzian FWHM versus storage time at 23 °C ( —▲— ) and 5 °C ( —△— ) for 20% PVA-B. Error in the measurements is  $\pm 200$  Hz.

The Lorentzian FWHM and Gaussian FWHM for 20% PVA-C are plotted as a function of storage time at 23 °C and 5 °C (Figure 26). The initial Gaussian FWHM of the sample stored at 5 °C is considerably larger than the Gaussian FWHM of the sample stored at 23 °C (Figure 26a). The larger FWHM indicates that the chains in the immobile component of the sample stored at 5 °C have less motion than those chains in the immobile component of the sample stored at 23 °C. The larger FWHM of the Lorentzian component of the PVA-C sample stored at 23 °C indicates that the chains in the mobile component have less motion than those chains in the mobile component of the PVA-C sample stored at 5 °C. At 5 °C, the chains in the immobile component are entangled and occupy a smaller free volume than the chains in the immobile component of the sample stored at 23 °C. This provides a greater available free volume to the mobile component and in effect dilutes the chains in the mobile component enabling them to move more freely at the lower storage temperature.

The FWHM of the Lorentzian component gives information about the relative molecular mobility of the polymer within the solvent-rich portion of the sample. The polymer chains in the Lorentzian component of the PVA-C sample stored at 5 °C have a greater free volume and hence more mobility than the polymer chains in the Lorentzian component of the corresponding sample stored at 23 °C as indicated by a more narrow Lorentzian FWHM (Figure 26b). The 5 °C quench causes the chains in the immobile portion to compact, increasing the available volume of the mobile portion of the sample. Chain entanglement in PVA-C stored at 5 °C progresses by further immobilizing the PVA chains in the Gaussian component without recruitment of chains from the Lorentzian component. Chain entanglement in the PVA-C sample stored at 23 °C, however, occurs in the Lorentzian component, indicated by an increase in the Lorentzian FWHM, and in the Gaussian component, indicated by a steady increase in



**Figure 26 .** (a) Gaussian FWHM versus storage time at 23 °C (—●—) and 5 °C (—○—) and (b) Lorentzian FWHM versus storage time at 23 °C (—▲—) and 5 °C (—△—) for 20% PVA-C.

the Gaussian FWHM. This explains the significant progression of network formation in the PVA-C sample beyond the initial quench.

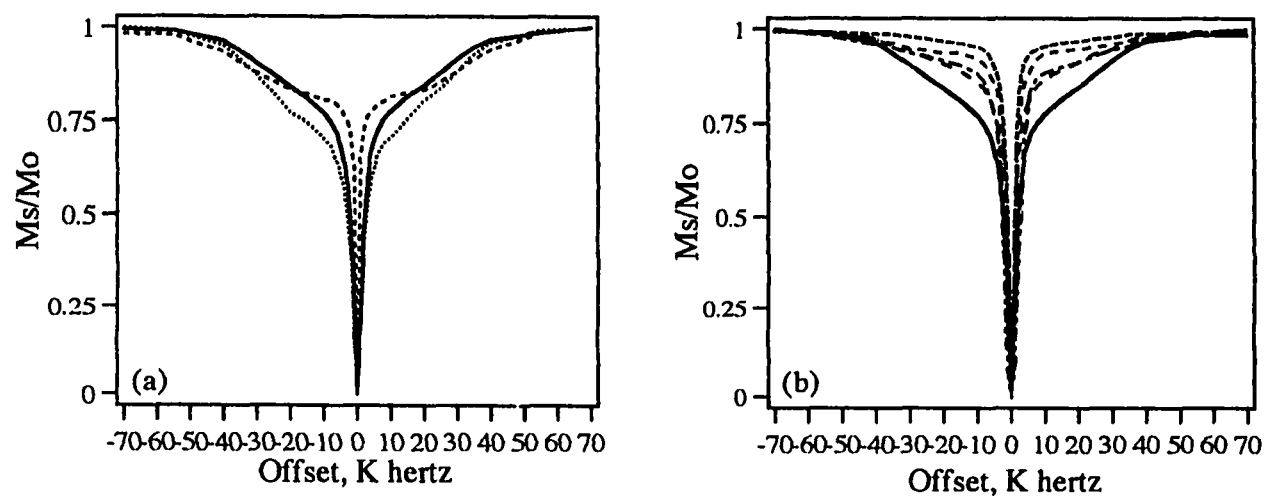
Network formation in PVA-C occurs by a different mechanism than network formation in PVA-A and PVA-B. The difference is caused by immediate inter- and intrachain hydrogen-bonding and molecular order in PVA-A and PVA-B resulting from the 5 °C quench. The low concentration of residual vinyl acetate in PVA-A and PVA-B allows for the promotion of efficient chain packing and leads to a densely packed Gaussian component. In the PVA-C sample, polymer-solvent interactions are favored, which significantly hinders polymer-polymer interactions and network formation.

Regarding the balance between self-association and solvent interaction, at 5 °C, the small change in the Gaussian FWHM in 20% PVA-A over time reflects the diminished molecular mobility of a sample in which self association is favored over solvent interaction. At 5 °C, the polymer chains in PVA-B and PVA-C are still mobile enough to continue to form an extensive network over time; they self associated to a lesser degree that in PVA-A.

## Effect of Viscosity Stabilizing and Destabilizing Agents on Network Formation

Literature data as well as data presented herein have shown that aqueous solutions prepared from PVA with a high degree of hydrolysis undergo network formation. The literature has shown that the development of the network responsible for the increase in viscosity can be affected by additives. Additives destabilize viscosity by inducing network formation or stabilize viscosity by hindering network formation.<sup>1</sup> Organic compounds such as methanol, acetone and ethylene glycol are known to induce network formation while isopropanol, isobutanol, n-butanol and n-propanol hinder network formation. Inorganic salts such as NaCl, Na<sub>2</sub>SO<sub>4</sub> and NaOCOCH<sub>3</sub> enhance network formation while thiocyanates hinder network formation.<sup>81-82</sup> Thiocyanates in particular destroy hydrophobic associations induced during cluster formation among water molecules when the hydrophobic portion of a polymer comes in contact with water. Thiocyanates should hinder network formation in aqueous PVA system where the increase in viscosity is due to intermolecular interactions between the hydrophobic portions of the PVA followed by entanglements due to hydrogen bonding.

Viscosity stabilizing and viscosity destabilizing agents were added as 10% of the aqueous phase in 20% PVA-A to investigate their effect on network formation. The samples were analyzed after 14 days of storage at 23 °C (Figure 27). Comparing the three profiles in Figure 27a, it is evident that the Na<sub>2</sub>SO<sub>4</sub> promotes network formation and reduces viscosity stability in the polymer rich region by a “salting-out effect” indicated by broadening only in the Gaussian component. Conversely, NaOCOCH<sub>3</sub> promotes network formation by reducing viscosity stabilization in both the immobile and mobile portions indicated by broadening of both the Gaussian and Lorentzian



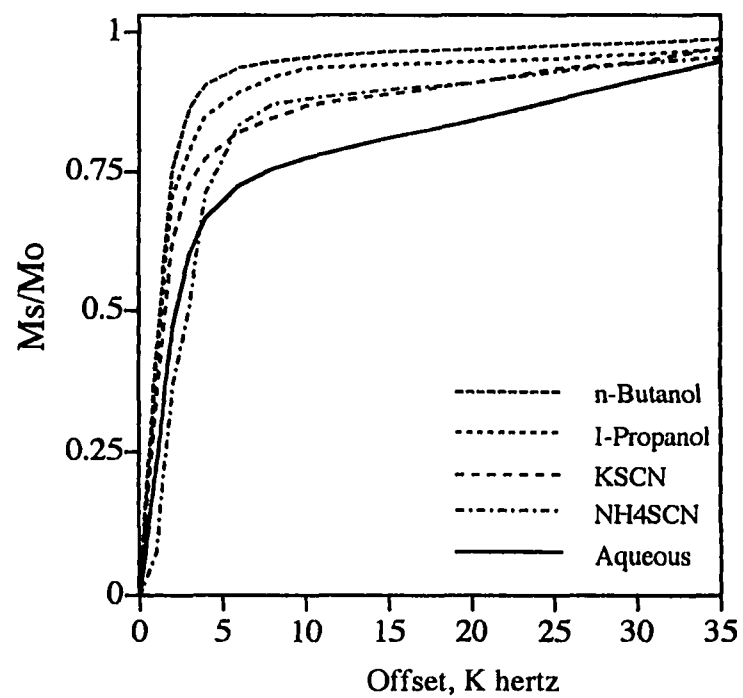
**Figure 27.** Magnetization-transfer profiles for 20% samples of PVA-A stored at 23 °C for 14 days (a) containing viscosity destabilizing agents:  $\text{Na}_2\text{SO}_4$  (.....) and  $\text{NaOCOCH}_3$  (.....) and (b) containing viscosity stabilizing agents: Iso-propanol (-----), KSCN (-----), n-butanol (-----),  $\text{NH}_4\text{SCN}$  (-----). Aqueous 20% PVA-A (——) shown in both figures.

components. The effect of the viscosity stabilization agents on network formation is shown in Figure 27b. An expansion of the data shown in Figure 27b shows that the order of viscosity stabilization is consistent with the literature whereby n-butanol > iso-propanol > NH<sub>4</sub>SCN > KSCN (Figure 28).

A closer evaluation of the data reveals that the order of viscosity stabilization is n-butanol > iso-propanol > KSCN > NH<sub>4</sub>SCN (Figure 28). These results are consistent with literature data showing that KSCN is more efficient at stabilizing viscosity than NH<sub>4</sub>SCN and n-butanol is better stabilizing viscosity than iso-propanol.<sup>1, 81-82</sup>

MT analysis provides additional detailed information compared to viscosity data in that it indicates if the agent works on the polymer-rich or solvent-rich regions of the sample. For example, Na<sub>2</sub>SO<sub>4</sub> has a pronounced effect in the polymer-rich region of the sample, while NaOCOCH<sub>3</sub> effects both the polymer-rich and solvent-rich components of the sample. Na<sub>2</sub>SO<sub>4</sub> may disrupt intermolecular interactions between the hydrophobic portions of the PVA, while sodium acetate may lower the solvent power of water.<sup>1</sup> Ammonium thiocyanate promotes viscosity stabilization in the Gaussian component and acts to destabilize the Lorentzian component unlike all the other viscosity stabilizing agents. The known viscosity stabilizing agent, NH<sub>4</sub>SCN, destroys the hydrophobic bonding induced during cluster formation among water molecules when the hydrophobic parts of the polymer chain come in contact with water. A reduction of cluster formation favors a decrease in the Gaussian component area and promotes an increase in the Lorentzian component area as a result of more chains being in the mobile phase rather than restricted in the immobile phase.

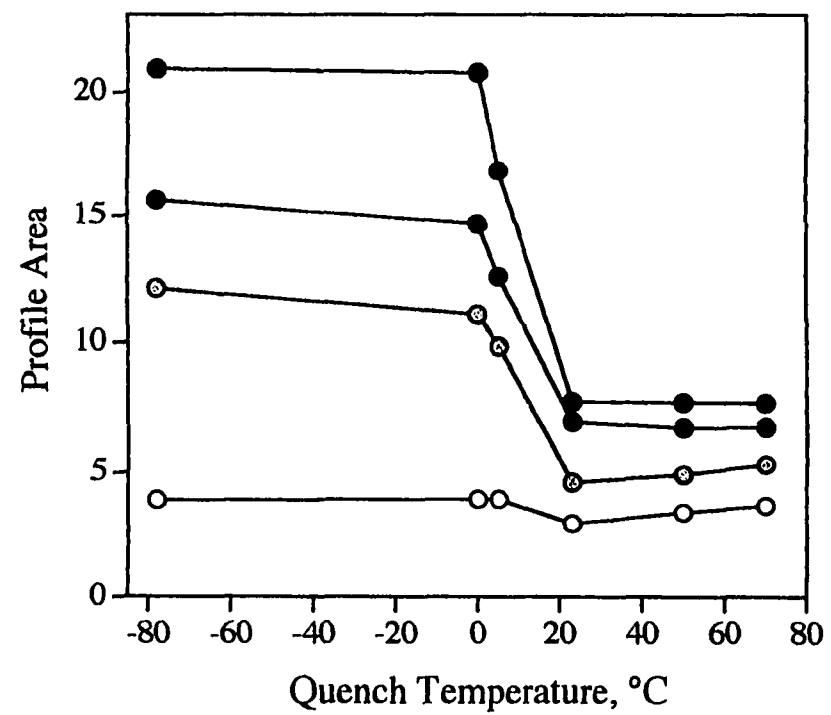




**Figure 28.** Expanded region of figure 28. The effect of viscosity stabilizing agents on the degree of network formation in 20% PVA-A stored at 23 °C for 14 days

## Effect of Quench Temperature on Network Formation

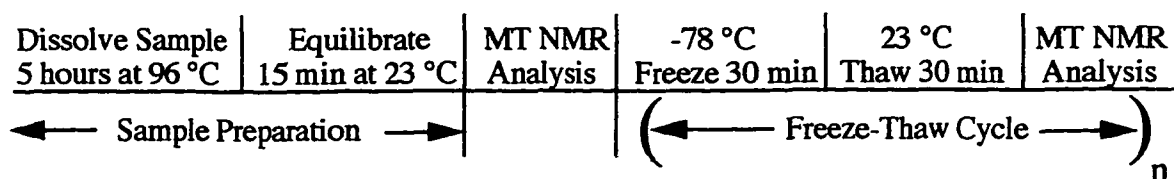
Due to the pronounced effect of storage temperature on the progression of network formation, the effect of quench temperature on network formation in 20% aqueous PVA gels was monitored. PVA-A, B, C and D samples were prepared at 96 °C then quenched at temperatures between 75 and -78 °C for 1 hour. The MT profiles were acquired after the samples were then stored for 23 hours at 23 °C for a total ageing period of 24 hours (Figure 29). A plot of quench temperature versus profile area shows a significant increase in the MT profile area between 23 °C and 0 °C. At temperatures below 0 °C the MT profile areas are large and well differentiated relative to the MT profile areas of samples quenched at temperatures above 23 °C. The values of profile areas at 0 °C and -78 °C represent the limiting values of profile areas achieved after 18 weeks of ageing (refer to Table 14 and Figure 18). Quench temperatures below 0 °C for all samples at one day of ageing cause the maximum degree of network formation. The samples quenched at and below 0 °C show no further development of the network even after ageing for 2 weeks at 23 °C. These samples are visually turbid, whereby the turbidity increases with decreasing quench temperature, suggesting that significant phase separation has occurred. The pronounced phase separation in these samples significantly hinders the development of the network over time.



**Figure 29.** Profile Area as a function of quench temperature for 20% samples of PVA-A (—●—), PVA-B (—●—), PVA-C (—○—) and PVA-D (—○—).

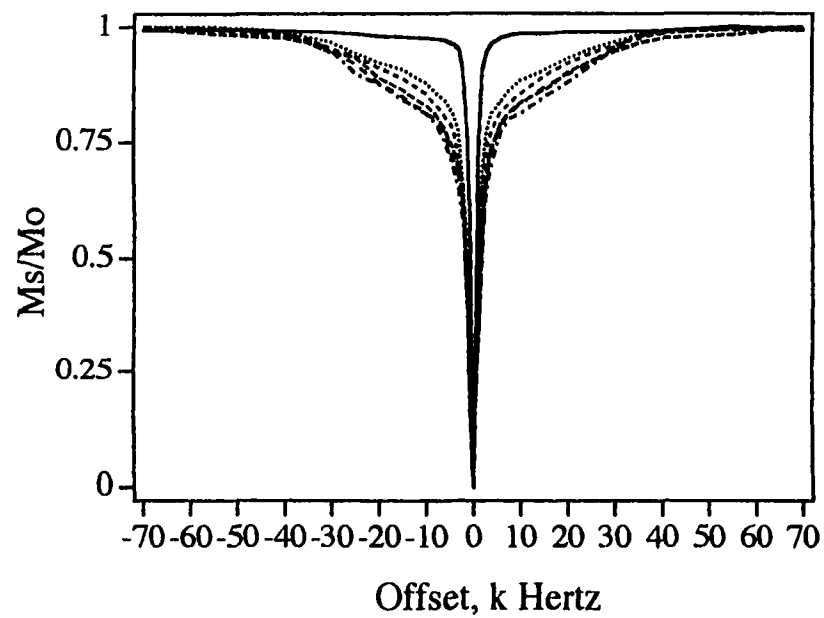
## The Effect of Freeze-Thaw Cycles on Network Formation

The effect of repetitive freezing and thawing on the degree of network formation in PVA samples was evaluated by MT analysis. The freeze-thaw procedure is represented as a time line in Figure 30 where (n) is the number of freeze-thaw cycles. A 10% PVA-A sample was exposed to 5 freeze-thaw cycles. MT analysis shows that the first



**Figure 30.** Freeze-thaw cycle.

freeze-thaw cycle significantly enhances network formation indicated by a large, broad profile area at  $n=1$  (Figure 31). Consecutive freeze-thaw cycles increase network formation to a slight degree. The profile area levels off at  $n=4$  and does not significantly increase after  $n=5$  freeze-thaw cycles.



Number of Freeze-thaw Cycles	Profile Area
0	4.9
1	9.1
2	10.5
3	12.1
4	12.7
5	12.8

**Figure 31** . Magnetization-transfer profiles of 10% PVA-A sample ( — ) after 1 ( ..... ), 2 ( ..... ), 3 ( ..... ), 4 ( ..... ) and 5 ( ..... ) freeze-thaw cycles. Profile areas are calculated from the magnetization-transfer profiles.

## **The Effect of Solvent Extraction on Network Formation**

To verify that the differences in the detected network formation by MT analysis were not due to impurities in the different PVA samples, MT analysis was performed on samples that were extracted. PVA was extracted with methanol in a Soxhlet extractor for 100 cycles and dried to remove the methanol with vacuum until a constant mass was obtained. Proton NMR spectra were acquired to verify the absence of sodium acetate and to assure that all methanol was removed from the extracted PVA samples. Sodium acetate was the main concern because it is known to destabilize viscosity. The sample with the highest degree of hydrolysis, i.e., PVA-A, has the highest concentration of sodium acetate that if in high enough concentration would destabilize viscosity and enhance network formation. PVA samples that were extracted were analyzed by MT analysis and no difference in the degree of network formation was observed. The concentration of sodium acetate, 0.91%, is not enough to induce measurable network formation. The amount of sodium acetate added in the viscosity destabilizing experiments in the previous section was 30 times greater than the residual sodium acetate present in PVA-A as a result of hydrolysis.

## **The Effect of Preheating on Network Formation**

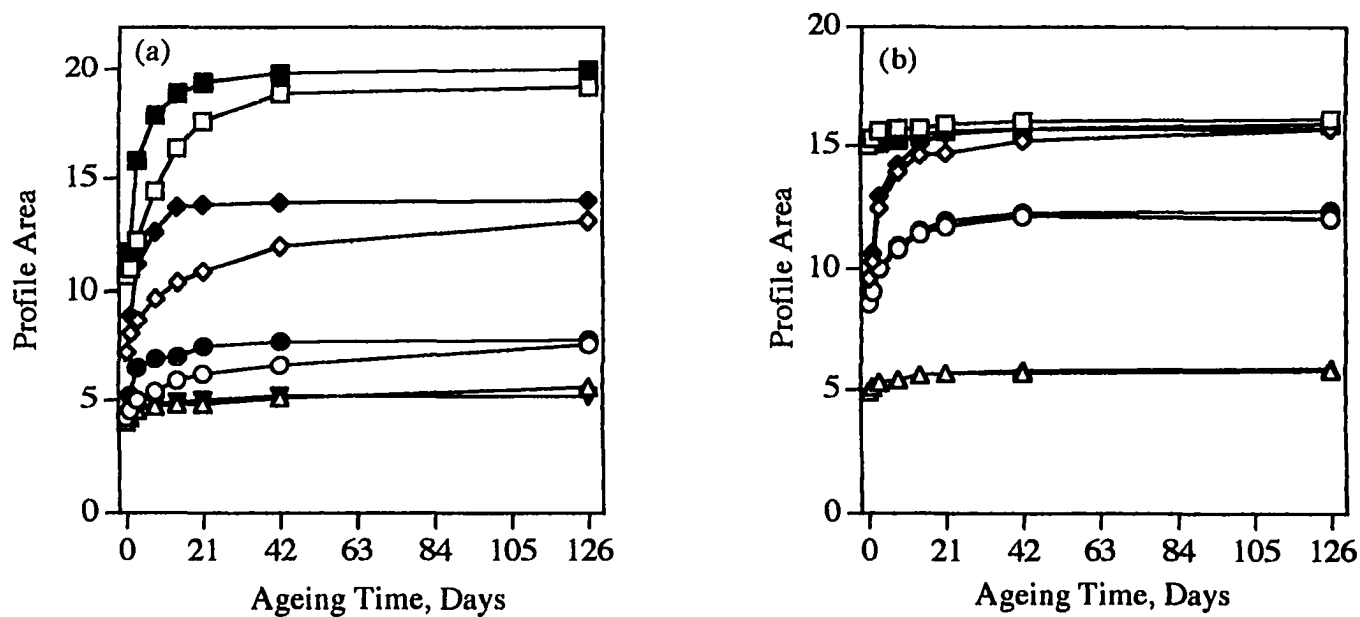
The effect of thermal prehistory on the degree of crystallinity has been observed in PVA systems.<sup>15-19</sup> The effect of preheating on network formation was determined. The PVA-A, B, C and D samples were preheated at 110 °C for 1 hour and cooled at room temperature for 1 hour prior to dissolution. Four 20% samples of PVA-A, B, C

and D were dissolved by heating for 5 hours at 96 °C. The samples were quenched and stored in a water bath for 24 hours prior to MT analysis. There was no detectable difference in the MT profiles between samples preheated and those that were not. This suggests that heating at 96 °C for 5 hours destroys any thermal prehistory that may have existed in the samples prior to dissolution.

### Thermoreversibility of Network Formation

The thermoreversibility of network formation was determined by treating aged samples at 96 °C for 5 hours. The 5, 10, 20 and 30% PVA-A, B, C and D samples stored at 23 °C and 5 °C for 21 weeks were placed in a 96 °C water bath for 5 hours then allowed to equilibrate at their previous storage temperature for 24 hours. All samples were completely thermoreversible; the total area of the MT profile as well as the areas of the Gaussian and Lorentzian components returned to the original value.

Network formation in the reheated 20% PVA-A, B, C and D aged for 21 weeks at 23 °C and 5 °C was monitored as the samples aged again at their initial temperature after being heated at 96 °C for 5 hours (Figure 32, Table 21). At 23 °C network formation proceeded faster in the reheated samples than in the initial samples (Table 14); at 5 °C there was little difference. The 23 °C samples that were aged for 21 weeks, reheated and allowed to age again at 23 °C, became more visually turbid with age than the original samples (Table 22). The samples stored at 5 °C, reheated and aged at 5 °C did not look visibly turbid.



**Figure 32** . Area of magnetization-transfer profiles of 20% PVA-A ( —□— ), PVA-B ( —◇— ), PVA-C ( —○— ) and PVA-D ( —△— ) stored at 23 °C (a) and 5 °C (b). MT profile areas of 20% PVA-A ( —■— ), PVA-B ( —◆— ), PVA-C ( —●— ) and PVA-D ( —▲— ) stored at 23 °C (a) and 5 °C (b) after the samples were reheated at 96 °C for 5 hours.



Ageing Time, Days	23 °C				5 °C			
	PVA-A	PVA-B	PVA-C	PVA-D	PVA-A	PVA-B	PVA-C	PVA-D
0	10.7	7.2	4.2	4.0	15.0	9.6	8.6	4.9
1	11.7	8.9	5.2	4.2	15.1	10.6	9.1	5.1
3	15.8	11.2	6.5	4.6	15.1	12.9	10.0	5.3
8	17.9	12.6	6.9	4.8	15.2	14.2	10.9	5.4
14	18.9	13.7	7.0	4.9	15.4	15.1	11.5	5.6
21	19.4	13.8	7.5	5.0	15.6	15.5	11.9	5.7
42	19.8	13.9	7.7	5.2	15.7	15.7	12.2	5.8
126	20.0	14.0	7.8	5.2	15.9	15.7	12.3	5.9

**Table 21** . Magnetization-transfer profile areas of 20% PVA-A, B, C and D samples aged at 23 °C and 5 °C for 21 weeks, reheated at 96 °C for 5 hours and aged again at 23 °C and 5 °C.

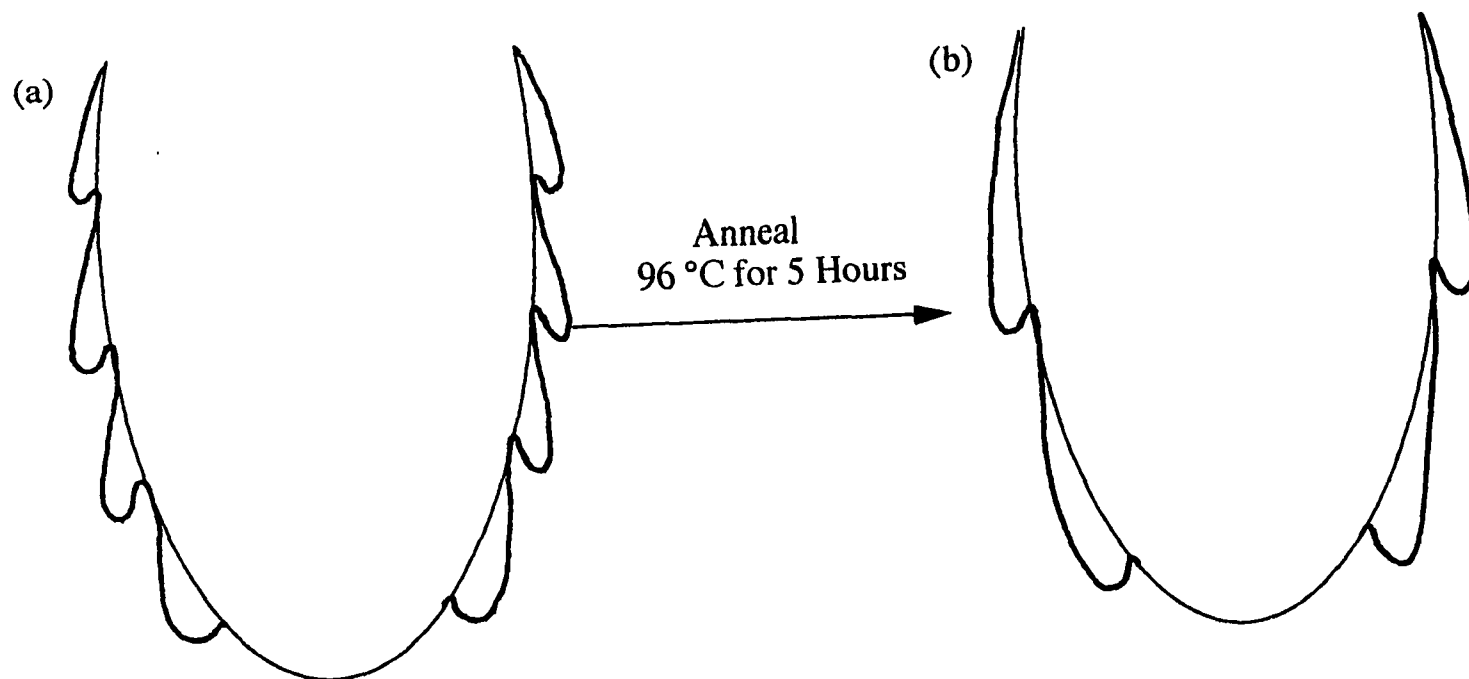
Ageing Time, Days	Original Samples Aged at 23 °C				Reheated Samples Aged at 23 °C			
	PVA-A	PVA-B	PVA-C	PVA-D	PVA-A	PVA-B	PVA-C	PVA-D
15 min	0.020	0.018	0.016	0.010	0.025	0.018	0.015	0.011
1 hr	0.041	0.020	0.015	0.010	0.048	0.035	0.019	0.010
17 hr	0.060	0.041	0.030	0.020	0.072	0.045	0.029	0.018
2 d	0.062	0.041	0.030	0.020	0.084	0.048	0.034	0.020
5 d	0.062	0.041	0.030	0.020	0.092	0.049	0.035	0.022
9 d	0.062	0.041	0.030	0.020	0.092	0.050	0.035	0.024
18 d	0.062	0.041	0.030	0.020	0.092	0.050	0.035	0.024
47 d	0.062	0.041	0.030	0.020	0.093	0.050	0.035	0.024
126 d	0.062	0.041	0.030	0.020	0.093	0.050	0.035	0.024

**Table 22 .** Measured turbidity as a function of ageing time for 20% PVA-A, B, C and D initially stored at 23 °C (left side of table) and as a function of ageing time after heating to 96 °C for 5 hours (right side of table).

At least two explanations for the fast return of network formation in the reheated samples are possible. Any entangled physical crosslinks or residual crystallites that are not fully destroyed in the heating process may nucleate network formation. Second, the chains may retain a memory of their previous alignment, even in a mobile state. Prior to reheating, the aged samples exist in a metastable state at a local energy minimum in the potential energy surface that describes the conformational possibilities. After heating, the system is in a high energy state and as it proceeds toward equilibrium again, the system reaches again a local minimum faster than it initially did (Figure 33). The return to a metastable state is faster in the reheated samples because the original potential wells on the energy surface are annealed by reheating. The removal of the local minima in the potential energy wells allows the reheated sample to attain a metastable state faster than the original sample.

The minimum time required for destruction of the network can be determined by MT-NMR analysis. The MT profiles of 20% samples of PVA-A aged for 126 days at 23 °C (Table 23) and 5 °C (Table 24) were monitored after the samples were heated at 96 °C for various periods of time. The 20% PVA-A sample returns to its initial profile area after being heated at 96 °C for 3 hours. The majority of the network is in fact destroyed after 1 hour of heating; the percent Gaussian drops from 81.5% to 58.6%.

The MT profiles of 20% samples of PVA-A aged for 126 days at 5 °C (Table 24) were monitored after the samples were heated at 96 °C for varying periods of time. The 20% PVA-A sample returns to its initial profile area after being heated at 96 °C for 4 hours. The destruction of the network as a result of heating is much slower in the 5 °C sample relative to the 23 °C sample. The majority of the network remains even after 3 hours of heating at 96 °C. This indicates that the tightly entangled network requires



**Figure 33.** Cartoon of a portion of a potential energy surface, (a) aged sample with many possible metastable states with local energy minima and (b) reheated sample after annealing at 96 °C for 5 hours.

Ageing Time	Profile Area	Gaussian Area	Lorentzian Area	% Gaussian
15 min	10.7	5.5	5.2	51.4
126 d	20.0	16.3	3.7	81.5
20% PVA-A aged for 126 days at 23 °C Heating Time                      heated at 96 °C				
15 min	18.8	14.9	3.9	79.2
1 hr	12.1	7.1	5.0	58.6
2 hr	11.2	6.0	5.2	53.6
3 hr	10.9	5.7	5.2	52.2
4 hr	10.7	5.5	5.2	51.4
5 hr	10.7	5.5	5.2	51.4

**Table 23.** Magnetization-transfer profile area, Gaussian and Lorentzian areas and % Gaussian area for 20% PVA-A heated for various times at 96 °C after being aged at 23 °C for 126 days. Magnetization-transfer analysis was performed after a 15 minute equilibration at 23 °C.

Ageing Time	Profile Area	Gaussian Area	Lorentzian Area	% Gaussian
15 min	15.0	10.5	4.5	70.0
126 d	16.1	12.2	4.9	75.8
20% PVA-A aged for 126 days at 5 °C Heating Time                      heated at 96 °C				
15 min	16.0	12.1	3.9	75.6
1 h	15.9	12.0	3.9	75.5
2 h	15.7	11.7	3.9	75.2
3 h	15.4	11.0	4.4	71.4
4 h	15.0	10.5	4.5	70.0
5 h	15.0	10.5	4.5	70.0

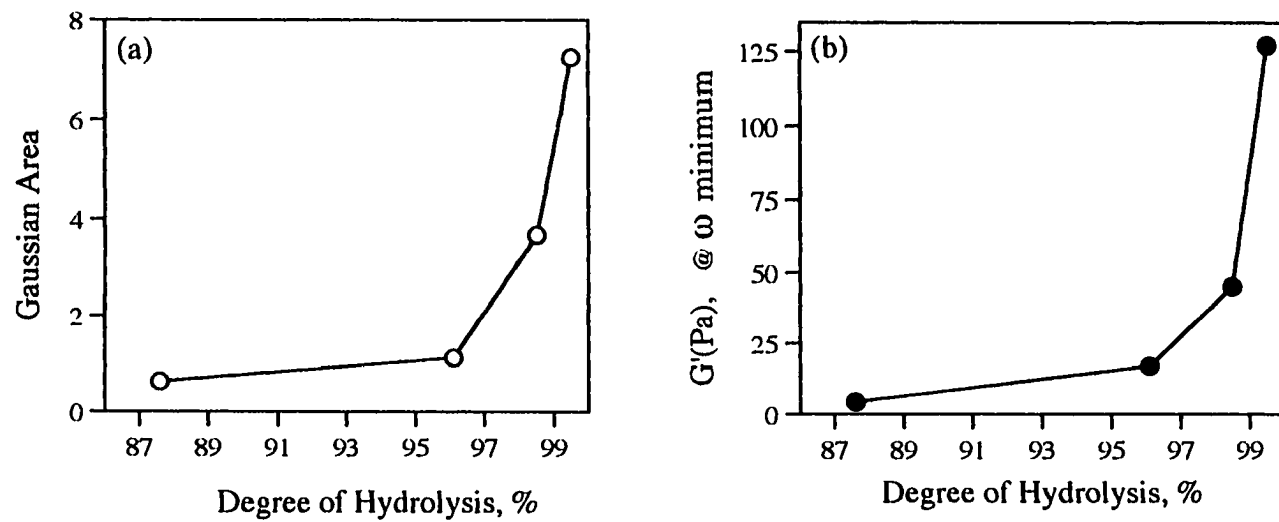
**Table 24.** Magnetization-transfer profile area, Gaussian and Lorentzian areas and % Gaussian area for 20% PVA-A heated for various times at 96 °C after being aged at 5 °C for 126 days. Magnetization-transfer analysis was performed after a 15 minute quench at 5 °C.

more time to allow disentanglement of the chains. Heating for 5 hours at 96 °C is sufficient for the full destruction of the network in the samples stored at 5 °C.

## Measurement of Rigidity

The MT profile area represents the bulk ensemble average of the mobile and immobile components that contribute to the overall rigidity of the gel. The increase in the Gaussian component with increasing concentration, degree of hydrolysis and age of the sample suggests an increase in the amount of PVA chains in highly restricted conformations, which may occur in polymer-rich regions in the sample such as aggregates or crystallites.

To confirm the relationship between the Gaussian component and the gel rigidity, the gel rigidity was measured by dynamic mechanical testing. The gel rigidity was determined for 20% samples of A-D stored at 23 °C for 3 days. The measured rigidity is expressed as the limiting value of the frequency-dependent storage modulus and is plotted as a function of the degree of hydrolysis (Figure 34). The gel rigidity measured by this method follows the same trend as the Gaussian area of the MT profile with increasing degree of hydrolysis. The Gaussian area of a gel can estimate of the rigidity of the gel without mechanical disruption or destruction of the gel.



**Figure 34** . a) Gaussian area of the MT profiles measured for 20% PVA samples stored at 23 °C for 3 Days. b) Gel rigidity measured at 23 °C for 20% PVA samples stored at 23 °C for 3 Days.



## Conclusions

Although spin lattice and spin-spin relaxation times for water protons vary with increasing polymer concentration, as has long been established in the literature, values of the relaxation times alone did not enable discrimination between samples with respect to the degree of hydrolysis nor did they allow us to monitor changes in the degree of network formation as the samples aged. Hence, magnetization-transfer (MT) experiments were explored as a means to determine differences in network formation with respect to the degree of hydrolysis of the polymer.

MT analysis can be used to observe the effects of the degree of hydrolysis, concentration, quench and storage conditions on the ageing process in polymer solutions and gels. Experiments with non-network forming polymers such as poly (ethylene oxide) and poly (acrylic acid) established that changes in the MT profiles are clearly due to network formation and are not simply an artifact of viscosity. We have further demonstrated that MT is sensitive to network formation in physically crosslinked, homogeneous solutions and gels of PVA, in the same manner as Eads and others have demonstrated for chemically crosslinked, heterogeneous biopolymers.

Furthermore, we have demonstrated that MT profiles yield distinct information about the mobile and immobile components of the gel and hence can provide a novel view of the processes occurring at a molecular level that cause transitions in properties between solutions and gels and between gels and heterogeneous mixtures. As a function of concentration, the processes that control the rigidity of the gel change. The differences in the degree of network formation in 20% samples of PVA with varying degrees of hydrolysis are a result of the differences in the degree of polymer-polymer

self interaction. Turbidity measurements indicate that gelation occurs without detectable phase separation. At 30%, however, phase separation is the dominate mechanism that contributes to the overall rigidity of the sample indicated by a significant increase in turbidity with age and temperature. The process of phase separation is most pronounced in samples with the highest degree of hydrolysis and dominates over network formation as a result of polymer-polymer self interaction.

Differentiation between samples with different degrees of hydrolysis is possible by MT analysis. Temperature has the most pronounced effect on network formation in samples with the highest degree of hydrolysis. At the low quench and storage temperature, network formation is hindered in the super hydrolyzed sample indicated by a negligible increase in network formation after the initial quench. The Gaussian component is extremely rigid indicating that the chains are immobilized in a tightly entangled network that does not further entangle with the age of the sample as it does in the corresponding sample stored at the higher storage temperature. The low temperature quench promotes network formation in the fully and intermediately hydrolyzed grades of PVA indicated by a significant increase in profile area after the initial quench. The area of the Gaussian component continues to increase with age indicating that the initial quench promotes a loosely entangled network that tightens as the sample ages. This mechanism of network formation in the fully and intermediately hydrolysed samples is further substantiated by an increase in the free volume available to the Lorentzian component over time as a result of a decrease in the volume occupied of the Gaussian component due to network tightening. The partially hydrolyzed grade of PVA is least sensitive temperature changes.

Further insight into the effect of degree of hydrolysis and temperature on network

formation was gained by evaluating the multicomponent nature of the MT profiles. Curve fitting analysis revealed information regarding the balance between the polymer-rich and solution-rich portions of the sample as it ages. Full evaluation of the multicomponent nature of the MT profiles allowed us to determine the gel point from the perspective of the NMR, whereby samples with a percent Gaussian area 50% or greater are gels. A comparison of the gel point determined by NMR and the gel point determined by the 90 ° tilt method reveals that NMR may be sensitive to the bulk gel point of the system. The gelation time determined by NMR is consistently longer for all samples than the gelation time determined by the 90 ° tilt method. The surface of the sample may crust over and not deform although the bulk of the sample may remain a solution.

In a related series of experiments, compounds known to modify the behavior of potential gel-forming polymers by stabilizing or destabilizing viscosity have yielded to MT analysis. Multi-component analysis of PVA solutions containing compounds such as KSCN and NH<sub>4</sub>SCN that are known to destabilize viscosity has provided insight into the actual mechanism of influence of the additives on the mobile and immobile components and water in the phase. The cations of such viscosity stabilizing agents bind by ionic interactions to the polar hydroxyl groups, thereby lowering the salting-out effect, while the anions destroy hydrophobic bonding and cluster formation. The literature suggests that K<sup>+</sup> ions are more efficient at stabilizing viscosity than NH<sub>4</sub><sup>+</sup>. MT analysis confirms, in general, that KSCN is more efficient at viscosity stabilization than NH<sub>4</sub>SCN.

## References

- 1) *Poly (Vinyl Alcohol), Recent Developments and Applications*; Finch, C.A., Ed., John Wiley, London, 1992.
- 2) Toyoshima, K. 'General Properties of Poly(Vinyl Alcohol) in Relationship to Its Applications' In *Poly(Vinyl Alcohol)*, Finch, C.A., Ed., John Wiley, London, 1973.
- 3) Sakurada, I. *Poly(Vinyl Alcohol) Fibers* Marcel Dekker, New York, 1985.
- 4) Fukae, R., Yamamoto, T., Sengen, O., Saso, T., Kako, T., Kamacho, M. *Polym. J.* **1990**, 22, 636-638.
- 5) Yamaura, K., Takahasi, S., Tanigami, T, Matsuzawa, S. *J. Appl. Polym. Sci.* **1987**, 33, 1982-1991.
- 6) Jamaura, K., Katoh, H., Tanigami, T. Matsuzawa, S. *Appl. Polym. Sci.* **1987**, 34, 2347-2354.
- 7) *Poly(Vinyl Alcohol), Basic Properties and Uses* , Pritchard, J.G., Ed., Gordon Breach, London, 1970.
- 8) Sawatari, C., Yamamoto, Y., Yanagida, N., Matsuo, M. *Polymer*, **1993**, 34, 956-966.
- 9) Lazareva, T.G., li'yushchenko, I.A., Alimov, I.F. *Polym.Sci, Ser A.* **1994**, 36, 1231-1235.
- 10) Fang, L., Brown, W. *Macromolecules* **1990**, 23, 3284-3290.
- 11) Koike, A. Nemoto, N., Inoue, T., Osaki, K. *Macromolecules*, **1995**, 28, 2339-2344.

- 12) Takahashi, A., Hiramitsu, S. *Polym. J.* **1974**, 6, 103-107.
- 13) Kanaya, T., Ohkura, M., Takeshita, H., Kaji, K., Furshaka, M., Yamaoka, H., Wignall, G.D. *Macromolecules* **1995**, 28, 3168-3174.
- 14) Wu, W., Shibayama, M., Roy, S., Kurokawa, H., Coyne, L., Nomura, S., Stein, R.S. *Macromolecules* **1990**, 23, 2245-2251.
- 15) Stern, P., Prokopova, E., Quadrat, O. *Colloid Polym. Sci.* **1985**, 263, 899-904.
- 16) Stern, P., Prokopova, E., Quadrat, O. *Colloid Polym. Sci.* **1987**, 265, 234-238.
- 17) Prokopova, E., Stern, P., Quadrat, O. *Colloid Polym. Sci.* **1987**, 265, 903-907.
- 18) Mrkvickova, L., Prokopova, E., Quadrat, O. *Colloid Polym. Sci.* **1987**, 265, 978-981.
- 19) Stern, P., Prokopova, E., Quadrat, O. *Colloid Polym. Sci.* **1992**, 270, 1066-1068.
- 20) Ohkura, M., Kanaya, T., Kaji, K. *Polymer* **1992**, 33, 5044-5047.
- 21) Gyorgyi-Edelenyi, J., Nagy, M. *Acta Chimica Hungarica* **1991**, 128, 411-417.
- 22) Lloyd, D.J., "The Problem of Gel Structure" In *Colloid Chemistry*, Alexander, J., Ed., Chem Catalogue, New York, Vol. 1, 1926.
- 23) Hermands, P.H., 'Gels' In *Colloid Science*, Kruyt, H.R., Ed. Elsevier, Amsterdam, Vol. 2, 1949.

- 24) Flory, P.J. *Disc. Faraday Soc.* **1974**, 57, 7-18.
- 25) Ferry, J.D., *Viscoelastic Properties of Polymers*, John Wiley, New York, 1980, 529-530.
- 26) Prokopova, E., Biro, J., Lednický, F. *Euro. Polym. J.* **1988**, 24, 621-64.
- 27) Overloop, K., Van Gerven, L. *J. Mag. Res.* **1992**, 100, 303-315.
- 28) Hanus, F., Gillis, P. *J. Magn. Reson.* **1984**, 59, 427-445.
- 29) Van der Beek, G.P., Cohen Stuart, M.A. *Langmuir* **1991**, 7, 327-334.
- 30) Olabisi, O., Bobeson, L.M., Shaw, M.T. *Polymer-Polymer Miscibility*, Academic Press, New York, 1979, 185-190.
- 31) Riggan, M.T., Sharp, A.R., Kaiser, R. *J. Appl. Polym. Sci.* **1979**, 23, 3147-3154.
- 32) Menon, R.S., Mackay, A.L., Hailey, J.R.T., Bloom, M., Burgess, A.E. *J. Appl. Polym. Sci.* **1987**, 33, 1141-1155.
- 33) Abaujo, C. D., MacKay, A.L., Whittall, K.P., Hailey, J.R. *J. Magn. Res. Ser. B*, **1993**, 101, 248-261.
- 34) Froix, M.F., Nelson, R. *Macromolecules* **1975**, 8, 726-730.
- 35) Ceckler, T.L. Balaban, R.S. *J. Magn. Reson.* **1991**, 93, 572-588.
- 36) Koenig, J.L., *Spectroscopy of Polymers*, American Chemical Society, Washington, D.C., 1992, Ch 10
- 37) Pimenov, G.G., Tyurina, N.V., Golyakova, E. Sh. *Polym. Sci.* **1992**, 34, 1018- 1021.

- 38) Cha, W-I, Hyon, S-H, Ikada, Y., *Makromol. Chem.* **1993**, *194*, 2433-2441.
- 39) Froix, M.F., Nelson, R. *Macromolecules* **1975**, *8*, 726-730.
- 40) Hatakeyema, T., Jamauchi, F., Hatakeyema, T. *Euro. Polym. J.* **1984**, *20*, 61- 64;
- 41) Hatakeyema, T., Jamauchi, F., Hatakeyema, H. *Euro. Polym. J.* **1987**, *23*, 361-365.
- 42) Cechler, T.L., Wolff, S.D., Yip, V., Simon, S.A., Balaban, R.S. *J. Mag. Res.* **1992**, *98*, 637-645.
- 43) Wu, J.Y., Eads, T.M. *Carbohydrate Polymers* **1993**, *20*, 51-60.
- 44) Ni, Q.X., Eads, T.M.J. *Agric. Food Chem.* **1993**, *41*, 1035-1040.
- 45) Gore, J.C., Brown, M.S., Armitage, I.M. *Magn. Reson. Med.* **1989**, *6*, 333-342.
- 46) Hills, B.P. *Molecular Physics* **1992**, *76*, 489-508.
- 47) Hua, J., Hurst, G.C. *J. Magn. Res. Series A* **1994**, *107*, 220-224.
- 48) Forsen, S., Hoffman, R.A. *J. Chem Phys.* **1963**, *39*, 2892-2898.
- 49) Brooks, D., Kuwata, K., Schleich, T. *Magn. Reson. Med.* **1994**, *31*, 331-336.
- 50) Koenig, S.H., Brown III, R.D. *Magn. Reson. Med.* **1993**, *30*, 685-695.
- 51) Farr, T.C., Becker, E.D. *Pulse Fourier Transform NMR*, Academic Press, New York, 1971.

- 52) Carr, H.Y., Purcell, E.M. *Phys. Rev.* **1954**, *94*, 630-637; Meiboom, S., Gill, D. *Rev. Sci. Instr.* **1958**, *29*, 688-695.
- 53) Carles, J.E., Scallan, A.M. *J. App. Polym. Sci.* **1973**, *17*, 1855-1865.
- 54) Grad, J., Mendelson, D., Hyder, F., Bryant, R.G. *J. Magn. Reson.* **1990**, *86*, 416-419.
- 55) Grad, J., Bryant, R.G. *J. Magn. Reson.* **1990**, *90*, 1-8.
- 56) Kennan, R.P., Richardson, K.A., Zhong, J., Maryanski, M.J., Gore, J.C. *Magn. Reson., Ser B* **1996**, *110*, 267-277.
- 57) Hua, J., Hurst, G. *J. Mag. Res. Ser. A* **1994**, *107*, 220-224.
- 58) Henkelman, R. M., Huang, X., Xiang, Q-S. Stanis, G.J., Swanson, S.D., Bronskill, M.J. *Mag. Res. Med.* **1993**, *29*, 759-766.
- 59) Komatsu, M., Inoue, T., Miyasaka, K. *J. Polym. Sci., Polym. Phys. Ed.* **1986**, *24*, 303-311.
- 60) Overall, D. W. *Macromolecules* **1984**, *17*, 1458-1464.
- 61) Li, Y., Wang, G, Hu, Z. *Macromolecules* **1995**, *28*, 4194-4197.
- 62) Shen, W., Smith, G.R., Knobler, C.M., Scott, R.L. *J. Chem. Phys.* **1991**, *95*, 3376-3381.
- 63) DaMire, L.W., Jacobs, D.T. *J. Chem. Phys.* **1992**, *97*, 464-468.
- 64) Almdal, K., Dyre, J., Hvidt, S., Kramer, O. *Polymer Gels and Networks* **1993**, *1*, 5-17.



- 65) Hvidt, S., Heller, K., 'Viscoelastic Properties of Biological Networks and Gels' In *Physical Networks, Polymers and Gels* Buchard, W., Ross-Murphy, R.B. Ed., Elsevier Applied Science, New York, 1990.
- 66) Djabourov, M., 'Gelation- A Review' In *Polym. International*, **1991**, 25, 135-143.
- 67) Bovey, F.A., Jelinski, L., Mirau, P.A. *Nuclear Magnetic Resonance Spectroscopy*, Academic Press, New York, 1988, Chapter 7.
- 68) Wu, T.K., Sheer, M.L. *Macromolecules* **1977**, 10, 529-532.
- 69) Wu, T.K., Overnall, D.W. *Macromolecules* **1973**, 6, 582-584.
- 70) Overnall, D. W. *Macromolecules* **1984**, 17, 1458-1464.
- 71) Terao, T., Maeda, S., Saika, A. *Macromolecules* **1983**, 16, 1535-1538.
- 72) Pham, Q.T., Petiaud, R., Waton, H. Llauro-Darricades, M.F. *Proton and Carbon NMR Spectra of Polymers*, Prenton Press, London, 1991.
- 73) Moritani, T., Kuruma, I., Shibantani, K., Fujiwara, Y. *Macromolecules* **1972**, 5, 577-580.
- 74) Hoeve, C.A.J. 'The Structure of Water in Polymers' In *Water in Polymers*, ACS Symp. Ser, **1980**, 127, 135-146.
- 75) Nakamura, K., Hatakeyama, T., Hatakeyama, H. *Polymer* **1983**, 24, 871-876.
- 76) Quinn, F.X., Kampff, E., Smyth, G., Mc Breietry, V.J. *Macromolecules* **1988**, 21, 3191-3198.

- 77) Rault, J. '*T<sub>g</sub> Regulation Effects in Polymer-Water Systems*' In *Hydrogen Bond Networks*, Bellissent-Funel, M.C., Dore, J.C. Ed., Kluwer Academic, Netherlands, 1994, 441-445.
- 78) Hutchinson, J. M. *Prog. Polym. Sci.* **1995**, 20, 703-760.
- 79) Prins, E., Prins, W. *Macromolecules* **1973**, 6, 888-895.
- 80) Matsuo, M., Kawase, M., Sugiura, Y., Takematsu, S., Hara, C. *Macromolecules* **1993**, 26, 4461-4471.
- 81) Bekturou, E.A., Bakauorova, Z.K. '*Poly (vinyl alcohol), Poly (propylene glycol) and other Non-inorganic Polymers*' In *Synthetic Water Soluble Polymers in Solution*, Huthig Wepf Verlag, Germany, 1986, Chapter 4.
- 82) Bekturou, E.A., Bakauorova, Z.K. '*Non-ionic Water-soluble Polymers*' In *Synthetic Water Soluble Polymers in Solution*, Huthig Wepf Verlag, Germany, 1981, Chapter 3.

## Vita

Lori Ellen Stephans was born to Frederick and Joan Stephans on November 28, 1967 in Morristown, NJ. She was raised on a small Christmas tree farm in Hope, NJ. She received a B.S. Degree in chemistry from East Stroudsburg University in East Stroudsburg, PA in June 1990. That same year, she came to Lehigh University where she began graduate work involving the modification of polyethylene and polypropylene surfaces under the direction of Dr. Gregory S. Ferguson. She received a Masters Degree in October of 1993. She later completed her research and received her Ph.D. in Chemistry from Lehigh University in June 1997 under the guidance of Dr. Natalie Foster. Lori accepted a position as assistant professor in the Department of Chemistry at Rowan University in Glassboro, NJ.